

Robust Spectral Compressed Sensing via Structured Matrix Completion

Yuxin Chen[†], Yuejie Chi[‡]

[†]Electrical Engineering, Stanford University

[‡]Electrical and Computer Engineering, The Ohio State University *

Abstract

The paper explores the problem of *spectral compressed sensing*, which aims to recover a spectrally sparse signal from a small random subset of its n time domain samples. The signal of interest is assumed to be a superposition of r multi-dimensional complex sinusoids, while the underlying frequencies can assume any *continuous* values on the unit interval. Conventional compressed sensing paradigms suffer from the *basis mismatch* issue when imposing a discrete dictionary on the Fourier representation. To address this problem, we develop a novel algorithm, called Enhanced Matrix Completion (EMaC), based on structured matrix completion that does not require prior knowledge of the model order. The algorithm starts by arranging the data into a low-rank enhanced form exhibiting multi-fold Hankel structure, and then attempts recovery via nuclear norm minimization. Under mild incoherence conditions, EMaC allows perfect recovery as soon as the number of samples exceeds the order of $r \log^3(n)$, and is stable against bounded noise. Even if a constant portion of samples are corrupted with arbitrary magnitude, EMaC can still allow accurate recovery, provided that the sample complexity exceeds the order of $r^2 \log^3(n)$. Along the way, our results demonstrate the power of convex relaxation in completing a low-rank multi-fold Hankel matrix from a minimal number of observed entries. The performance of our algorithm and its applicability to super resolution are further validated by numerical experiments.

1 Introduction

1.1 Motivation and Contributions

A large class of practical applications features high-dimensional signals that can be modeled or approximated by a superposition of spikes in the spectral (resp. time) domain, and involves estimation of the signal from its time (resp. frequency) domain samples. Examples include acceleration of medical imaging [1], target localization in radar and sonar systems [2], inverse scattering in seismic imaging [3], fluorescence microscopy [4], channel estimation in wireless communications [5], analog-to-digital conversion [6], etc. The data acquisition devices, however, are often limited by hardware and physical constraints, precluding sampling with the desired resolution. It is thus of paramount interest to reduce the sensing complexity while retaining the recovery accuracy.

In this paper, we investigate the *spectral compressed sensing* problem, which aims to recover a spectrally sparse signal from a small number of randomly observed time domain samples. The signal of interest $x(t)$ with ambient dimension n is assumed to be a weighted sum of multi-dimensional complex sinusoids at r distinct frequencies $\{\mathbf{f}_i \in [0, 1)^K : 1 \leq i \leq r\}$, where the underlying frequencies can assume any continuous values on the unit interval.

Spectral compressed sensing is closely related to the problem of *harmonic retrieval*, which seeks to extract the underlying frequencies of a signal from a collection of its time domain samples. Conventional methods

*Y. Chen is with the Department of Electrical Engineering, Stanford University, Stanford, CA 94305, USA (email: yx-chen@stanford.edu). Y. Chi is with Department of Electrical and Computer Engineering and Department of Biomedical Informatics, The Ohio State University, Columbus, OH 43210, USA (email: chi.97@osu.edu). This work has been presented in part at the 2013 International Conference on Machine Learning. Manuscript date: August 15, 2018.

for harmonic retrieval include Prony’s method [7], ESPRIT [8], the matrix pencil method [9], the Tufts and Kumaresan approach [10], the finite rate of innovation approach [11, 12], etc. These methods routinely exploit the *shift invariance* of the harmonic structure, namely, a consecutive segment of time domain samples lies in the same subspace irrespective of the beginning of the segment. However, one weakness of these techniques is that they require prior knowledge of the model order, that is, the number of underlying frequency spikes of the signal or at least an estimate of it. Besides, these techniques heavily rely on the knowledge of the noise spectra, and are often sensitive against noise and outliers [13].

Another line of work is concerned with Compressed Sensing (CS) [14, 15] over a discrete domain, which suggests that it is possible to recover a signal even when the number of samples is far below its ambient dimension, provided that the signal enjoys a *sparse representation* in the transform domain. In particular, tractable algorithms based on convex surrogates become popular due to their computational efficiency and robustness against noise and outliers [16, 17]. Furthermore, they do not require prior information on the model order. Nevertheless, the success of CS relies on sparse representation or approximation of the signal of interest in a finite discrete dictionary, while the true parameters in many applications are actually specified in a *continuous* dictionary. The *basis mismatch* between the true frequencies and the discretized grid [18] results in loss of sparsity due to spectral leakage along the Dirichlet kernel, and hence degeneration in the performance of conventional CS paradigms.

In this paper, we develop an algorithm, called Enhanced Matrix Completion (EMaC), that simultaneously exploits the shift invariance of harmonic structures and the spectral sparsity of signals. Inspired by the conventional matrix pencil form [19], EMaC starts by arranging the data samples into an enhanced matrix exhibiting K -fold Hankel structures, whose rank is bounded above by the spectral sparsity r . This way we convert the spectral sparsity into the low-rank structure without imposing any pre-determined grid. EMaC then invokes a nuclear norm minimization program to complete the enhanced matrix from partially observed samples. When a sparse proportion of the observed samples are corrupted with arbitrary magnitudes, EMaC solves a weighted nuclear norm minimization and ℓ_1 norm minimization to recover the signal as well as the sparse corruption.

The performance of EMaC depends on an incoherence condition that depends only on the frequency locations regardless of their respective amplitudes. The incoherence measure is characterized by the reciprocal of the smallest singular value of some Gram matrix, which is defined by sampling the *Dirichlet kernel* at the wrap-around differences of all frequency pairs. The signal of interest is said to obey the incoherence condition if the Gram matrix is well conditioned, which arises over a broad class of spectrally sparse signals. We demonstrate that, under this incoherence condition, EMaC enables exact recovery from $\mathcal{O}(r \log^3 n)$ random samples¹, and is stable against bounded noise. Moreover, EMaC admits perfect signal recovery from $\mathcal{O}(r^2 \log^3 n)$ random samples even when a constant proportion of the samples are corrupted with arbitrary magnitudes. Finally, numerical experiments validate our theoretical findings, and indicate the applicability of EMaC in super resolution.

Along the way, we provide theoretical guarantee for low-rank matrix completion of Hankel matrices and Toeplitz matrices, which is of great importance in control, natural language processing, and computer vision. To the best of our knowledge, our results provide the first theoretical guarantees that are close to the information theoretic limit.

1.2 Connection and Comparison to Prior Work

The K -fold Hankel structure, which plays a central role in the EMaC algorithm, roots from the traditional spectral estimation technique named Matrix Enhancement Matrix Pencil (MEMP) [19] for multi-dimensional harmonic retrieval. The conventional MEMP algorithm assumes equi-spaced time domain samples for estimation, and require prior knowledge on the model order. Cadzow’s denoising method [20] also exploits the low-rank structure of the matrix pencil form for denoising line spectrum, but the method is non-convex and lacks performance guarantees.

When the frequencies of the signal indeed fall on a grid, CS algorithms based on ℓ_1 minimization [14, 15] assert that it is possible to recover the spectrally sparse signal from $\mathcal{O}(r \log n)$ random time domain samples. These algorithms admit faithful recovery even when the samples are contaminated by bounded noise [16, 21]

¹The standard notation $f(n) = \mathcal{O}(g(n))$ means that there exists a constant $c > 0$ such that $f(n) \leq cg(n)$; $f(n) = \Theta(g(n))$ means there are numerical constants $c_1, c_2 > 0$ such that $c_1g(n) \leq f(n) \leq c_2g(n)$.

or arbitrary sparse outliers [17]. When the inevitable *basis mismatch* issue [18] is present, several remedies of CS algorithms have been proposed to mitigate the effect [22, 23], although theoretical guarantees are in general lacking.

More recently, Candes and Fernandez-Granda [24] proposed a total-variation norm minimization algorithm to super-resolve a sparse signal from frequency samples at the *low end* of the spectrum. This algorithm allows accurate super-resolution when the point sources are sufficiently separated, and is stable against noise [25]. Inspired by this approach, Tang et. al. [26] then developed an atomic norm minimization algorithm for line spectral estimation from $\mathcal{O}(r \log r \log n)$ random time domain samples, which enables exact recovery when the frequencies are separated by at least $4/n$. However, the results of [26] are limited to line spectrum (1-D frequency model), and are established under a random signal model, i.e. the complex signs of the frequency spikes are assumed to be i.i.d. drawn from a uniform distribution. The robustness of the method against outliers is not known either. In contrast, our approach can accommodate multi-dimensional frequencies, and yields deterministic conditions for perfect recovery. We will provide detailed comparison with the approach of Tang et. al. after we formally present our results. A numerical comparison is also presented in Section 5.3 for the line spectrum model.

Our algorithm is inspired by recent advances of Matrix Completion (MC) [27, 28], which aims at recovering a low-rank matrix from partial entries. It has been shown [29–31] that exact recovery is possible via nuclear norm minimization, as soon as the number of observed entries exceeds the order of the information theoretic limit. This line of algorithms is also robust against noise and outliers [32, 33], and allow exact recovery even in the presence of a constant portion of maliciously corrupted entries [34–36], which have found numerous applications in collaborative filtering [37], medical imaging [38], etc. Nevertheless, the theoretical guarantees of these algorithms do not apply to the more structured observation models associated with the proposed multi-fold Hankel structure. Consequently, direct application of existing MC results delivers pessimistic sample complexity, which far exceeds the degrees of freedom underlying the signal.

1.3 Organization

The rest of the paper is organized as follows. The signal and sampling models are described in Section 2. By restricting our attention to two-dimensional (2-D) frequency models, we present the enhanced matrix form and the associated structured matrix completion algorithms. The extension to multi-dimensional frequency models is discussed in Section 3.3. The main theoretical guarantees are summarized in Section 3, based on the incoherence condition introduced in Section 3.1. We then discuss the extension to low-rank Hankel and Toeplitz matrix completion in Section 4. Section 5 presents the numerical validation of our algorithms. The proofs of Theorems 1 and 3 are based on duality analysis followed by a golfing scheme, which are supplied in Section 6 and Section 7, respectively. Section 8 concludes the paper with a short summary of our findings as well as a discussion of potential extensions and improvements. Finally, the proofs of auxiliary lemmas supporting our results are deferred to the appendices.

2 Model and Algorithm

Assume that the signal of interest $x(\mathbf{t})$ can be modeled as a weighted sum of K -dimensional complex sinusoids at r distinct frequencies $\mathbf{f}_i \in [0, 1)^K$, $1 \leq i \leq r$, i.e.

$$x(\mathbf{t}) = \sum_{i=1}^r d_i e^{j2\pi \langle \mathbf{t}, \mathbf{f}_i \rangle}, \quad \mathbf{t} \in \mathbb{Z}^K. \quad (1)$$

It is assumed throughout that the frequencies \mathbf{f}_i 's are normalized with respect to the Nyquist frequency of $x(\mathbf{t})$ and the time domain samples are sampled at integer values. The d_i 's represent the complex amplitudes, and $\langle \cdot, \cdot \rangle$ denotes the inner product. For concreteness, our discussion is mainly devoted to a 2-D frequency model when $K = 2$. This subsumes line spectral estimation as a special case, and indicates how to address multi-dimensional models. The algorithms for higher dimensional scenarios closely parallel the 2-D case, which will be briefly discussed in Section 3.3.

2.1 2-D Frequency Model

Consider a data matrix $\mathbf{X} = [X_{k,l}]_{0 \leq k < n_1, 0 \leq l < n_2}$ of ambient dimension $n := n_1 n_2$, which is obtained by sampling (1) on a uniform grid at the Nyquist rate. From (1) each entry $X_{k,l}$ can be expressed as

$$X_{k,l} = x(k, l) = \sum_{i=1}^r d_i y_i^k z_i^l, \quad (2)$$

where for any i ($1 \leq i \leq r$) we define

$$y_i := \exp(j2\pi f_{1i}) \quad \text{and} \quad z_i := \exp(j2\pi f_{2i})$$

for some frequency pairs $\{\mathbf{f}_i = (f_{1i}, f_{2i}) \mid 1 \leq i \leq r\}$. We can then express \mathbf{X} in a matrix form as follows

$$\mathbf{X} = \mathbf{Y} \mathbf{D} \mathbf{Z}^\top, \quad (3)$$

where the above matrices are defined as

$$\mathbf{Y} := \begin{bmatrix} 1 & 1 & \cdots & 1 \\ y_1 & y_2 & \cdots & y_r \\ \vdots & \vdots & \vdots & \vdots \\ y_1^{n_1-1} & y_2^{n_1-1} & \cdots & y_r^{n_1-1} \end{bmatrix}, \quad (4)$$

$$\mathbf{Z} := \begin{bmatrix} 1 & 1 & \cdots & 1 \\ z_1 & z_2 & \cdots & z_r \\ \vdots & \vdots & \vdots & \vdots \\ z_1^{n_2-1} & z_2^{n_2-1} & \cdots & z_r^{n_2-1} \end{bmatrix}, \quad (5)$$

and

$$\mathbf{D} := \text{diag}[d_1, d_2, \dots, d_r]. \quad (6)$$

The above form (3) is sometimes referred to as the Vandermonde decomposition of \mathbf{X} .

Suppose that there exists a location set Ω of size m such that the $X_{k,l}$ is observed if and only if $(k, l) \in \Omega$. It is assumed that Ω is sampled uniformly at random. Define $\mathcal{P}_\Omega(\mathbf{X})$ as the orthogonal projection of \mathbf{X} onto the subspace of matrices that vanish outside Ω . We aim at recovering \mathbf{X} from $\mathcal{P}_\Omega(\mathbf{X})$.

2.2 Matrix Enhancement

One might naturally attempt recovery by applying the low-rank MC algorithms [27], arguing that when r is small, perfect recovery of \mathbf{X} is possible from partial measurements since \mathbf{X} is low rank if $r \ll \min\{n_1, n_2\}$. Specifically, this corresponds to the following algorithm:

$$\begin{aligned} & \underset{\mathbf{M} \in \mathbb{C}^{n_1 \times n_2}}{\text{minimize}} \quad \|\mathbf{M}\|_* \\ & \text{subject to} \quad \mathcal{P}_\Omega(\mathbf{M}) = \mathcal{P}_\Omega(\mathbf{X}), \end{aligned} \quad (7)$$

where $\|\mathbf{M}\|_*$ denotes the nuclear norm (or sum of all singular values) of a matrix $\mathbf{M} = [M_{k,l}]$. This is a convex relaxation paradigm of the rank minimization problem. However, naive MC algorithms [30] require at least the order of $r \max(n_1, n_2) \log(n_1 n_2)$ samples, which far exceeds the degrees of freedom (which is $\Theta(r)$) in our problem. What is worse, since r can be as large as $n_1 n_2$, \mathbf{X} will no longer be low-rank when $r > \min(n_1, n_2)$. This motivates us to seek other forms that better capture the harmonic structure.

In this paper, we adopt one effective enhanced form of \mathbf{X} based on the following two-fold Hankel structure. The enhanced matrix \mathbf{X}_e with respect to \mathbf{X} is defined as a $k_1 \times (n_1 - k_1 + 1)$ block Hankel matrix

$$\mathbf{X}_e := \begin{bmatrix} \mathbf{X}_0 & \mathbf{X}_1 & \cdots & \mathbf{X}_{n_1-k_1} \\ \mathbf{X}_1 & \mathbf{X}_2 & \cdots & \mathbf{X}_{n_1-k_1+1} \\ \vdots & \vdots & \vdots & \vdots \\ \mathbf{X}_{k_1-1} & \mathbf{X}_{k_1} & \cdots & \mathbf{X}_{n_1-1} \end{bmatrix}, \quad (8)$$

where $1 \leq k_1 \leq n_1$ is a pencil parameter, and each block is a $k_2 \times (n_2 - k_2 + 1)$ Hankel matrix defined such that for every ℓ ($0 \leq \ell < n_1$):

$$\mathbf{X}_\ell := \begin{bmatrix} X_{\ell,0} & X_{\ell,1} & \cdots & X_{\ell,n_2-k_2} \\ X_{\ell,1} & X_{\ell,2} & \cdots & X_{\ell,n_2-k_2+1} \\ \vdots & \vdots & \vdots & \vdots \\ X_{\ell,k_2-1} & X_{\ell,k_2} & \cdots & X_{\ell,n_2-1} \end{bmatrix}, \quad (9)$$

where $1 \leq k_2 \leq n_2$ is another pencil parameter. This enhanced form allows us to express each block as²

$$\mathbf{X}_\ell = \mathbf{Z}_L \mathbf{Y}_d^\ell \mathbf{D} \mathbf{Z}_R, \quad (10)$$

where \mathbf{Z}_L , \mathbf{Z}_R and \mathbf{Y}_d are defined as

$$\mathbf{Z}_L := \begin{bmatrix} 1 & 1 & \cdots & 1 \\ z_1 & z_2 & \cdots & z_r \\ \vdots & \vdots & \vdots & \vdots \\ z_1^{k_2-1} & z_2^{k_2-1} & \cdots & z_r^{k_2-1} \end{bmatrix}, \quad \mathbf{Z}_R := \begin{bmatrix} 1 & z_1 & \cdots & z_1^{n_2-k_2} \\ 1 & z_2 & \cdots & z_2^{n_2-k_2} \\ \vdots & \vdots & \vdots & \vdots \\ 1 & z_r & \cdots & z_r^{n_2-k_2} \end{bmatrix}$$

and

$$\mathbf{Y}_d := \text{diag}[y_1, y_2, \dots, y_r].$$

Substituting (10) into (8) yields the following:

$$\mathbf{X}_e = \underbrace{\begin{bmatrix} \mathbf{Z}_L \\ \mathbf{Z}_L \mathbf{Y}_d \\ \vdots \\ \mathbf{Z}_L \mathbf{Y}_d^{k_1-1} \end{bmatrix}}_{\sqrt{k_1 k_2} \mathbf{E}_L} \underbrace{\mathbf{D} [\mathbf{Z}_R, \mathbf{Y}_d \mathbf{Z}_R, \dots, \mathbf{Y}_d^{n_1-k_1} \mathbf{Z}_R]}_{\sqrt{(n_1-k_1+1)(n_2-k_2+1)} \mathbf{E}_R}, \quad (11)$$

where \mathbf{E}_L and \mathbf{E}_R characterize the column and row space of \mathbf{X}_e , respectively. This immediately implies that \mathbf{X}_e is *low-rank*, i.e.

$$\text{rank}(\mathbf{X}_e) \leq r. \quad (12)$$

The rank of \mathbf{X}_e is strictly smaller than r if two distinct frequencies take the same value along one direction [19]. This form is closely aligned with the traditional matrix pencil approach proposed in [9, 19] to estimate harmonic frequencies if *all* entries of \mathbf{X} are available. Thus, one can extract all underlying frequencies of \mathbf{X} using methods proposed in [19], as long as \mathbf{X} can be faithfully recovered.

2.3 The EMaC Algorithm without Noise

We then attempt recovery through the following Enhancement Matrix Completion (EMaC) algorithm:

$$\begin{aligned} (\text{EMaC}) \quad & \underset{\mathbf{M} \in \mathbb{C}^{n_1 \times n_2}}{\text{minimize}} \quad \|\mathbf{M}_e\|_* \\ & \text{subject to} \quad \mathcal{P}_\Omega(\mathbf{M}) = \mathcal{P}_\Omega(\mathbf{X}), \end{aligned} \quad (13)$$

where \mathbf{M}_e denotes the enhanced form of \mathbf{M} . In other words, EMaC minimizes the nuclear norm of the enhanced form over all matrices compatible with the samples. This convex program can be rewritten into a

²Note that the l th ($0 \leq l < n_1$) row \mathbf{X}_{l*} of \mathbf{X} can be expressed as

$$\mathbf{X}_{l*} = [y_1^l, \dots, y_r^l] \mathbf{D} \mathbf{Z}^\top = [y_1^l d_1, \dots, y_r^l d_r] \mathbf{Z}^\top,$$

and hence we only need to find the Vandemonde decomposition for \mathbf{X}_0 and then replace d_i by $y_i^l d_i$.

semidefinite program (SDP) [39]

$$\begin{aligned} & \underset{\mathbf{M} \in \mathbb{C}^{n_1 \times n_2}}{\text{minimize}} && \frac{1}{2} \text{Tr}(\mathbf{Q}_1) + \frac{1}{2} \text{Tr}(\mathbf{Q}_2) \\ & \text{subject to} && \mathcal{P}_\Omega(\mathbf{M}) = \mathcal{P}_\Omega(\mathbf{X}), \\ & && \begin{bmatrix} \mathbf{Q}_1 & \mathbf{M}_e^* \\ \mathbf{M}_e & \mathbf{Q}_2 \end{bmatrix} \succeq 0, \end{aligned}$$

which can be solved using off-the-shelf solvers in a tractable manner (see, e.g., [39]). It is worth mentioning that EMaC has a similar computational complexity as the atomic norm minimization method [26] when restricted to the 1-D frequency model.

Careful readers will remark that the performance of EMaC must depend on the choices of the pencil parameters k_1 and k_2 . In fact, if we define a quantity

$$c_s := \max \left(\frac{n_1 n_2}{k_1 k_2}, \frac{n_1 n_2}{(n_1 - k_1 + 1)(n_2 - k_2 + 1)} \right) \quad (14)$$

that measures how close \mathbf{X}_e is to a square matrix, then it will be shown later that the required sample complexity for faithful recovery is an increasing function of c_s . In fact, both our theory and empirical experience are in favor of a small c_s , corresponding to the choices $k_1 = \Theta(n_1)$, $n_1 - k_1 + 1 = \Theta(n_1)$, $k_2 = \Theta(n_2)$, and $n_2 - k_2 + 1 = \Theta(n_2)$.

2.4 The Noisy-EMaC Algorithm with Bounded Noise

In practice, measurements are contaminated by a certain amount of noise. To make our model and algorithm more practically applicable, we replace our measurements by $\mathbf{X}^\circ = [X_{k,l}^\circ]_{0 \leq k < n_1, 0 \leq l < n_2}$ through the following noisy model

$$X_{k,l}^\circ = X_{k,l} + N_{k,l}, \quad \forall (k, l) \in \Omega, \quad (15)$$

where $X_{k,l}^\circ$ is the observed (k, l) -th entry, and $\mathbf{N} = [N_{k,l}]_{0 \leq k < n_1, 0 \leq l < n_2}$ denotes some unknown noise. We assume that the noise magnitude is bounded by a known amount $\|\mathcal{P}_\Omega(\mathbf{N})\|_F \leq \delta$, where $\|\cdot\|_F$ denotes the Frobenius norm. In order to adapt our algorithm to such noisy measurements, one wishes that small perturbation in the measurements should result in small variation in the estimate. Our algorithm is then modified as follows

$$\begin{aligned} \text{(Noisy-EMaC)} : & \underset{\mathbf{M} \in \mathbb{C}^{n_1 \times n_2}}{\text{minimize}} && \|\mathbf{M}_e\|_* \\ & \text{subject to} && \|\mathcal{P}_\Omega(\mathbf{M} - \mathbf{X}^\circ)\|_F \leq \delta. \end{aligned} \quad (16)$$

That said, the algorithm searches for a candidate with minimum nuclear norm among all signals close to the measurements.

2.5 The Robust-EMaC Algorithm with Sparse Outliers

An outlier is a data sample that can deviate arbitrarily from the true data point. Practical data samples one collects may contain a certain portion of outliers due to abnormal behavior of data acquisition devices such as amplifier saturation, sensor failures, and malicious attacks. A desired recovery algorithm should be able to automatically prune all outliers even when they corrupt up to a constant portion of all data samples.

Specifically, suppose that our measurements \mathbf{X}° are given by

$$X_{k,l}^\circ = X_{k,l} + S_{k,l}, \quad \forall (k, l) \in \Omega, \quad (17)$$

where $X_{k,l}^\circ$ is the observed (k, l) -th entry, and $\mathbf{S} = [S_{k,l}]_{0 \leq k < n_1, 0 \leq l < n_2}$ denotes the outliers, which is assumed to be a sparse matrix supported on some location set $\Omega^{\text{dirty}} \subseteq \Omega$. We assume that the sparsity pattern of \mathbf{S} is selected uniformly at random conditioned on Ω . The sampling model is formally described as follows.

1. Suppose that Ω is obtained by sampling m entries uniformly at random, and define $\rho := \frac{m}{n_1 n_2}$.

2. Conditioning on $(k, l) \in \Omega$, the events $\{(k, l) \in \Omega^{\text{dirty}}\}$ are independent with conditional probability

$$\mathbb{P}\{(k, l) \in \Omega^{\text{dirty}} \mid (k, l) \in \Omega\} = s$$

for some small constant corruption fraction $0 < s < 1$.

3. Define $\Omega^{\text{clean}} := \Omega \setminus \Omega^{\text{dirty}}$ as the location set of *uncorrupted* measurements.

EMaC is then modified as follows to accommodate sparse outliers:

$$\begin{aligned} (\text{Robust-EMaC}) \quad & \underset{\mathbf{M}, \hat{\mathbf{S}} \in \mathbb{C}^{n_1 \times n_2}}{\text{minimize}} \quad \|\mathbf{M}_e\|_* + \lambda \|\hat{\mathbf{S}}_e\|_1 \\ & \text{subject to} \quad \mathcal{P}_\Omega(\mathbf{M} + \hat{\mathbf{S}}) = \mathcal{P}_\Omega(\mathbf{X} + \mathbf{S}), \end{aligned} \quad (18)$$

where $\lambda > 0$ is a regularization parameter that will be specified later. \mathbf{M}_e and $\hat{\mathbf{S}}_e$ denote the enhanced form of \mathbf{M} and $\hat{\mathbf{S}}$, respectively. Here, $\|\hat{\mathbf{S}}_e\|_1 := \|\text{vec}(\hat{\mathbf{S}}_e)\|_1$ denotes the elementwise ℓ_1 -norm of $\hat{\mathbf{S}}_e$. Robust-EMaC promotes the low-rank structure of the enhanced data matrix as well as the sparsity of the outliers via convex relaxation with respective structures.

2.6 Notations

Before continuing, we introduce a few notations that will be used throughout. Let the singular value decomposition (SVD) of \mathbf{X}_e be $\mathbf{X}_e = \mathbf{U}\mathbf{\Lambda}\mathbf{V}^*$. Denote by

$$T := \left\{ \mathbf{U}\mathbf{M}^* + \tilde{\mathbf{M}}\mathbf{V}^* : \mathbf{M} \in \mathbb{C}^{(n_1-k_1+1)(n_2-k_1+1) \times r}; \tilde{\mathbf{M}} \in \mathbb{C}^{k_1 k_2 \times r} \right\}$$

the tangent space with respect to \mathbf{X}_e , and T^\perp the orthogonal complement of T . Denote by \mathcal{P}_U (resp. \mathcal{P}_V , \mathcal{P}_T) the orthogonal projections onto the column (resp. row, tangent) space of \mathbf{X}_e , i.e. for any \mathbf{M}

$$\mathcal{P}_U \mathbf{M} = \mathbf{U}\mathbf{U}^* \mathbf{M}; \mathcal{P}_V \mathbf{M} = \mathbf{M}\mathbf{V}\mathbf{V}^*; \mathcal{P}_T = \mathcal{P}_U + \mathcal{P}_V - \mathcal{P}_U \mathcal{P}_V.$$

We let $\mathcal{P}_{T^\perp} = \mathcal{I} - \mathcal{P}_T$ be the orthogonal complement of \mathcal{P}_T , where \mathcal{I} denotes the identity operator.

Denote by $\|\mathbf{M}\|$, $\|\mathbf{M}\|_F$ and $\|\mathbf{M}\|_*$ the spectral norm (operator norm), Frobenius norm, and nuclear norm of \mathbf{M} , respectively. Also, $\|\mathbf{M}\|_1$ and $\|\mathbf{M}\|_\infty$ are defined to be the elementwise ℓ_1 and ℓ_∞ norm of \mathbf{M} . Denote by \mathbf{e}_i the i th standard basis vector. Additionally, we use $\text{sgn}(\mathbf{M})$ to denote the elementwise complex sign of \mathbf{M} .

On the other hand, we denote by $\Omega_e(k, l)$ the set of locations of the enhanced matrix \mathbf{X}_e containing copies of $X_{k,l}$. Due to the Hankel and multi-fold Hankel structures, one can easily verify the following: for any $\Omega_e(k, l)$, there exists at most one index in any given row of the enhanced form, and at most one index in any given column. For each $(k, l) \in [n_1] \times [n_2]$, we use $\mathbf{A}_{(k,l)}$ to denote a basis matrix that extracts the average of all entries in $\Omega_e(k, l)$. Specifically,

$$(\mathbf{A}_{(k,l)})_{\alpha,\beta} := \begin{cases} \frac{1}{\sqrt{|\Omega_e(k,l)|}}, & \text{if } (\alpha, \beta) \in \Omega_e(k, l), \\ 0, & \text{else.} \end{cases} \quad (19)$$

We will use $\omega_{k,l} := |\Omega_e(k, l)|$ as a short-hand notation.

3 Main Results

This section delivers the following encouraging news: under mild incoherence conditions, EMaC enables faithful signal recovery from a small number of time-domain samples, even when the samples are contaminated by bounded noise and a constant portion of arbitrary outliers.

3.1 Incoherence Measure

In general, matrix completion from a few entries is hopeless unless the underlying structure is uncorrelated with the observation basis. This inspires us to introduce certain incoherence measures. To this end, we define the 2-D Dirichlet kernel as

$$\mathcal{D}(k_1, k_2, \mathbf{f}) := \frac{1}{k_1 k_2} \left(\frac{1 - e^{-j2\pi k_1 f_1}}{1 - e^{-j2\pi f_1}} \right) \left(\frac{1 - e^{-j2\pi k_2 f_2}}{1 - e^{-j2\pi f_2}} \right), \quad (20)$$

where $\mathbf{f} = (f_1, f_2) \in [-1/2, 1/2]^2$. Fig. 1 (a) illustrates the amplitude of $\mathcal{D}(k_1, k_2, \mathbf{f})$ when $k_1 = k_2 = 6$. The value of $|\mathcal{D}(k_1, k_2, \mathbf{f})|$ decays inverse proportionally with respect to the frequency \mathbf{f} . Set \mathbf{G}_L and \mathbf{G}_R to be two $r \times r$ Gram matrices such that their entries are given respectively by

$$\begin{aligned} (\mathbf{G}_L)_{i,l} &= \mathcal{D}(k_1, k_2, \mathbf{f}_i - \mathbf{f}_l), \\ (\mathbf{G}_R)_{i,l} &= \mathcal{D}(n_1 - k_1 + 1, n_2 - k_2 + 1, \mathbf{f}_i - \mathbf{f}_l), \end{aligned}$$

where the difference $\mathbf{f}_i - \mathbf{f}_l$ is understood as the wrap-around distance in the interval $[-1/2, 1/2]^2$. Simple manipulation reveals that

$$\mathbf{G}_L = \mathbf{E}_L^* \mathbf{E}_L, \quad \mathbf{G}_R = (\mathbf{E}_R \mathbf{E}_R^*)^\top,$$

where \mathbf{E}_L and \mathbf{E}_R are defined in (11).

The incoherence measure is defined as follows.

Definition 1. [*Incoherence*] The incoherence measure of the data matrix \mathbf{X} is defined as μ_1 if

$$\sigma_{\min}(\mathbf{G}_L) \geq \frac{1}{\mu_1} \quad \text{and} \quad \sigma_{\min}(\mathbf{G}_R) \geq \frac{1}{\mu_1}. \quad (21)$$

where $\sigma_{\min}(\mathbf{G}_L)$ and $\sigma_{\min}(\mathbf{G}_R)$ represent the least singular values of \mathbf{G}_L and \mathbf{G}_R , respectively.

The incoherence measure μ_1 only depends on the locations of the frequency spikes, irrespective of their amplitudes. As will be shown later, we would like μ_1 to behave as a small number, which occurs when \mathbf{G}_L and \mathbf{G}_R are both well-conditioned. Our incoherence measure naturally requires certain separation among all frequency pairs, as when two frequency spikes are closely located, μ_1 gets undesirably large. However, it does not impose a strict separation condition among all frequency pairs (i.e. minimum frequency spacing exceeds $4/n$) as required in [26] and is thereby applicable to a broader class of spectrally sparse signals.

To give the reader a flavor of the incoherence condition, we list two examples below. For ease of presentation, we assume below 2-D frequency models with $n_1 = n_2$. Note, however, that the asymmetric cases and general K -D frequency models can be analyzed in the same manner.

- *Random frequency locations*: suppose that the r frequencies are generated uniformly at random, then the minimum pairwise separation can be crudely bounded by $\Theta\left(\frac{1}{r^2 \log n_1}\right)$. If $n_1 \gg r^{2.5} \log n_1$, then a crude bound reveals that

$$\max \left\{ \frac{1}{k_1} \frac{1 - (y_{i_1}^* y_{i_2})^{k_1}}{1 - y_{i_1}^* y_{i_2}}, \frac{1}{k_2} \frac{1 - (z_{i_1}^* z_{i_2})^{k_2}}{1 - z_{i_1}^* z_{i_2}} \right\} \ll \frac{1}{\sqrt{r}}, \quad \forall i_1 \neq i_2,$$

indicating that the off-diagonal entries of \mathbf{G}_L and \mathbf{G}_R are much smaller than $1/r$ in magnitude. Simple manipulation then allows us to conclude that $\sigma_{\min}(\mathbf{G}_L)$ and $\sigma_{\min}(\mathbf{G}_R)$ are bounded below by positive constants. Fig. 1 (b) shows the minimum eigenvalue of \mathbf{G}_L for different $k = k_1 = k_2 = 6, 36, 72$ when the spikes are randomly generated and the number of spikes is given as the sparsity level. The minimum eigenvalue of \mathbf{G}_L gets closer to one as k grows, confirming our argument.

- *Small perturbation off the grid*: suppose that all frequencies are within a distance at most $\frac{1}{n_1 r^{1/4}}$ from some grid points $\left(\frac{l_1}{k_1}, \frac{l_2}{k_2}\right)$ ($0 \leq l_1 < k_1, 0 \leq l_2 < k_2$). One can verify that

$$\max \left\{ \frac{1}{k_1} \frac{1 - (y_{i_1}^* y_{i_2})^{k_1}}{1 - y_{i_1}^* y_{i_2}}, \frac{1}{k_2} \frac{1 - (z_{i_1}^* z_{i_2})^{k_2}}{1 - z_{i_1}^* z_{i_2}} \right\} < \frac{1}{2\sqrt{r}}, \quad \forall i_1 \neq i_2,$$

and hence the magnitude of all off-diagonal entries of \mathbf{G}_L and \mathbf{G}_R are no larger than $1/(4r)$. This immediately suggests that $\sigma_{\min}(\mathbf{G}_L)$ and $\sigma_{\min}(\mathbf{G}_R)$ are lower bounded by $3/4$.

Note, however, that the class of incoherent signals are far beyond the ones discussed above.

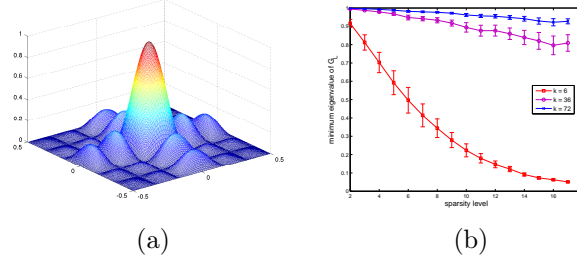


Figure 1: (a) The 2-D Dirichlet kernel when $k = k_1 = k_2 = 6$; (b) The empirical distribution of the minimum eigenvalue $\sigma_{\min}(\mathbf{G}_L)$ for various choices of k with respect to the sparsity level.

3.2 Theoretical Guarantees

With the above incoherence measure, the main theoretical guarantees are provided in the following three theorems each accounting for a distinct data model: 1) noiseless measurements, 2) measurements contaminated by bounded noise, and 3) measurements corrupted by a constant proportion of arbitrary outliers.

3.2.1 Exact Recovery from Noiseless Measurements

Exact recovery is possible from a minimal number of noise-free samples, as asserted in the following theorem.

Theorem 1. *Let \mathbf{X} be a data matrix of form (3), and Ω the random location set of size m . Suppose that the incoherence property (21) holds and that all measurements are noiseless. Then there exists a universal constant $c_1 > 0$ such that \mathbf{X} is the unique solution to EMaC with probability exceeding $1 - (n_1 n_2)^{-2}$, provided that*

$$m > c_1 \mu_1 c_s r \log^3(n_1 n_2). \quad (22)$$

Remark 1. Theorem 1 significantly strengthens our prior results reported in [40] by improving the required sample complexity from $\mathcal{O}(\mu_1^2 c_s^2 r^2 \text{poly} \log(n_1 n_2))$ to $\mathcal{O}(\mu_1 c_s r \text{poly} \log(n_1 n_2))$.

Theorem 1 asserts that under some mild *deterministic* incoherence condition such that μ_1 scales as a small constant, EMaC admits perfect recovery as soon as the number of measurements exceeds $\mathcal{O}(r \log^3(n_1 n_2))$. Since there are $\Theta(r)$ degrees of freedom in total, the lower bound should be no smaller than $\Theta(r)$. This demonstrates the orderwise optimality of EMaC except for a logarithmic gap. We note, however, that the polylog factor might be further refined via finer tuning of concentration of measure inequalities.

It is worth emphasizing that while we assume random observation models, the data model is assumed deterministic. This differs significantly from [26], which relies on randomness in both the observation model and the data model. In particular, our theoretical performance guarantees rely solely on the frequency locations irrespective of the associated amplitudes. In contrast, the results in [26] require the phases of all frequency spikes to be i.i.d. drawn in a uniform manner in addition to a separation condition.

3.2.2 Stable Recovery in the Presence of Bounded Noise

Our method enables stable recovery even when the time domain samples are noisy copies of the true data. Here, we say the recovery is stable if the solution of Noisy-EMaC is “close” to the ground truth. To this end, we provide the following theorem, which is a counterpart of Theorem 1 in the noisy setting, whose proof is inspired by [41].

Theorem 2. Suppose \mathbf{X}° is a noisy copy of \mathbf{X} that satisfies $\|\mathcal{P}_\Omega(\mathbf{X} - \mathbf{X}^\circ)\|_F \leq \delta$. Under the conditions of Theorem 1, the solution to Noisy-EMaC in (16) satisfies

$$\|\hat{\mathbf{X}}_e - \mathbf{X}_e\|_F \leq \left\{ 2\sqrt{n_1 n_2} + 8n_1 n_2 + \frac{8\sqrt{2}n_1^2 n_2^2}{m} \right\} \delta \quad (23)$$

with probability exceeding $1 - (n_1 n_2)^{-2}$.

Proof. See Appendix L. □

Theorem 2 reveals that the recovered enhanced matrix (which contains $\Theta(n_1^2 n_2^2)$ entries) is close to the true enhanced matrix at high signal-to-noise ratio. In particular, the average entry inaccuracy of the enhance matrix is bounded above by $\mathcal{O}(\frac{n_1 n_2}{m}\delta)$, amplified by the subsampling factor. In practice, one is interested in an estimate of \mathbf{X} , which can be obtained naively by randomly selecting an entry in $\Omega_e(k, l)$ as $\hat{X}_{k,l}$, then we have

$$\|\hat{\mathbf{X}} - \mathbf{X}\|_F \leq \|\hat{\mathbf{X}}_e - \mathbf{X}_e\|_F.$$

This yields that the per-entry noise of $\hat{\mathbf{X}}$ is about $\mathcal{O}(\frac{(n_1 n_2)^{3/2}}{m}\delta)$, which is further amplified due to enhancement by a factor of $n_1 n_2$. However, this factor arises from an analysis artifact due to our simple strategy to deduce $\hat{\mathbf{X}}$ from $\hat{\mathbf{X}}_e$, and may be elevated. We note that in numerical experiments, Noisy-EMaC usually generates much better estimates, usually by a polynomial factor. The practical applicability will be illustrated in Section 5.

It is worth mentioning that to the best of our knowledge, our result is the first stability result with partially observed data for spectral compressed sensing off the grid. While the atomic norm approach is near-minimax with full data [42], it is not clear how it performs with partially observed data.

3.2.3 Robust Recovery in the Presence of Sparse Outliers

Interestingly, Robust-EMaC can provably tolerate a constant portion of arbitrary outliers. The theoretical performance is formally summarized in the following theorem.

Theorem 3. Let \mathbf{X} be a data matrix with matrix form (3), and Ω a random location set of size m . Set $\lambda = \frac{1}{\sqrt{m \log(n_1 n_2)}}$, and assume $s \leq 0.1$ is some small positive constant. Then there exist a numerical constant $c_1 > 0$ depending only on s such that if (21) holds and

$$m > c_1 \mu_1^2 c_s^2 r^2 \log^3(n_1 n_2), \quad (24)$$

then Robust-EMaC is exact, i.e. the minimizer $(\hat{\mathbf{M}}, \hat{\mathbf{S}})$ satisfies $\hat{\mathbf{M}} = \mathbf{X}$, with probability exceeding $1 - (n_1 n_2)^{-2}$.

Theorem 3 specifies a candidate choice of the regularization parameter λ that allows recovery from a few samples, which only depends on the size of Ω but is otherwise parameter-free. In practice, however, λ may better be selected via cross validation. Furthermore, Theorem 3 demonstrates the possibility of robust recovery under a constant proportion of sparse corruptions. Under the same mild incoherence condition as for Theorem 1, robust recovery is possible from $\mathcal{O}(r^2 \log^3(n_1 n_2))$ samples, even when a constant proportion of the samples are arbitrarily corrupted.

3.3 Extension to Higher-Dimensional and Damping Frequency Models

By letting $n_2 = 1$ the above 2-D frequency model reverts to the line spectrum model. The EMaC algorithm also extends to higher dimensional frequency models without difficulty. In fact, for K -dimensional frequency models, one can arrange the original data into a K -fold Hankel matrix of rank at most r . For instance, consider a 3-D model such that

$$X_{l_1, l_2, l_3} = \sum_{i=1}^r d_i y_i^{l_1} z_i^{l_2} w_i^{l_3}, \quad \forall (l_1, l_2, l_3) \in [n_1] \times [n_2] \times [n_3].$$

An enhanced form can be defined as a 3-fold Hankel matrix such that

$$\mathbf{X}_e := \begin{bmatrix} \mathbf{X}_{0,e} & \mathbf{X}_{1,e} & \cdots & \mathbf{X}_{n_3-k_3,e} \\ \mathbf{X}_{1,e} & \mathbf{X}_{2,e} & \cdots & \mathbf{X}_{n_3-k_3+1,e} \\ \vdots & \vdots & \ddots & \vdots \\ \mathbf{X}_{k_3-1,e} & \mathbf{X}_{k_1,e} & \cdots & \mathbf{X}_{n_3-1,e} \end{bmatrix},$$

where $\mathbf{X}_{i,e}$ denotes the 2-D enhanced form of the matrix consisting of all entries X_{l_1,l_2,l_3} obeying $l_3 = i$. One can verify that \mathbf{X}_e is of rank at most r , and can thereby apply EMaC on the 3-D enhanced form. To summarize, for K -dimensional frequency models, EMaC (resp. Noisy-EMaC, Robust-EMaC) searches over all K -fold Hankel matrices that are consistent with the measurements. The theoretical performance guarantees can be similarly extended defining the respective Dirichlet kernel in 3-D and the coherence measure. In fact, all our analysis can be extended to handle *damping* modes, when the frequencies are not of unit amplitude. We omit the details for conciseness.

4 Structured Matrix Completion

One problem closely related to our method is completion of multi-fold Hankel matrices from a small number of entries. While each spectrally sparse signal can be mapped to a low-rank multi-fold Hankel matrix, it is not clear whether all multi-fold Hankel matrices of rank r can be written as the enhanced form of a signal with spectral sparsity r . Therefore, one can think of recovery of multi-fold Hankel matrices as a more general problem than the spectral compressed sensing problem. Indeed, Hankel matrix completion has found numerous applications in system identification [43, 44], natural language processing [45], computer vision [46], magnetic resonance imaging [47], etc.

There has been several work concerning algorithms and numerical experiments for Hankel matrix completions [43, 44, 48]. However, to the best of our knowledge, there has been little theoretical guarantee that addresses directly Hankel matrix completion. Our analysis framework can be straightforwardly adapted to the general K -fold Hankel matrix completions. Below we present the performance guarantee for the two-fold Hankel matrix completion without loss of generality. Notice that we need to modify the definition of μ_1 as stated in the following theorem.

Theorem 4. *Consider a two-fold Hankel matrix \mathbf{X}_e of rank r . The bounds in Theorems 1, 2 and 3 continue to hold, if the incoherence μ_1 is defined as the smallest number that satisfies*

$$\max_{(k,l) \in [n_1] \times [n_2]} \{ \|\mathbf{U}\mathbf{U}^* \mathbf{A}_{(k,l)}\|_F^2, \|\mathbf{A}_{(k,l)} \mathbf{V}\mathbf{V}^*\|_F^2 \} \leq \frac{\mu_1 c_s r}{n_1 n_2}. \quad (25)$$

Condition (25) requires that the left and right singular vectors are sufficiently uncorrelated with the observation basis. In fact, condition (25) is a weaker assumption than (21).

It is worth mentioning that a low-rank Hankel matrix can often be converted to its low-rank Toeplitz counterpart, by reversely ordering all rows of the Hankel matrix. Both Hankel and Toeplitz matrices are effective forms that capture the underlying harmonic structures. Our results and analysis framework extend to low-rank Toeplitz matrix completion problem without difficulty.

5 Numerical Experiments

In this section, we present numerical examples to evaluate the performance of EMaC and its variants under different scenarios. We further examine the application of EMaC in image super resolution. Finally, we propose an extension of singular value thresholding (SVT) developed by Cai et. al. [49] that exploits the multi-fold Hankel structure to handle larger scale data sets.

5.1 Phase Transition in the Noiseless Setting

To evaluate the practical ability of the EMaC algorithm, we conducted a series of numerical experiments to examine the phase transition for exact recovery. Let $n_1 = n_2$, and we take $k_1 = k_2 = \lceil (n_1 + 1)/2 \rceil$

which corresponds to the smallest c_s . For each (r, m) pair, 100 Monte Carlo trials were conducted. We generated a spectrally sparse data matrix \mathbf{X} by randomly generating r frequency spikes in $[0, 1) \times [0, 1)$, and sampled a subset Ω of size m entries uniformly at random. The EMaC algorithm was conducted using the convex programming modeling software CVX with the interior-point solver SDPT3 [50]. Each trial is declared successful if the normalized mean squared error (NMSE) satisfies $\|\hat{\mathbf{X}} - \mathbf{X}\|_F / \|\mathbf{X}\|_F \leq 10^{-3}$, where $\hat{\mathbf{X}}$ denotes the estimate returned by EMaC. The empirical success rate is calculated by averaging over 100 Monte Carlo trials.

Fig. 2 illustrates the results of these Monte Carlo experiments when the dimensions of \mathbf{X} are 11×11 and 15×15 . The horizontal axis corresponds to the number m of samples revealed to the algorithm, while the vertical axis corresponds to the spectral sparsity level r . The empirical success rate is reflected by the color of each cell. It can be seen from the plot that the number of samples m grows approximately linearly with respect to the spectral sparsity r , and that the slopes of the phase transition lines for two cases are approximately the same. These observations are in line with our theoretical guarantee in Theorem 1. This phase transition diagrams justify the practical applicability of our algorithm in the noiseless setting.

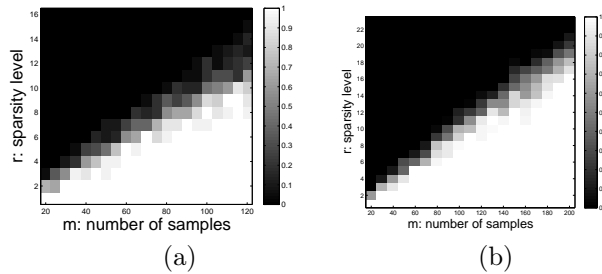


Figure 2: Phase transition plots where frequency locations are randomly generated. The plot (a) concerns the case where $n_1 = n_2 = 11$, whereas the plot (b) corresponds to the situation where $n_1 = n_2 = 15$. The empirical success rate is calculated by averaging over 100 Monte Carlo trials.

5.2 Stable Recovery from Noisy Data

Fig. 3 further examines the stability of the proposed algorithm by performing Noisy-EMaC with respect to different parameter δ on a noise-free dataset of $r = 4$ complex sinusoids with $n_1 = n_2 = 11$. The number of random samples is $m = 50$. The reconstructed NMSE grows approximately linear with respect to δ , validating the stability of the proposed algorithm.

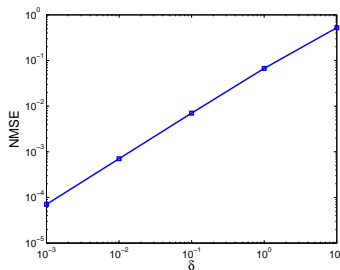


Figure 3: The reconstruction NMSE with respect to δ for a dataset with $n_1 = n_2 = 11$, $r = 4$ and $m = 50$.

5.3 Comparison with Existing Approaches for Line Spectrum Estimation

Suppose that we randomly observe 64 entries of an n -dimensional vector ($n = 127$) composed of $r = 4$ modes. For such 1-D signals, we compare EMaC with the atomic norm approach [26] as well as basis pursuit [51] assuming a grid of size 2^{12} . For the atomic norm and the EMaC algorithm, the modes are recovered via

linear prediction using the recovered data [52]. Fig. 4 demonstrates the recovery of mode locations for three cases, namely when (a) all the modes are on the DFT grid along the unit circle; (b) all the modes are on the unit circle except two closely located modes that are off the presumed grid; (c) all the modes are on the unit circle except that one of the two closely located modes is a damping mode with amplitude 0.99. In all cases, the EMaC algorithm successfully recovers the underlying modes, while the atomic norm approach fails to recover damping modes, and basis pursuit fails with both off-the-grid modes and damping modes.

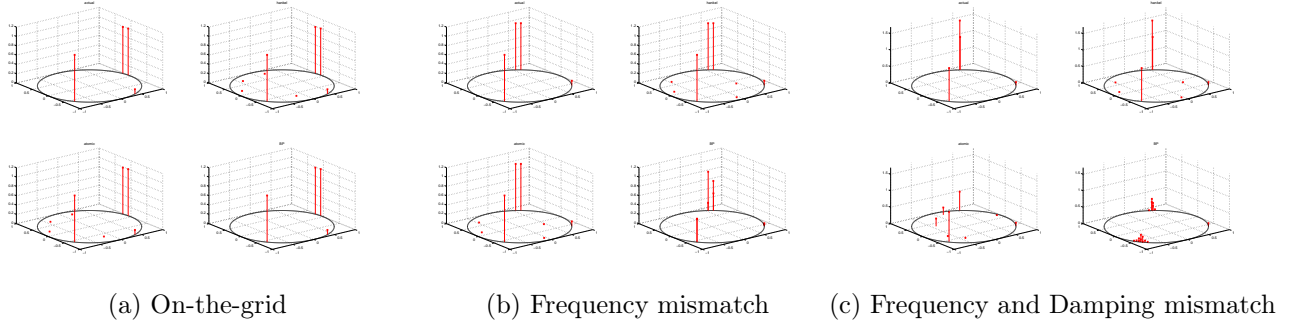
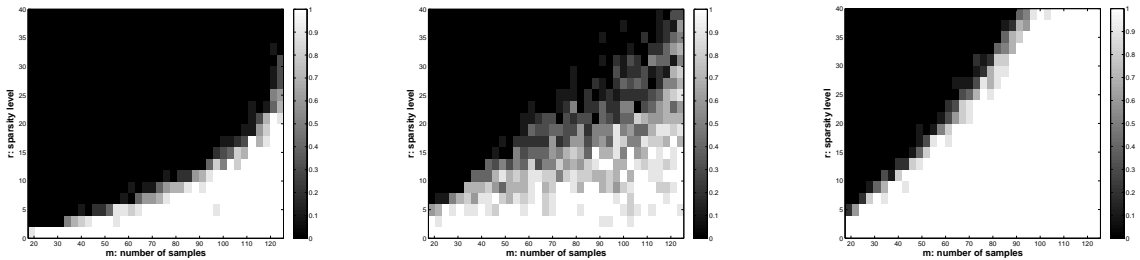


Figure 4: Recovery of mode locations when (a) all the modes are on the DFT grid along the unit circle; (b) all the modes are on the unit circle except two closely located modes that are off the DFT grid; (c) all the modes are on the unit circle except that one of the two closely located modes is a damping mode. The panels from the upper left, clockwise, are the ground truth, the EMaC algorithm, the atomic norm approach [26], and basis pursuit [51] assuming a grid of size 2^{12} .

We further compare the phase transition of the EMaC algorithm and the atomic norm approach in [26] for line spectrum estimation. We assume a 1-D signal of length $n = n_1 = 127$ and the pencil parameter k_1 of EMaC is chosen to be 64. The phase transition experiments are conducted in the same manner as Fig. 2. In the first case, the spikes are generated randomly as Fig. 2 on a unit circle; in the second case, the spikes are generated until a separation condition is satisfied $\Delta := \min_{i_1 \neq i_2} |f_{i_1} - f_{i_2}| \geq 1.5/n$. Fig. 5 (a) and (b) illustrate the phase transition of EMaC and the atomic norm approach when the frequencies are randomly generated without imposing the separation condition. The performance of the atomic norm approach degenerates severely when the separation condition is not met; on the other hand, the EMaC gives a sharp phase transition similar to the 2D case. When the separation condition is imposed, the phase transition of the atomic norm approach greatly improves as shown in Fig. 5 (c), while the phase transition of EMaC still gives similar performance as in Fig. 5 (a) (We omit the actual phase transition in this case.) However, it is worth mentioning that when the sparsity level is relatively high, the required separation condition is in general difficult to be satisfied in practice. In comparison, EMaC is less sensitive to the separation requirement.



(a) EMaC without separation (b) Atomic Norm without separation (c) Atomic Norm with separation

Figure 5: Phase transition for line spectrum estimation of EMaC and the atomic norm approach [26]. (a) EMaC without imposing separation; (b) atomic norm approach without imposing separation; (c) atomic norm approach with separation.

5.4 Robust Line Spectrum Estimation

Consider the problem of line spectrum estimation, where the time domain measurements are contaminated by a constant portion of outliers. We conducted a series of Monte Carlo trials to illustrate the phase transition for perfect recovery of the ground truth. The true data \mathbf{X} is assumed to be a 125-dimensional vector, where the locations of the underlying frequencies are randomly generated. The simulations were carried out again using CVX with SDPT3.

Fig. 6(a) illustrates the phase transition for robust line spectrum estimation when 10% of the entries are corrupted, which showcases the tradeoff between the number m of measurements and the recoverable spectral sparsity level r . One can see from the plot that m is approximately linear in r on the phase transition curve even when 10% of the measurements are corrupted, which validates our finding in Theorem 3. Fig. 6(b) illustrates the success rate of exact recovery when we obtain samples for all entry locations. This plot illustrates the tradeoff between the spectral sparsity level and the number of outliers when all entries of the corrupted \mathbf{X}^o are observed. It can be seen that there is a large region where exact recovery can be guaranteed, demonstrating the power of our algorithms in the presence of sparse outliers.

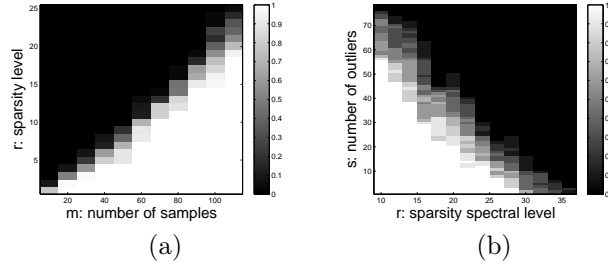


Figure 6: Robust line spectrum estimation where mode locations are randomly generated: (a) Phase transition plots when $n = 125$, and 10% of the entries are corrupted; the empirical success rate is calculated by averaging over 100 Monte Carlo trials. (b) Phase transition plots when $n = 125$, and all the entries are observed; the empirical success rate is calculated by averaging over 20 Monte Carlo trials.

5.5 Synthetic Super Resolution

The proposed EMaC algorithm works beyond the random observation model in Theorem 1. Fig. 7 considers a synthetic super resolution example motivated by [24], where the ground truth in Fig. 7(a) contains 6 point sources with constant amplitude. The low-resolution observation in Fig. 7(b) is obtained by measuring low-frequency components $[-f_{lo}, f_{lo}]$ of the ground truth. Due to the large width of the associated point-spread function, both the locations and amplitudes of the point sources are distorted in the low-resolution image.

We apply EMaC to extrapolate high-frequency components up to $[-f_{hi}, f_{hi}]$, where $f_{hi}/f_{lo} = 2$. The reconstruction in Fig. 7(c) is obtained via applying directly inverse Fourier transform of the spectrum to avoid parameter estimation such as the number of modes. The resolution is greatly enhanced from Fig. 7(b), suggesting that EMaC is a promising approach for super resolution tasks. The theoretical performance is left for future work.

5.6 Singular Value Thresholding for EMaC

The above Monte Carlo experiments were conducted using the advanced SDP solver SDPT3. This solver and many other popular ones (e.g. SeDuMi) are based on interior point methods, which are typically inapplicable to large-scale data. In fact, SDPT3 fails to handle an $n \times n$ data matrix when n exceeds 19, which corresponds to a 100×100 enhanced matrix.

One alternative for large-scale data is the first-order algorithms tailored to matrix completion problems, e.g. the singular value thresholding (SVT) algorithm [49]. We propose a modified SVT algorithm in Algorithm 1 to exploit the Hankel structure.

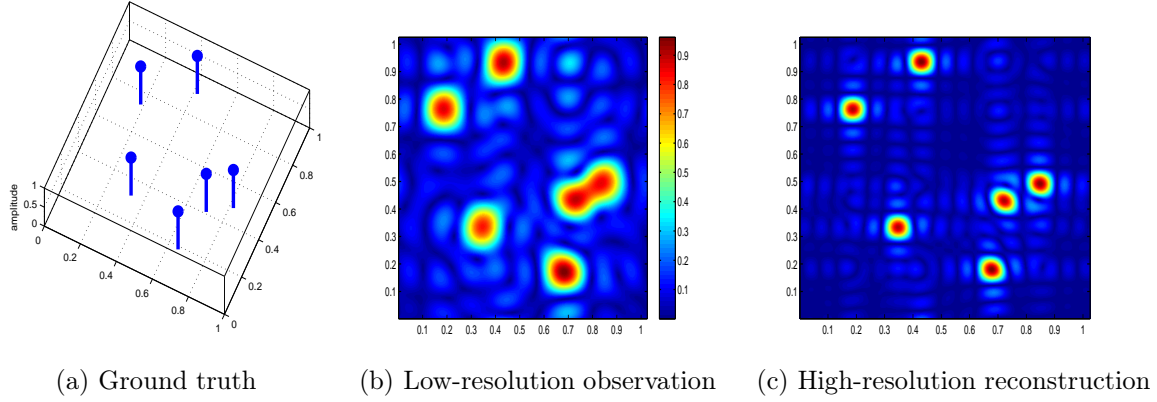


Figure 7: A synthetic super resolution example, where the observation (b) is taken from the low-frequency components of the ground truth in (a), and the reconstruction (c) is done via inverse Fourier transform of the extrapolated high-frequency components.

Algorithm 1 Singular Value Thresholding for EMaC.

Input: The observed data matrix \mathbf{X}° on the location set Ω .

initialize: let \mathbf{X}_e° denote the enhanced form of $\mathcal{P}_\Omega(\mathbf{X}^\circ)$;

set $\mathbf{M}_0 = \mathbf{X}_e^\circ$ and $t = 0$.

repeat

1) $\mathbf{Q}_t \leftarrow \mathcal{D}_{\tau_t}(\mathbf{M}_t)$

2) $\mathbf{M}_t \leftarrow \mathcal{H}_{\mathbf{X}^\circ}(\mathbf{Q}_t)$

3) $t \leftarrow t + 1$

until convergence

output $\hat{\mathbf{X}}$ as the data matrix with enhanced form \mathbf{M}_t .

In particular, two operators are defined as follows:

- $\mathcal{D}_{\tau_t}(\cdot)$ in Algorithm 1 denotes the singular value shrinkage operator. Specifically, if the SVD of \mathbf{X} is given by $\mathbf{X} = \mathbf{U}\mathbf{\Sigma}\mathbf{V}^*$ with $\mathbf{\Sigma} = \text{diag}(\{\sigma_i\})$, then

$$\mathcal{D}_{\tau_t}(\mathbf{X}) := \mathbf{U} \text{diag}(\{(\sigma_i - \tau_t)_+\}) \mathbf{V}^*,$$

where $\tau_t > 0$ is the soft-thresholding level.

- In the K -dimensional frequency model, $\mathcal{H}_{\mathbf{X}^\circ}(\mathbf{Q}_t)$ denotes the projection of \mathbf{Q}_t onto the subspace of enhanced matrices (i.e. K -fold Hankel matrices) that are consistent with the observed entries.

Consequently, at each iteration, a pair $(\mathbf{Q}_t, \mathbf{M}_t)$ is produced by first performing singular value shrinkage and then projecting the outcome onto the space of K -fold Hankel matrices that are consistent with observed entries.

The key parameter that one needs to tune is the threshold τ_t . Unfortunately, there is no universal consensus regarding how to tweak the threshold for SVT type of algorithms. One suggested choice is $\tau_t = 0.1\sigma_{\max}(\mathbf{M}_t) / \lceil \frac{t}{10} \rceil$, which works well based on our empirical experiments.

Fig. 8 illustrates the performance of Algorithm 1. We generated a true 101×101 data matrix \mathbf{X} through a superposition of 30 random complex sinusoids, and revealed 5.8% of the total entries (i.e. $m = 600$) uniformly at random. The noise was i.i.d. Gaussian giving a signal-to-noise amplitude ratio of 10. The reconstructed vectorized signal is superimposed on the ground truth in Fig. 8. The normalized reconstruction error was $\|\hat{\mathbf{X}} - \mathbf{X}\|_F / \|\mathbf{X}\|_F = 0.1098$, validating the stability of our algorithm in the presence of noise.

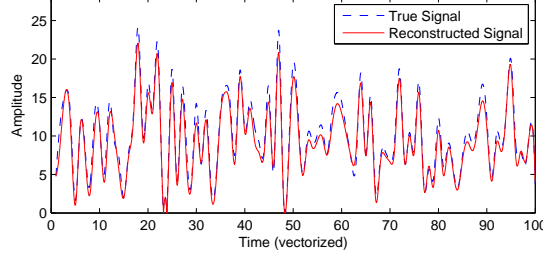


Figure 8: The performance of SVT for Noisy-EMaC for a 101×101 data matrix that contains 30 random frequency spikes. 5.8% of all entries ($m = 600$) are observed with signal-to-noise amplitude ratio 10. Here, $\tau_t = 0.1\sigma_{\max}(\mathbf{M}_t) / \lceil \frac{t}{10} \rceil$ empirically. For concreteness, the reconstructed data against the true data for the first 100 time instances (after vectorization) are plotted.

6 Proof of Theorems 1 and 4

EMaC has similar spirit as the well-known matrix completion algorithms [27, 30], except that we impose Hankel and multi-fold Hankel structures on the matrices. While [30] has presented a general sufficient condition for exact recovery (see [30, Theorem 3]), the basis in our case does not exhibit desired coherence properties as required in [30], and hence these results cannot deliver informative estimates when applied to our problem. Nevertheless, the beautiful golfing scheme introduced in [30] lays the foundation of our analysis in the sequel. We also note that the analyses adopted in [27, 30] rely on a desired joint incoherence property on \mathbf{UV}^* , which was recently shown to be unnecessary [31]. The analysis framework presented here is inspired by [31].

For concreteness, the analysis in this paper focuses on recovering harmonically sparse signals as stated in Theorem 1, since proving Theorem 1 is slightly more involved than proving Theorem 4. We note, however, that our analysis already entails all reasoning required for establishing Theorem 4.

6.1 Dual Certification

Denote by $\mathcal{A}_{(k,l)}(\mathbf{M})$ the projection of \mathbf{M} onto the subspace spanned by $\mathbf{A}_{(k,l)}$, and define the projection operator onto the space spanned by all $\mathbf{A}_{(k,l)}$ and its orthogonal complement as

$$\mathcal{A} := \sum_{(k,l) \in [n_1] \times [n_2]} \mathcal{A}_{(k,l)}, \quad \text{and} \quad \mathcal{A}^\perp = \mathcal{I} - \mathcal{A}. \quad (26)$$

There are two common ways to describe the randomness of Ω : one corresponds to sampling *without* replacement, and another concerns sampling *with* replacement (i.e. Ω contains m indices $\{\mathbf{a}_i \in [n_1] \times [n_2] : 1 \leq i \leq m\}$ that are i.i.d. generated). As discussed in [30, Section II.A], while both situations result in the same order-wise bounds, the latter situation admits simpler analysis due to independence. Therefore, we will assume that Ω is a multi-set (possibly with repeated elements) and \mathbf{a}_i 's are independently and uniformly distributed throughout the proofs of this paper, and define the associated operators as

$$\mathcal{A}_\Omega := \sum_{i=1}^m \mathcal{A}_{\mathbf{a}_i}. \quad (27)$$

We also define another projection operator \mathcal{A}'_Ω similar to (27), but with the sum extending only over *distinct* samples. Its complement operator is defined as $\mathcal{A}'_{\Omega^\perp} := \mathcal{A} - \mathcal{A}'_\Omega$. Note that $\mathcal{A}_\Omega(\mathbf{M}) = 0$ is equivalent to $\mathcal{A}'_\Omega(\mathbf{M}) = 0$. With these definitions, EMaC can be rewritten as the following general matrix completion problem:

$$\begin{aligned} & \underset{\mathbf{M}}{\text{minimize}} && \|\mathbf{M}\|_* \\ & \text{subject to} && \mathcal{A}'_\Omega(\mathbf{M}) = \mathcal{A}'_\Omega(\mathbf{X}_e), \\ & && \mathcal{A}^\perp(\mathbf{M}) = \mathcal{A}^\perp(\mathbf{X}_e) = 0. \end{aligned} \quad (28)$$

To prove exact recovery of convex optimization, it suffices to produce an appropriate dual certificate, as stated in the following lemma.

Lemma 1. *Consider a multi-set Ω that contains m random indices. Suppose that the sampling operator \mathcal{A}_Ω obeys*

$$\left\| \mathcal{P}_T \mathcal{A} \mathcal{P}_T - \frac{n_1 n_2}{m} \mathcal{P}_T \mathcal{A}_\Omega \mathcal{P}_T \right\| \leq \frac{1}{2}. \quad (29)$$

If there exists a matrix \mathbf{W} satisfying

$$\mathcal{A}'_{\Omega^\perp}(\mathbf{W}) = 0, \quad (30)$$

$$\|\mathcal{P}_T(\mathbf{W} - \mathbf{U}\mathbf{V}^*)\|_F \leq \frac{1}{2n_1^2 n_2^2}, \quad (31)$$

and

$$\|\mathcal{P}_{T^\perp}(\mathbf{W})\| \leq \frac{1}{2}, \quad (32)$$

then \mathbf{X}_e is the unique solution to (28) or, equivalently, \mathbf{X} is the unique minimizer of EMaC.

Proof. See Appendix B. □

Condition (29) will be analyzed in Section 6.2, while a dual certificate \mathbf{W} will be constructed in Section 6.3. The validity of \mathbf{W} as a dual certificate will be established in Sections 6.3 - 6.5. These are the focus of the remaining section.

6.2 Deviation of $\left\| \mathcal{P}_T \mathcal{A} \mathcal{P}_T - \frac{n_1 n_2}{m} \mathcal{P}_T \mathcal{A}_\Omega \mathcal{P}_T \right\|$

Lemma 1 requires that \mathcal{A}_Ω be sufficiently incoherent with respect to the tangent space T . The following lemma quantifies the projection of each $\mathbf{A}_{(k,l)}$ onto the subspace T .

Lemma 2. *Under the hypothesis (21), one has*

$$\|\mathbf{U}\mathbf{U}^* \mathbf{A}_{(k,l)}\|_F^2 \leq \frac{\mu_1 c_s r}{n_1 n_2}, \quad \|\mathbf{A}_{(k,l)} \mathbf{V}\mathbf{V}^*\|_F^2 \leq \frac{\mu_1 c_s r}{n_1 n_2}, \quad (33)$$

for all $(k, l) \in [n_1] \times [n_2]$. For any $\mathbf{a}, \mathbf{b} \in [n_1] \times [n_2]$, one has

$$|\langle \mathbf{A}_b, \mathcal{P}_T \mathbf{A}_a \rangle| \leq \sqrt{\frac{\omega_b}{\omega_a}} \frac{3\mu_1 c_s r}{n_1 n_2}. \quad (34)$$

Proof. See Appendix C. □

Recognizing that (33) is the same as (25), the following proof also establishes Theorem 4. Note that Lemma 2 immediately leads to

$$\|\mathcal{P}_T(\mathbf{A}_{(k,l)})\|_F^2 \leq \|\mathcal{P}_U(\mathbf{A}_{(k,l)})\|_F^2 + \|\mathcal{P}_V(\mathbf{A}_{(k,l)})\|_F^2 \leq \frac{2\mu_1 c_s r}{n_1 n_2}. \quad (35)$$

As long as (35) holds, the deviation of $\mathcal{P}_T \mathcal{A}_\Omega \mathcal{P}_T$ can be controlled reasonably well, as stated in the following lemma. This justifies Condition (29) as required by Lemma 1.

Lemma 3. *Suppose that (35) holds. Then for any small constant $0 < \epsilon \leq \frac{1}{2}$, one has*

$$\left\| \frac{n_1 n_2}{m} \mathcal{P}_T \mathcal{A}_\Omega \mathcal{P}_T - \mathcal{P}_T \mathcal{A} \mathcal{P}_T \right\| \leq \epsilon \quad (36)$$

with probability exceeding $1 - (n_1 n_2)^{-4}$, provided that $m > c_1 \mu_1 c_s r \log(n_1 n_2)$ for some universal constant $c_1 > 0$.

Proof. See Appendix D. □

6.3 Construction of Dual Certificate

Now we are in a position to construct the dual certificate, for which we will employ the golfing scheme introduced in [30]. Suppose that we generate j_0 independent random location multi-sets Ω_i ($1 \leq i \leq j_0$), each containing $\frac{m}{j_0}$ i.i.d. samples. This way the distribution of Ω is the same as $\Omega_1 \cup \Omega_2 \cup \dots \cup \Omega_{j_0}$. Note that Ω_i 's correspond to sampling *with* replacement. Let

$$\rho := \frac{m}{n_1 n_2} \quad \text{and} \quad q := \frac{\rho}{j_0} \quad (37)$$

represent the undersampling factors of Ω and Ω_i , respectively.

Consider a small constant $\epsilon < \frac{1}{e}$, and pick $j_0 := 3 \log_{\frac{1}{\epsilon}} n_1 n_2$. The construction of the dual matrix \mathbf{W} then proceeds as follows:

Construction of a dual certificate \mathbf{W} via the golfing scheme.

1. Set $\mathbf{F}_0 = \mathbf{U}\mathbf{V}^*$, and $j_0 := 5 \log_{\frac{1}{\epsilon}}(n_1 n_2)$.
 2. For all i ($1 \leq i \leq j_0$), let $\mathbf{F}_i = \mathcal{P}_T \left(\mathcal{A} - \frac{1}{q} \mathcal{A}_{\Omega_i} \right) \mathcal{P}_T(\mathbf{F}_{i-1})$.
 3. Set $\mathbf{W} := \sum_{j=1}^{j_0} \left(\frac{1}{q} \mathcal{A}_{\Omega_j} + \mathcal{A}^\perp \right) \mathbf{F}_{j-1}$.
-

We will establish that \mathbf{W} is a valid dual certificate by showing \mathbf{W} satisfies the conditions stated in Lemma 1, which we now proceed step by step.

First, by construction, all summands

$$\left(\frac{1}{q} \mathcal{A}_{\Omega_i} + \mathcal{A}^\perp \right) \mathbf{F}_{i-1}$$

lie within the subspace of matrices supported on Ω or the subspace \mathcal{A}^\perp . This validates that $\mathcal{A}'_{\Omega^\perp}(\mathbf{W}) = 0$, as required in (30).

Secondly, the recursive construction procedure of \mathbf{F}_i allows us to write

$$\begin{aligned} -\mathcal{P}_T(\mathbf{W} - \mathbf{F}_0) &= \mathcal{P}_T(\mathbf{F}_0) - \sum_{j=1}^{j_0} \mathcal{P}_T \left(\frac{1}{q} \mathcal{A}_{\Omega_j} + \mathcal{A}^\perp \right) \mathbf{F}_{j-1} \\ &= \mathcal{P}_T(\mathbf{F}_0) - \mathcal{P}_T \left(\frac{1}{q} \mathcal{A}_{\Omega_i} + \mathcal{A}^\perp \right) \mathcal{P}_T(\mathbf{F}_0) - \sum_{j=2}^{j_0} \mathcal{P}_T \left(\frac{1}{q} \mathcal{A}_{\Omega_j} + \mathcal{A}^\perp \right) \mathbf{F}_{j-1} \\ &= \mathcal{P}_T \left(\mathcal{A} - \frac{1}{q} \mathcal{A}_{\Omega_i} \right) \mathcal{P}_T(\mathbf{F}_0) - \sum_{j=2}^{j_0} \mathcal{P}_T \left(\frac{1}{q} \mathcal{A}_{\Omega_j} + \mathcal{A}^\perp \right) \mathbf{F}_{j-1} \\ &= \mathcal{P}_T(\mathbf{F}_1) - \sum_{j=2}^{j_0} \mathcal{P}_T \left(\frac{1}{q} \mathcal{A}_{\Omega_j} + \mathcal{A}^\perp \right) \mathbf{F}_{j-1} \\ &= \dots = \mathcal{P}_T(\mathbf{F}_{j_0}). \end{aligned} \quad (38)$$

Lemma 3 asserts the following: if $qn_1 n_2 \geq c_1 \mu_1 c_s r \log(n_1 n_2)$ or, equivalently, $m \geq \tilde{c}_1 \mu_1 c_s r \log^2(n_1 n_2)$, then with overwhelming probability one has

$$\left\| \mathcal{P}_T - \mathcal{P}_T \left(\frac{1}{q} \mathcal{A}_{\Omega_i} + \mathcal{A}^\perp \right) \mathcal{P}_T \right\| = \left\| \mathcal{P}_T \mathcal{A} \mathcal{P}_T - \frac{1}{q} \mathcal{P}_T \mathcal{A}_{\Omega_i} \mathcal{P}_T \right\| \leq \epsilon < \frac{1}{2}.$$

This allows us to bound $\|\mathcal{P}_T(\mathbf{F}_i)\|_F$ as

$$\|\mathcal{P}_T(\mathbf{F}_i)\|_F \leq \epsilon^i \|\mathcal{P}_T(\mathbf{F}_0)\|_F \leq \epsilon^i \|\mathbf{U}\mathbf{V}^*\|_F = \epsilon^i \sqrt{r},$$

which together with (38) gives

$$\|\mathcal{P}_T(\mathbf{W} - \mathbf{U}\mathbf{V}^*)\|_F = \|\mathcal{P}_T(\mathbf{W} - \mathbf{F}_0)\|_F = \|\mathcal{P}_T(\mathbf{F}_{j_0})\|_F \leq \epsilon^{j_0} \sqrt{r} < \frac{1}{2n_1^2 n_2^2} \quad (39)$$

as required in Condition (31).

Finally, it remains to be shown that $\|\mathcal{P}_{T^\perp}(\mathbf{W})\| \leq \frac{1}{2}$, which we will establish in the next two subsections. In particular, we first introduce two key metrics and characterize their relationships in Section 6.4. These metrics are crucial in bounding $\|\mathcal{P}_{T^\perp}(\mathbf{W})\|$, which will be the focus of Section 6.5.

6.4 Two Metrics and Key Lemmas

In this subsection, we introduce the following two norms

$$\|\mathbf{M}\|_{\mathcal{A},\infty} := \max_{(k,l) \in [n_1] \times [n_2]} \left| \frac{\langle \mathbf{A}_{(k,l)}, \mathbf{M} \rangle}{\sqrt{\omega_{k,l}}} \right|, \quad (40)$$

$$\|\mathbf{M}\|_{\mathcal{A},2} := \sqrt{\sum_{(k,l) \in [n_1] \times [n_2]} \frac{|\langle \mathbf{A}_{(k,l)}, \mathbf{M} \rangle|^2}{\omega_{k,l}}}. \quad (41)$$

Based on these two metrics, we can derive several technical lemmas which, taken collectively, allow us to control $\|\mathcal{P}_{T^\perp}(\mathbf{W})\|$. Specifically, these lemmas characterize the mutual dependence of three norms $\|\cdot\|$, $\|\cdot\|_{\mathcal{A},2}$ and $\|\cdot\|_{\mathcal{A},\infty}$.

Lemma 4. *For any given matrix \mathbf{M} , there exists some numerical constant $c_2 > 0$ such that*

$$\left\| \left(\frac{n_1 n_2}{m} \mathcal{A}_\Omega - \mathcal{A} \right) (\mathbf{M}) \right\| \leq c_2 \left(\sqrt{\frac{n_1 n_2 \log(n_1 n_2)}{m}} \|\mathbf{M}\|_{\mathcal{A},2} + \frac{n_1 n_2 \log(n_1 n_2)}{m} \|\mathbf{M}\|_{\mathcal{A},\infty} \right) \quad (42)$$

with probability at least $1 - (n_1 n_2)^{-10}$.

Proof. See Appendix E. □

Lemma 5. *Suppose that \mathbf{M} is fixed, and assume that there exists a quantity μ_5 such that*

$$\left\| \mathcal{P}_T(\omega_{\alpha,\beta} \mathbf{A}_{(\alpha,\beta)}) \right\|_{\mathcal{A},2}^2 \leq \frac{\mu_5 r}{n_1 n_2}, \quad (\alpha, \beta) \in [n_1] \times [n_2]. \quad (43)$$

Then with probability exceeding $1 - (n_1 n_2)^{-10}$, one has

$$\left\| \left(\frac{n_1 n_2}{m} \mathcal{P}_T \mathcal{A}_\Omega - \mathcal{P}_T \mathcal{A} \right) (\mathbf{M}) \right\|_{\mathcal{A},2} \leq c_3 \sqrt{\frac{\mu_5 r \log(n_1 n_2)}{m}} \left(\|\mathbf{M}\|_{\mathcal{A},2} + \sqrt{\frac{n_1 n_2 \log(n_1 n_2)}{m}} \|\mathbf{M}\|_{\mathcal{A},\infty} \right) \quad (44)$$

for some absolute constant $c_3 > 0$.

Proof. See Appendix F. □

Lemma 6. *For any given matrix $\mathbf{M} \in T$, there is some absolute constant $c_4 > 0$ such that*

$$\left\| \left(\frac{n_1 n_2}{m} \mathcal{P}_T \mathcal{A}_\Omega - \mathcal{P}_T \mathcal{A} \right) (\mathbf{M}) \right\|_{\mathcal{A},\infty} \leq c_4 \left(\sqrt{\frac{\mu_1 c_s r \log(n_1 n_2)}{m}} \cdot \sqrt{\frac{\mu_1 c_s r}{n_1 n_2}} \|\mathbf{M}\|_{\mathcal{A},2} + \frac{\mu_1 c_s r \log(n_1 n_2)}{m} \|\mathbf{M}\|_{\mathcal{A},\infty} \right) \quad (45)$$

with probability exceeding $1 - (n_1 n_2)^{-10}$.

Proof. See Appendix G. □

Lemma 5 combined with Lemma 6 gives rise to the following inequality. Consider any given matrix $\mathbf{M} \in T$. Applying the bounds (44) and (45), one can derive

$$\begin{aligned}
& \left\| \left(\frac{n_1 n_2}{m} \mathcal{P}_T \mathcal{A}_\Omega - \mathcal{P}_T \mathcal{A} \right) (\mathbf{M}) \right\|_{\mathcal{A},2} + \sqrt{\frac{n_1 n_2 \log(n_1 n_2)}{m}} \left\| \left(\frac{n_1 n_2}{m} \mathcal{P}_T \mathcal{A}_\Omega - \mathcal{P}_T \mathcal{A} \right) (\mathbf{M}) \right\|_{\mathcal{A},\infty} \\
& \leq c_3 \sqrt{\frac{\mu_5 r \log(n_1 n_2)}{m}} \left(\|\mathbf{M}\|_{\mathcal{A},2} + \sqrt{\frac{n_1 n_2 \log(n_1 n_2)}{m}} \|\mathbf{M}\|_{\mathcal{A},\infty} \right) + \\
& \quad c_4 \sqrt{\frac{n_1 n_2 \log(n_1 n_2)}{m}} \left(\sqrt{\frac{\mu_1 c_s r \log(n_1 n_2)}{m}} \cdot \sqrt{\frac{\mu_1 c_s r}{n_1 n_2}} \|\mathbf{M}\|_{\mathcal{A},2} + \frac{\mu_1 c_s r \log(n_1 n_2)}{m} \|\mathbf{M}\|_{\mathcal{A},\infty} \right) \\
& \leq c_5 \left(\sqrt{\frac{\mu_5 r \log(n_1 n_2)}{m}} + \frac{\mu_1 c_s r \log(n_1 n_2)}{m} \right) \left\{ \|\mathbf{M}\|_{\mathcal{A},2} + \sqrt{\frac{n_1 n_2 \log(n_1 n_2)}{m}} \|\mathbf{M}\|_{\mathcal{A},\infty} \right\}, \tag{46}
\end{aligned}$$

with probability exceeding $1 - (n_1 n_2)^{-10}$, where $c_5 = \max\{c_3, c_4\}$.

6.5 An Upper Bound on $\|\mathcal{P}_{T^\perp}(\mathbf{W})\|$

Now we are ready to show how we may combine the above lemmas to develop an upper bound on $\|\mathcal{P}_{T^\perp}(\mathbf{W})\|$. By construction, one has

$$\|\mathcal{P}_{T^\perp}(\mathbf{W})\| \leq \sum_{l=1}^{j_0} \left\| \mathcal{P}_{T^\perp} \left(\frac{1}{q} \mathcal{A}_{\Omega_l} + \mathcal{A}^\perp \right) \mathcal{P}_T(\mathbf{F}_{l-1}) \right\|.$$

Each summand can be bounded above as follows

$$\begin{aligned}
\left\| \mathcal{P}_{T^\perp} \left(\frac{1}{q} \mathcal{A}_{\Omega_l} + \mathcal{A}^\perp \right) \mathcal{P}_T(\mathbf{F}_{l-1}) \right\| &= \left\| \mathcal{P}_{T^\perp} \left(\frac{1}{q} \mathcal{A}_{\Omega_l} - \mathcal{A} \right) \mathcal{P}_T(\mathbf{F}_{l-1}) \right\| \\
&\leq \left\| \left(\frac{1}{q} \mathcal{A}_{\Omega_l} - \mathcal{A} \right) (\mathbf{F}_{l-1}) \right\| \\
&\leq c_2 \left(\sqrt{\frac{\log(n_1 n_2)}{q}} \|\mathbf{F}_{l-1}\|_{\mathcal{A},2} + \frac{\log(n_1 n_2)}{q} \|\mathbf{F}_{l-1}\|_{\mathcal{A},\infty} \right) \tag{47}
\end{aligned}$$

$$\begin{aligned}
&\leq c_2 c_5 \left(\sqrt{\frac{\mu_5 r \log(n_1 n_2)}{q n_1 n_2}} + \frac{\mu_1 c_s r \log(n_1 n_2)}{q n_1 n_2} \right) \\
&\quad \cdot \left\{ \sqrt{\frac{\log(n_1 n_2)}{q}} \|\mathbf{F}_{l-2}\|_{\mathcal{A},2} + \frac{\log(n_1 n_2)}{q} \|\mathbf{F}_{l-2}\|_{\mathcal{A},\infty} \right\} \tag{48}
\end{aligned}$$

$$\leq \left(\frac{1}{2} \right)^{l-1} \left(\sqrt{\frac{\log(n_1 n_2)}{q}} \cdot \|\mathbf{F}_0\|_{\mathcal{A},2} + \frac{\log(n_1 n_2)}{q} \|\mathbf{F}_0\|_{\mathcal{A},\infty} \right), \tag{49}$$

where (47) follows from Lemma 4 together with the fact that $\mathbf{F}_i \in T$, and (48) is a consequence of (46). The last inequality holds under the hypothesis that $q n_1 n_2 \gg \max\{\mu_1 c_s, \mu_5\} r \log(n_1 n_2)$ or, equivalently, $m \gg \max\{\mu_1 c_s, \mu_5\} r \log^2(n_1 n_2)$.

Since $\mathbf{F}_0 = \mathbf{U}\mathbf{V}^*$, it remains to control $\|\mathbf{U}\mathbf{V}^*\|_{\mathcal{A},\infty}$ and $\|\mathbf{U}\mathbf{V}^*\|_{\mathcal{A},2}$. We have the following lemma.

Lemma 7. *With the incoherence measure μ_1 , one can bound*

$$\|\mathbf{U}\mathbf{V}^*\|_{\mathcal{A},\infty} \leq \frac{\mu_1 c_s r}{n_1 n_2}, \tag{50}$$

$$\|\mathbf{U}\mathbf{V}^*\|_{\mathcal{A},2}^2 \leq \frac{\mu_1 c_s r \log(n_1 n_2)}{n_1 n_2}, \tag{51}$$

and for any $(\alpha, \beta) \in [n_1] \times [n_2]$,

$$\left\| \mathcal{P}_T(\omega_{\alpha, \beta} \mathbf{A}_{(\alpha, \beta)}) \right\|_{\mathcal{A}, 2}^2 \leq \frac{c_6 \mu_1 c_s \log(n_1 n_2) r}{n_1 n_2} \quad (52)$$

for some numerical constant $c_6 > 0$.

Proof. See Appendix H. □

In particular, the bound (52) translates into

$$\mu_5 \leq c_6 \mu_1 c_s \log(n_1 n_2).$$

Substituting (50) and (51) into (49) gives

$$\left\| \mathcal{P}_{T^\perp} \left(\frac{n_1 n_2}{m} \mathcal{A}_{\Omega_l} + \mathcal{A}^\perp \right) \mathcal{P}_T(\mathbf{F}_{l-1}) \right\| \leq \left(\frac{1}{2} \right)^{l-1} \left(\sqrt{\frac{\mu_1 c_s r \log(n_1 n_2)}{q n_1 n_2}} + \frac{\mu_1 c_s r}{q n_1 n_2} \right) \ll \frac{1}{2} \cdot \left(\frac{1}{2} \right)^l,$$

as soon as $m > c_7 \max \{ \mu_1 c_s \log^2(n_1 n_2), \mu_5 \log^2(n_1 n_2) \} r$ or $m > \tilde{c}_7 \mu_1 c_s \log^3(n_1 n_2)$ for some constants $c_7, \tilde{c}_7 > 0$, indicating that

$$\left\| \mathcal{P}_{T^\perp}(\mathbf{W}) \right\| \leq \sum_{l=1}^{j_0} \left\| \mathcal{P}_{T^\perp} \left(\frac{1}{q} \mathcal{A}_{\Omega_l} + \mathcal{A}^\perp \right) \mathcal{P}_T(\mathbf{F}_{l-1}) \right\| \leq \frac{1}{2} \cdot \sum_{l=1}^{\infty} \left(\frac{1}{2} \right)^l \leq \frac{1}{2} \quad (53)$$

as required. So far, we have successfully verified that with high probability, \mathbf{W} is a valid dual certificate, and hence by Lemma 1 the solution to EMaC is exact.

7 Proof of Theorem 3

The algorithm Robust-EMaC is inspired by the well-known robust principal component analysis [17, 32] that seeks a decomposition of low-rank plus sparse matrices, except that we impose multi-fold Hankel structures on both the low-rank and sparse matrices. Following similar spirit as to the proof of Theorem 1, the proof here is based on duality analysis, and relies on the golfing scheme [30] to construct a valid dual certificate.

In this section, we prove the results for a slightly different sampling model as follows.

- The location multi-set Ω^{clean} of observed uncorrupted entries is generated by sampling $(1-s)\rho n_1 n_2$ i.i.d. entries uniformly at random.
- The location multi-set Ω of observed entries is generated by sampling $\rho n_1 n_2$ i.i.d. entries uniformly at random, with the first $(1-s)\rho n_1 n_2$ entries coming from Ω^{clean} .
- The location set Ω^{dirty} of observed corrupted entries is given by $\Omega' \setminus \Omega^{\text{clean}'}$, where Ω' and $\Omega^{\text{clean}'}$ denote the sets of distinct entry locations in Ω and Ω^{clean} , respectively.

As mentioned in the proof of Theorem 1, this slightly different sampling model, while resulting in the same order-wise bounds, significantly simplifies the analysis due to the independence assumptions.

We will prove Theorem 3 under an additional random sign condition, that is, the signs of all non-zero entries of \mathbf{S} are *independent zero-mean* random variables. Specifically, we will prove the following theorem.

Theorem 5 (Random sign). *Suppose that \mathbf{X} obeys the incoherence condition with parameter μ_1 , and let $\lambda = \frac{1}{\sqrt{m \log(n_1 n_2)}}$. Assume that $s \leq 0.2$ is some small positive constant, and that the signs of nonzero entries of \mathbf{S} are independently generated with zero mean. If*

$$m > c_0 \mu_1^2 c_s^2 r^2 \log^3(n_1 n_2),$$

then Robust-EMaC succeeds in recovering \mathbf{X} with probability exceeding $1 - (n_1 n_2)^{-2}$.

In fact, a simple derandomization argument introduced in [32, Section 2.2] immediately suggests that the performance of Robust-EMaC under the fixed-sign pattern is no worse than that under the random-sign pattern with sparsity parameter $2s$, i.e. the condition on the signs pattern of \mathbf{S} is unnecessary and Theorem 3 follows after we establish Theorem 5. As a result, the section will focus on Theorem 3 with random sign patterns, which are much easier to analyze.

7.1 Dual Certification

We adopt similar notations as in Section 6.1. That said, if we generate $\rho n_1 n_2$ i.i.d. entry locations \mathbf{a}_i 's uniformly at random, and let the multi-sets Ω and Ω^{clean} contain respectively $\{\mathbf{a}_i | 1 \leq i \leq \rho n_1 n_2\}$ and $\{\mathbf{a}_i | 1 \leq i \leq \rho(1-s)n_1 n_2\}$, then

$$\mathcal{A}_\Omega := \sum_{i=1}^{\rho n_1 n_2} \mathcal{A}_{\mathbf{a}_i}, \quad \text{and} \quad \mathcal{A}_{\Omega^{\text{clean}}} := \sum_{i=1}^{\rho(1-s)n_1 n_2} \mathcal{A}_{\mathbf{a}_i},$$

corresponding to sampling with replacement. Besides, \mathcal{A}'_Ω (resp. $\mathcal{A}'_{\Omega^{\text{clean}}}$) is defined similar to \mathcal{A}_Ω (resp. $\mathcal{A}_{\Omega^{\text{clean}}}$), but with the sum extending only over *distinct* samples.

We will establish that exact recovery can be guaranteed, if we can produce a valid dual certificate as follows.

Lemma 8. *Suppose that s is some small positive constant. Suppose that the associated sampling operator $\mathcal{A}_{\Omega^{\text{clean}}}$ obeys*

$$\left\| \mathcal{P}_T \mathcal{A} \mathcal{P}_T - \frac{1}{\rho(1-s)} \mathcal{P}_T \mathcal{A}_{\Omega^{\text{clean}}} \mathcal{P}_T \right\| \leq \frac{1}{2}, \quad (54)$$

and

$$\|\mathcal{A}_{\Omega^{\text{clean}}}(\mathbf{M})\|_F \leq 10 \log(n_1 n_2) \|\mathcal{A}'_{\Omega^{\text{clean}}}(\mathbf{M})\|_F, \quad (55)$$

for any matrix \mathbf{M} . If there exist a regularization parameter λ ($0 < \lambda < 1$) and a matrix \mathbf{W} obeying

$$\begin{cases} \|\mathcal{P}_T(\mathbf{W} + \lambda \text{sgn}(\mathbf{S}_e) - \mathbf{U}\mathbf{V}^*)\|_F \leq \frac{\lambda}{n_1^2 n_2^2}, \\ \|\mathcal{P}_{T^\perp}(\mathbf{W} + \lambda \text{sgn}(\mathbf{S}_e))\| \leq \frac{1}{4}, \\ \mathcal{A}'_{(\Omega^{\text{clean}})^\perp}(\mathbf{W}) = 0, \\ \|\mathcal{A}'_{\Omega^{\text{clean}}}(\mathbf{W})\|_\infty \leq \frac{\lambda}{4}, \end{cases} \quad (56)$$

then Robust-EMaC is exact, i.e. the minimizer $(\hat{\mathbf{M}}, \hat{\mathbf{S}})$ satisfies $\hat{\mathbf{M}} = \mathbf{X}$.

Proof. See Appendix I. □

We note that a reasonably tight bound on $\left\| \mathcal{P}_T \mathcal{A} \mathcal{P}_T - \frac{1}{\rho(1-s)} \mathcal{P}_T \mathcal{A}_{\Omega^{\text{clean}}} \mathcal{P}_T \right\|$ has been developed by Lemma 3. Specifically, there exists some constant $c_1 > 0$ such that if $\rho(1-s)n_1 n_2 > c_1 \mu_1 c_s r \log(n_1 n_2)$, then one has

$$\left\| \mathcal{P}_T \mathcal{A} \mathcal{P}_T - \frac{1}{\rho(1-s)} \mathcal{P}_T \mathcal{A}_{\Omega^{\text{clean}}} \mathcal{P}_T \right\| \leq \frac{1}{2}$$

with probability exceeding $1 - (n_1 n_2)^{-4}$. Besides, Chernoff bound [53] indicates that with probability exceeding $1 - (n_1 n_2)^{-3}$, none of the entries is sampled more than $10 \log(n_1 n_2)$ times. Equivalently,

$$\mathbb{P}(\forall \mathbf{M} : \|\mathcal{A}_{\Omega^{\text{clean}}}(\mathbf{M})\|_F \leq 10 \log(n_1 n_2) \|\mathcal{A}'_{\Omega^{\text{clean}}}(\mathbf{M})\|_F) \geq 1 - (n_1 n_2)^{-3}.$$

Our objective in the remainder of this section is to produce a dual matrix \mathbf{W} satisfying Condition (56).

7.2 Construction of Dual Certificate

Suppose that we generate j_0 independent random location multi-sets Ω_j^{clean} , where Ω_j^{clean} contains $q n_1 n_2$ i.i.d. samples uniformly at random. Here, we set $q := \frac{(1-s)\rho}{j_0}$ and $\epsilon < \frac{1}{e}$. This way the distribution of the multi-set Ω is the same as $\Omega_1^{\text{clean}} \cup \Omega_2^{\text{clean}} \cup \dots \cup \Omega_{j_0}^{\text{clean}}$.

We now propose constructing a dual certificate \mathbf{W} as follows:

Construction of a dual certificate \mathbf{W} via the golfing scheme.

1. Set $\mathbf{F}_0 = \mathcal{P}_T(\mathbf{U}\mathbf{V}^* - \lambda \text{sgn}(\mathbf{S}_e))$, and $j_0 := 5 \log_{\frac{1}{\epsilon}} n_1 n_2$.
 2. For every i ($1 \leq i \leq j_0$), let $\mathbf{F}_i := \mathcal{P}_T\left(\mathcal{A} - \frac{1}{q} \mathcal{A}_{\Omega_i^{\text{clean}}}\right) \mathcal{P}_T(\mathbf{F}_{i-1})$.
 3. Set $\mathbf{W} := \sum_{j=1}^{j_0} \left(\frac{1}{q} \mathcal{A}_{\Omega_j^{\text{clean}}} + \mathcal{A}^\perp\right) \mathbf{F}_{j-1}$.
-

Take $\lambda = \frac{1}{\sqrt{m \log(n_1 n_2)}}$. Note that the construction of \mathbf{W} proceeds with a similar procedure as in Section 6.3, except that \mathbf{F}_0 and Ω_i are replaced by $\mathcal{P}_T(\mathbf{UV}^* - \lambda \text{sgn}(\mathbf{S}_e))$ and Ω_i^{clean} , respectively.

We will justify that \mathbf{W} is a valid dual certificate, by examining the conditions in (56) step by step.

(1) The first condition requires the term $\|\mathcal{P}_T(\mathbf{W} + \lambda \text{sgn}(\mathbf{S}_e) - \mathbf{UV}^*)\|_F = \|\mathcal{P}_T(\mathbf{W} - \mathbf{F}_0)\|_F$ to be reasonably small. Lemma 3 asserts that there exist some constants $c_1, \tilde{c}_1 > 0$ such that if $m = \rho n_1 n_2 > c_1 \mu_1 c_s r \log^2(n_1 n_2)$ or, equivalently, $q_i n_1 n_2 > \tilde{c}_1 \mu_1 c_s r \log^2(n_1 n_2)$, then

$$\begin{aligned} \|\mathcal{P}_T(\mathbf{F}_{j_0})\|_F &\leq \epsilon \|\mathcal{P}_T(\mathbf{F}_{j_0-1})\|_F \leq \dots \leq \epsilon^{j_0} \|\mathcal{P}_T(\mathbf{F}_0)\|_F \\ &\leq \frac{1}{n_1^5 n_2^5} (\|\mathbf{UV}^*\|_F + \lambda \|\text{sgn}(\mathbf{S}_e)\|_F) \end{aligned} \quad (57)$$

$$\leq \frac{1}{n_1^5 n_2^5} (\sqrt{r} + \lambda n_1 n_2) < \frac{1}{n_1^5 n_2^5} (n_1 n_2 + \lambda n_1 n_2) \leq \frac{\lambda}{n_1^2 n_2^2} \quad (58)$$

with probability exceeding $1 - (n_1 n_2)^{-3}$. Apply the same argument as for (38) to derive

$$-\mathcal{P}_T(\mathbf{W} - \mathbf{F}_0) = \mathcal{P}_T(\mathbf{F}_{j_0}).$$

Plugging this into (58) establishes that

$$\|\mathcal{P}_T(\mathbf{W} + \lambda \text{sgn}(\mathbf{S}_e) - \mathbf{UV}^*)\|_F = \|\mathcal{P}_T(\mathbf{F}_{j_0})\|_F \leq \frac{\lambda}{n_1^2 n_2^2}. \quad (59)$$

(2) The second condition relies on an upper bound on $\|\mathcal{P}_{T^\perp}(\mathbf{W} + \lambda \text{sgn}(\mathbf{S}_e))\|$. To this end, we proceed by controlling $\|\mathcal{P}_{T^\perp}(\mathbf{W})\|$ and $\|\mathcal{P}_{T^\perp}(\lambda \text{sgn}(\mathbf{S}_e))\|$ separately. Applying the same argument as for (49) suggests

$$\left\| \mathcal{P}_{T^\perp} \left(\frac{1}{q} \mathcal{A}_{\Omega_l} + \mathcal{A}^\perp \right) \mathcal{P}_T(\mathbf{F}_{l-1}) \right\| \leq \left(\frac{1}{2} \right)^{l-1} \left(\sqrt{\frac{\log(n_1 n_2)}{q}} \cdot \|\mathbf{F}_0\|_{\mathcal{A},2} + \frac{\log(n_1 n_2)}{q} \|\mathbf{F}_0\|_{\mathcal{A},\infty} \right) \quad (60)$$

$$\leq \left(\frac{1}{2} \right)^{l-1} \left(\sqrt{\frac{n_1 n_2 \log(n_1 n_2)}{q}} + \frac{\log(n_1 n_2)}{q} \right) \cdot \|\mathbf{F}_0\|_{\mathcal{A},\infty} \quad (61)$$

$$\leq \left(\frac{1}{2} \right)^{l-2} \frac{n_1 n_2 \log(n_1 n_2)}{\sqrt{m}} \|\mathbf{F}_0\|_{\mathcal{A},\infty}, \quad (62)$$

where the second inequality follows since $\|\mathbf{M}\|_{\mathcal{A},2} \leq \sqrt{n_1 n_2} \|\mathbf{M}\|_{\mathcal{A},\infty}$, and the last inequality arises from the fact that

$$\frac{\log(n_1 n_2)}{q} \leq \sqrt{\frac{n_1 n_2 \log(n_1 n_2)}{q}} = \frac{n_1 n_2 \log(n_1 n_2)}{\sqrt{m}}$$

when $m \gg \log^2(n_1 n_2)$. Note that $\mathbf{F}_0 = \mathbf{UV}^* - \lambda \mathcal{P}_T(\text{sgn}(\mathbf{S}_e))$. Since we have established an upper bound on $\|\mathbf{UV}^*\|_{\mathcal{A},\infty}$ in (50), what remains to be controlled is $\|\mathcal{P}_T(\text{sgn}(\mathbf{S}_e))\|_{\mathcal{A},\infty}$. This is achieved by the following lemma.

Lemma 9. *Suppose that s is a positive constant. then one has*

$$\|\mathcal{P}_T(\text{sgn}(\mathbf{S}_e))\|_{\mathcal{A},\infty} \leq c_9 \frac{\mu_1 c_s r}{n_1 n_2} \sqrt{m s \log(n_1 n_2)}$$

for some constant $c_9 > 0$ with probability at least $1 - (n_1 n_2)^{-4}$.

Proof. See Appendix J. □

From (50) and Lemma 9, we have

$$\begin{aligned} \|\mathbf{F}_0\|_{\mathcal{A},\infty} &\leq \|\mathbf{UV}^*\|_{\mathcal{A},\infty} + \lambda \|\mathcal{P}_T(\text{sgn}(\mathbf{S}_e))\|_{\mathcal{A},\infty} \\ &\leq \frac{\mu_1 c_s r}{n_1 n_2} + \frac{c_9 \mu_1 c_s r \sqrt{s}}{n_1 n_2} \\ &\leq \frac{\tilde{c}_9 \mu_1 c_s r}{n_1 n_2}, \end{aligned} \quad (63)$$

and substitute (63) into (62) we have

$$\left\| \mathcal{P}_{T^\perp} \left(\frac{1}{q} \mathcal{A}_{\Omega_l} + \mathcal{A}^\perp \right) \mathcal{P}_T(\mathbf{F}_{l-1}) \right\| \leq \left(\frac{1}{2} \right)^{l-2} \frac{\tilde{c}_9 \mu_1 c_s r \log(n_1 n_2)}{\sqrt{m}}.$$

In particular, if $m > c_8 \mu_1^2 c_s^2 r^2 \log^2(n_1 n_2)$ for some large enough constant c_8 , then one has

$$\left\| \mathcal{P}_{T^\perp} \left(\frac{1}{q} \mathcal{A}_{\Omega_l} + \mathcal{A}^\perp \right) \mathcal{P}_T(\mathbf{F}_{l-1}) \right\| \leq \left(\frac{1}{2} \right)^{l+4}.$$

As a result, we can obtain

$$\begin{aligned} \|\mathcal{P}_{T^\perp}(\mathbf{W})\| &\leq \sum_{i=1}^{j_0} \left\| \mathcal{P}_{T^\perp} \left(\frac{1}{q} \mathcal{A}_{\Omega_i^{\text{clean}}} + \mathcal{A}^\perp \right) \mathcal{P}_T(\mathbf{F}_{i-1}) \right\| \\ &\leq \sum_{i=0}^{j_0} \left(\frac{1}{2} \right)^{i+4} < \frac{1}{8} \end{aligned} \quad (64)$$

with probability exceeding $1 - (n_1 n_2)^{-4}$.

It remains to control the term $\|\mathcal{P}_{T^\perp}(\lambda \text{sgn}(\mathbf{S}_e))\|$, which is supplied in the following lemma.

Lemma 10. *Suppose that s is a small positive constant, then one has*

$$\|\text{sgn}(\mathbf{S}_e)\| \leq \sqrt{c_{10} \rho s n_1 n_2 \log^{\frac{1}{2}}(n_1 n_2)} \quad \text{and} \quad \|\mathcal{P}_{T^\perp}(\lambda \text{sgn}(\mathbf{S}_e))\| \leq \frac{1}{8} \quad (65)$$

with probability at least $1 - (n_1 n_2)^{-5}$.

Proof. See Appendix K. □

Putting (64) and (65) together yields

$$\|\mathcal{P}_{T^\perp}(\mathbf{W} + \lambda \text{sgn}(\mathbf{S}_e))\| \leq \|\mathcal{P}_{T^\perp}(\mathbf{W})\| + \|\mathcal{P}_{T^\perp}(\lambda \text{sgn}(\mathbf{S}_e))\| \leq \frac{1}{4}$$

with high probability.

(3) By construction, one has $\mathcal{A}'_{(\Omega^{\text{clean}})^\perp}(\mathbf{W}) = 0$.

(4) The last step is to bound $\|\mathcal{A}'_{\Omega^{\text{clean}}}(\mathbf{W})\|_\infty$, which is apparently bounded above by $\|\mathcal{A}_{\Omega^{\text{clean}}}(\mathbf{W})\|_\infty$. The construction procedure together with Lemma 6 allows us to bound

$$\|\mathbf{F}_i\|_{\mathcal{A}, \infty} \leq c_4 \left(\sqrt{\frac{\mu_1 c_s r \log(n_1 n_2)}{q n_1 n_2}} \cdot \sqrt{\frac{\mu_1 c_s r}{n_1 n_2}} \|\mathbf{F}_{i-1}\|_{\mathcal{A}, 2} + \frac{\mu_1 c_s r \log(n_1 n_2)}{q n_1 n_2} \|\mathbf{F}_{i-1}\|_{\mathcal{A}, \infty} \right) \quad (66)$$

$$\leq c_4 \left(\sqrt{\frac{\mu_1 c_s r \log(n_1 n_2)}{q n_1 n_2}} \cdot \sqrt{\mu_1 c_s r} + \frac{\mu_1 c_s r \log(n_1 n_2)}{q n_1 n_2} \right) \|\mathbf{F}_{i-1}\|_{\mathcal{A}, \infty} \quad (67)$$

$$\leq 2c_4 \mu_1 c_s r \sqrt{\frac{\log(n_1 n_2)}{q n_1 n_2}} \|\mathbf{F}_{i-1}\|_{\mathcal{A}, \infty}, \quad (68)$$

where the second inequality arises since $\|\mathbf{F}_i\|_{\mathcal{A}, 2} \leq \sqrt{n_1 n_2} \|\mathbf{F}_i\|_{\mathcal{A}, \infty}$, and the last step follows since $\sqrt{\frac{\log(n_1 n_2)}{q n_1 n_2}} \geq \frac{\log(n_1 n_2)}{q n_1 n_2}$ when $m \gg \log^2(n_1 n_2)$. Then there exists some constant $c_{11} > 0$ such that if $m > c_{11} \mu_1^2 c_s^2 r^2 \log^2(n_1 n_2)$, then

$$\|\mathbf{F}_i\|_{\mathcal{A}, \infty} \leq \frac{1}{4} \|\mathbf{F}_{i-1}\|_{\mathcal{A}, \infty} \leq \frac{1}{4^i} \|\mathbf{F}_0\|_{\mathcal{A}, \infty} \leq \frac{\tilde{c}_9 \mu_1 c_s r}{4^i n_1 n_2},$$

where the last inequality follows from (63). As a result, one can deduce

$$\begin{aligned}
\|\mathcal{A}_{\Omega^{\text{clean}}}(\mathbf{W})\|_{\infty} &= \left\| \sum_{i=1}^{j_0} \mathcal{A}_{\Omega^{\text{clean}}} \left(\frac{1}{q} \mathcal{A}_{\Omega_i^{\text{clean}}} + \mathcal{A}^{\perp} \right) \mathbf{F}_{i-1} \right\|_{\infty} = \left\| \sum_{i=1}^{j_0} \frac{1}{q} \mathcal{A}_{\Omega_i^{\text{clean}}} \mathbf{F}_{i-1} \right\|_{\infty} \\
&\leq \sum_{i=1}^{j_0} \frac{1}{q} \max_{(k,l) \in [n_1] \times [n_2]} \frac{|\langle \mathbf{A}_{(k,l)}, \mathbf{F}_{i-1} \rangle|}{\sqrt{\omega_{k,l}}} = \sum_{i=1}^{j_0} \frac{1}{q} \|\mathbf{F}_{i-1}\|_{\mathcal{A}, \infty} \\
&\leq \sum_{i=1}^{j_0} \frac{5 \log(n_1 n_2)}{\rho} \frac{\tilde{c}_9 \mu_1 c_s r}{4^{i-1} n_1 n_2} \\
&\leq \frac{20 \log(n_1 n_2) \tilde{c}_9 \mu_1 c_s r}{3m} \leq \frac{1}{4\sqrt{m \log(n_1 n_2)}}
\end{aligned}$$

when the last inequality is obtained by setting $m > c_{12} \mu_1^2 c_s^2 r^2 \log^3(n_1 n_2)$ for some constant $c_{12} > 0$.

To sum up, we have verified that \mathbf{W} satisfies the four conditions required in (56), and is hence a valid dual certificate. This concludes the proof.

8 Concluding Remarks

We present an efficient algorithm to estimate a spectrally sparse signal from its partial time-domain samples that does not require prior knowledge on the model order, which poses spectral compressed sensing as a low-rank Hankel structured matrix completion problem. Under mild incoherence conditions, our algorithm enables recovery of the multi-dimensional unknown frequencies with infinite precision, which remedies the basis mismatch issue that arises in conventional CS paradigms. We have shown both theoretically and numerically that our algorithm is stable against bounded noise and a constant proportion of arbitrary corruptions, and can be extended numerically to tasks such as super resolution. To the best of our knowledge, our result on Hankel matrix completion is also the first theoretical guarantee that is close to the information-theoretical limit (up to some logarithmic factor).

Our results are based on uniform random observation models. In particular, this paper considers directly taking a random subset of the time domain samples, it is also possible to take a random set of linear mixtures of the time domain samples, as in the renowned CS setting [14]. This again can be translated into taking linear measurements of the low-rank K -fold Hankel matrix, given as $\mathbf{y} = \mathcal{B}(\mathbf{X}_e)$. Unfortunately, due to the Hankel structures, it is not clear whether \mathcal{B} exhibits approximate isometry property. Nonetheless, the technique developed in this paper can be extended without difficulty to analyze linear measurements, in a similar flavor of a golfing scheme developed for CS in [21].

It remains to be seen whether it is possible to obtain performance guarantees of the proposed EMaC algorithm similar to that in [24] for super resolution. It is also of great interest to develop efficient numerical methods to solve the EMaC algorithm in order to accommodate large datasets.

A Bernstein Inequality

Our analysis relies heavily on the Bernstein inequality. To simplify presentation, we state below a user-friendly version of Bernstein inequality, which is an immediate consequence of [54, Theorem 1.6].

Lemma 11. *Consider m independent random matrices \mathbf{M}_l ($1 \leq l \leq m$) of dimension $d_1 \times d_2$, each satisfying $\mathbb{E}[\mathbf{M}_l] = 0$ and $\|\mathbf{M}_l\| \leq B$. Define*

$$\sigma^2 := \max \left\{ \left\| \sum_{l=1}^m \mathbb{E}[\mathbf{M}_l \mathbf{M}_l^*] \right\|, \left\| \sum_{l=1}^m \mathbb{E}[\mathbf{M}_l^* \mathbf{M}_l] \right\| \right\}.$$

Then there exists a universal constant $c_0 > 0$ such that for any integer $a \geq 2$,

$$\left\| \sum_{l=1}^m \mathbf{M}_l \right\| \leq c_0 \left(\sqrt{a \sigma^2 \log(d_1 + d_2)} + a B \log(d_1 + d_2) \right) \quad (69)$$

with probability at least $1 - (d_1 + d_2)^{-a}$.

B Proof of Lemma 1

Consider any valid perturbation \mathbf{H} obeying $\mathcal{P}_\Omega(\mathbf{X} + \mathbf{H}) = \mathcal{P}_\Omega(\mathbf{X})$, and denote by \mathbf{H}_e the enhanced form of \mathbf{H} . We note that the constraint requires $\mathcal{A}'_\Omega(\mathbf{H}_e) = 0$ (or $\mathcal{A}_\Omega(\mathbf{H}_e) = 0$) and $\mathcal{A}^\perp(\mathbf{H}_e) = 0$. In addition, set $\mathbf{Z}_0 = \mathcal{P}_{T^\perp}(\mathbf{B})$ for any \mathbf{B} that satisfies $\langle \mathbf{B}, \mathcal{P}_{T^\perp}(\mathbf{H}_e) \rangle = \|\mathcal{P}_{T^\perp}(\mathbf{H}_e)\|_*$ and $\|\mathbf{B}\| \leq 1$. Therefore, $\mathbf{Z}_0 \in T^\perp$ and $\|\mathbf{Z}_0\| \leq 1$, and hence $\mathbf{UV}^* + \mathbf{Z}_0$ is a sub-gradient of the nuclear norm at \mathbf{X}_e . We will establish this lemma by considering two scenarios separately.

(1) Consider first the case in which \mathbf{H}_e satisfies

$$\|\mathcal{P}_T(\mathbf{H}_e)\|_F \leq \frac{n_1^2 n_2^2}{2} \|\mathcal{P}_{T^\perp}(\mathbf{H}_e)\|_F. \quad (70)$$

Since $\mathbf{UV}^* + \mathbf{Z}_0$ is a sub-gradient of the nuclear norm at \mathbf{X}_e , it follows that

$$\begin{aligned} \|\mathbf{X}_e + \mathbf{H}_e\|_* &\geq \|\mathbf{X}_e\|_* + \langle \mathbf{UV}^* + \mathbf{Z}_0, \mathbf{H}_e \rangle \\ &= \|\mathbf{X}_e\|_* + \langle \mathbf{W}, \mathbf{H}_e \rangle + \langle \mathbf{Z}_0, \mathbf{H}_e \rangle - \langle \mathbf{W} - \mathbf{UV}^*, \mathbf{H}_e \rangle \\ &= \|\mathbf{X}_e\|_* + \langle (\mathcal{A}'_\Omega + \mathcal{A}^\perp)(\mathbf{W}), \mathbf{H}_e \rangle + \langle \mathbf{Z}_0, \mathbf{H}_e \rangle - \langle \mathbf{W} - \mathbf{UV}^*, \mathbf{H}_e \rangle \\ &\geq \|\mathbf{X}_e\|_* + \|\mathcal{P}_{T^\perp}(\mathbf{H}_e)\|_* - \langle \mathbf{W} - \mathbf{UV}^*, \mathbf{H}_e \rangle \end{aligned} \quad (71)$$

where (71) holds from (30), and (72) follows from the property of \mathbf{Z}_0 and the fact that $(\mathcal{A}'_\Omega + \mathcal{A}^\perp)(\mathbf{H}_e) = 0$. The last term of (72) can be bounded as

$$\begin{aligned} \langle \mathbf{W} - \mathbf{UV}^*, \mathbf{H}_e \rangle &= \langle \mathcal{P}_T(\mathbf{W} - \mathbf{UV}^*), \mathbf{H}_e \rangle + \langle \mathcal{P}_{T^\perp}(\mathbf{W} - \mathbf{UV}^*), \mathbf{H}_e \rangle \\ &\leq \|\mathcal{P}_T(\mathbf{W} - \mathbf{UV}^*)\|_F \|\mathcal{P}_T(\mathbf{H}_e)\|_F + \|\mathcal{P}_{T^\perp}(\mathbf{W})\| \|\mathcal{P}_{T^\perp}(\mathbf{H}_e)\|_* \\ &\leq \frac{1}{2n_1^2 n_2^2} \|\mathcal{P}_T(\mathbf{H}_e)\|_F + \frac{1}{2} \|\mathcal{P}_{T^\perp}(\mathbf{H}_e)\|_*, \end{aligned}$$

where the last inequality follows from the assumptions (31) and (32). Plugging this into (72) yields

$$\begin{aligned} \|\mathbf{X}_e + \mathbf{H}_e\|_* &\geq \|\mathbf{X}_e\|_* - \frac{1}{2n_1^2 n_2^2} \|\mathcal{P}_T(\mathbf{H}_e)\|_F + \frac{1}{2} \|\mathcal{P}_{T^\perp}(\mathbf{H}_e)\|_* \\ &\geq \|\mathbf{X}_e\|_* - \frac{1}{4} \|\mathcal{P}_{T^\perp}(\mathbf{H}_e)\|_F + \frac{1}{2} \|\mathcal{P}_{T^\perp}(\mathbf{H}_e)\|_F \\ &\geq \|\mathbf{X}_e\|_* + \frac{1}{4} \|\mathcal{P}_{T^\perp}(\mathbf{H}_e)\|_F \end{aligned} \quad (73)$$

where (73) follows from the inequality $\|\mathbf{M}\|_* \geq \|\mathbf{M}\|_F$ and (70). Therefore, \mathbf{X}_e is the minimizer of EMaC.

We still need to prove the uniqueness of the minimizer. The inequality (73) implies that $\|\mathbf{X}_e + \mathbf{H}_e\|_* = \|\mathbf{X}_e\|_*$ only when $\|\mathcal{P}_{T^\perp}(\mathbf{H}_e)\|_F = 0$. If $\|\mathcal{P}_{T^\perp}(\mathbf{H}_e)\|_F = 0$, then $\|\mathcal{P}_T(\mathbf{H}_e)\|_F \leq \frac{n_1^2 n_2^2}{2} \|\mathcal{P}_{T^\perp}(\mathbf{H}_e)\|_F = 0$, and hence $\mathcal{P}_{T^\perp}(\mathbf{H}_e) = \mathcal{P}_T(\mathbf{H}_e) = 0$, which only occurs when $\mathbf{H}_e = 0$. Hence, \mathbf{X}_e is the unique minimizer in this situation.

(2) On the other hand, consider the complement scenario where the following holds

$$\|\mathcal{P}_T(\mathbf{H}_e)\|_F \geq \frac{n_1^2 n_2^2}{2} \|\mathcal{P}_{T^\perp}(\mathbf{H}_e)\|_F. \quad (74)$$

We would first like to bound $\|(\frac{n_1 n_2}{m} \mathcal{A}_\Omega + \mathcal{A}^\perp) \mathcal{P}_T(\mathbf{H}_e)\|_F$ and $\|(\frac{n_1 n_2}{m} \mathcal{A}_\Omega + \mathcal{A}^\perp) \mathcal{P}_{T^\perp}(\mathbf{H}_e)\|_F$. The former

term can be lower bounded by

$$\begin{aligned}
& \left\| \left(\frac{n_1 n_2}{m} \mathcal{A}_\Omega + \mathcal{A}^\perp \right) \mathcal{P}_T(\mathbf{H}_e) \right\|_F^2 \\
&= \left\langle \left(\frac{n_1 n_2}{m} \mathcal{A}_\Omega + \mathcal{A}^\perp \right) \mathcal{P}_T(\mathbf{H}_e), \left(\frac{n_1 n_2}{m} \mathcal{A}_\Omega + \mathcal{A}^\perp \right) \mathcal{P}_T(\mathbf{H}_e) \right\rangle \\
&= \left\langle \frac{n_1 n_2}{m} \mathcal{A}_\Omega \mathcal{P}_T(\mathbf{H}_e), \frac{n_1 n_2}{m} \mathcal{A}_\Omega \mathcal{P}_T(\mathbf{H}_e) \right\rangle + \left\langle \mathcal{A}^\perp \mathcal{P}_T(\mathbf{H}_e), \mathcal{A}^\perp \mathcal{P}_T(\mathbf{H}_e) \right\rangle \\
&\geq \left\langle \mathcal{P}_T(\mathbf{H}_e), \frac{n_1 n_2}{m} \mathcal{A}_\Omega \mathcal{P}_T(\mathbf{H}_e) \right\rangle + \left\langle \mathcal{P}_T(\mathbf{H}_e), \mathcal{A}^\perp \mathcal{P}_T(\mathbf{H}_e) \right\rangle \\
&= \left\langle \mathcal{P}_T(\mathbf{H}_e), \mathcal{P}_T \left(\frac{n_1 n_2}{m} \mathcal{A}_\Omega + \mathcal{A}^\perp \right) \mathcal{P}_T(\mathbf{H}_e) \right\rangle \\
&= \left\langle \mathcal{P}_T(\mathbf{H}_e), \mathcal{P}_T(\mathbf{H}_e) \right\rangle + \left\langle \mathcal{P}_T(\mathbf{H}_e), \left(\frac{n_1 n_2}{m} \mathcal{P}_T \mathcal{A}_\Omega \mathcal{P}_T - \mathcal{P}_T \mathcal{A} \mathcal{P}_T \right) \mathcal{P}_T(\mathbf{H}_e) \right\rangle \\
&\geq \|\mathcal{P}_T(\mathbf{H}_e)\|_F^2 - \left\| \mathcal{P}_T \mathcal{A} \mathcal{P}_T - \frac{n_1 n_2}{m} \mathcal{P}_T \mathcal{A}_\Omega \mathcal{P}_T \right\| \|\mathcal{P}_T(\mathbf{H}_e)\|_F^2 \\
&\geq \left(1 - \left\| \mathcal{P}_T \mathcal{A} \mathcal{P}_T - \frac{n_1 n_2}{m} \mathcal{P}_T \mathcal{A}_\Omega \mathcal{P}_T \right\| \right) \|\mathcal{P}_T(\mathbf{H}_e)\|_F^2 \\
&\geq \frac{1}{2} \|\mathcal{P}_T(\mathbf{H}_e)\|_F^2.
\end{aligned} \tag{75}$$

$$\begin{aligned}
& \geq \|\mathcal{P}_T(\mathbf{H}_e)\|_F^2 - \left\| \mathcal{P}_T \mathcal{A} \mathcal{P}_T - \frac{n_1 n_2}{m} \mathcal{P}_T \mathcal{A}_\Omega \mathcal{P}_T \right\| \|\mathcal{P}_T(\mathbf{H}_e)\|_F^2 \\
&\geq \left(1 - \left\| \mathcal{P}_T \mathcal{A} \mathcal{P}_T - \frac{n_1 n_2}{m} \mathcal{P}_T \mathcal{A}_\Omega \mathcal{P}_T \right\| \right) \|\mathcal{P}_T(\mathbf{H}_e)\|_F^2 \\
&\geq \frac{1}{2} \|\mathcal{P}_T(\mathbf{H}_e)\|_F^2.
\end{aligned} \tag{76}$$

On the other hand, since the operator norm of any projection operator is bounded above by 1, one can verify that

$$\left\| \frac{n_1 n_2}{m} \mathcal{A}_\Omega + \mathcal{A}^\perp \right\| \leq \frac{n_1 n_2}{m} \left(\|\mathcal{A}_{a_1} + \mathcal{A}^\perp\| + \sum_{i=2}^m \|\mathcal{A}_{a_i}\| \right) \leq n_1 n_2,$$

where a_i ($1 \leq i \leq m$) are m uniform random indices that form Ω . This implies the following bound:

$$\left\| \left(\frac{n_1 n_2}{m} \mathcal{A}_\Omega + \mathcal{A}^\perp \right) \mathcal{P}_{T^\perp}(\mathbf{H}_e) \right\|_F \leq n_1 n_2 \|\mathcal{P}_{T^\perp}(\mathbf{H}_e)\|_F \leq \frac{2}{n_1 n_2} \|\mathcal{P}_T(\mathbf{H}_e)\|_F, \tag{78}$$

where the last inequality arises from our assumption. Combining this with the above two bounds yields

$$\begin{aligned}
0 &= \left\| \left(\frac{n_1 n_2}{m} \mathcal{A}_\Omega + \mathcal{A}^\perp \right) \mathcal{P}_{T^\perp}(\mathbf{H}_e) \right\|_F \geq \left\| \left(\frac{n_1 n_2}{m} \mathcal{A}_\Omega + \mathcal{A}^\perp \right) \mathcal{P}_T(\mathbf{H}_e) \right\|_F - \left\| \left(\frac{n_1 n_2}{m} \mathcal{A}_\Omega + \mathcal{A}^\perp \right) \mathcal{P}_{T^\perp}(\mathbf{H}_e) \right\|_F \\
&\geq \sqrt{\frac{1}{2}} \|\mathcal{P}_T(\mathbf{H}_e)\|_F - \frac{2}{n_1 n_2} \|\mathcal{P}_T(\mathbf{H}_e)\|_F \\
&\geq \frac{1}{2} \|\mathcal{P}_T(\mathbf{H}_e)\|_F \geq \frac{n_1^2 n_2^2}{4} \|\mathcal{P}_{T^\perp}(\mathbf{H}_e)\|_F \geq 0,
\end{aligned}$$

which immediately indicates $\mathcal{P}_{T^\perp}(\mathbf{H}_e) = 0$ and $\mathcal{P}_T(\mathbf{H}_e) = 0$. Hence, (74) can only hold when $\mathbf{H}_e = 0$.

C Proof of Lemma 2

Since \mathbf{U} (resp. \mathbf{V}) and \mathbf{E}_L (resp. \mathbf{E}_R) determine the same column (resp. row) space, we can write

$$\mathbf{U}\mathbf{U}^* = \mathbf{E}_L (\mathbf{E}_L^* \mathbf{E}_L)^{-1} \mathbf{E}_L^* \quad \text{and} \quad \mathbf{V}\mathbf{V}^* = \mathbf{E}_R^* (\mathbf{E}_R \mathbf{E}_R^*)^{-1} \mathbf{E}_R,$$

and thus

$$\begin{aligned}
\|\mathcal{P}_U(\mathbf{A}_{(k,l)})\|_F^2 &\leq \left\| \mathbf{E}_L (\mathbf{E}_L^* \mathbf{E}_L)^{-1} \mathbf{E}_L^* \mathbf{A}_{(k,l)} \right\|_F^2 \leq \frac{1}{\sigma_{\min}(\mathbf{E}_L^* \mathbf{E}_L)} \|\mathbf{E}_L^* \mathbf{A}_{(k,l)}\|_F^2 \\
\|\mathcal{P}_V(\mathbf{A}_{(k,l)})\|_F^2 &\leq \left\| \mathbf{A}_{(k,l)} \mathbf{E}_R^* (\mathbf{E}_R \mathbf{E}_R^*)^{-1} \mathbf{E}_R \right\|_F^2 \leq \frac{1}{\sigma_{\min}(\mathbf{E}_R \mathbf{E}_R^*)} \|\mathbf{A}_{(k,l)} \mathbf{E}_R^*\|_F^2.
\end{aligned}$$

Note that $\sqrt{\omega_{k,l}} \mathbf{E}_L^* \mathbf{A}_{(k,l)}$ consists of $\omega_{k,l}$ columns of \mathbf{E}_L^* (and hence it contains $r\omega_{k,l}$ nonzero entries in total). Owing to the fact that each entry of \mathbf{E}_L^* has magnitude $\frac{1}{\sqrt{k_1 k_2}}$, one can derive

$$\|\mathbf{E}_L^* \mathbf{A}_{(k,l)}\|_F^2 = \frac{1}{\omega_{k,l}} \cdot r\omega_{k,l} \cdot \frac{1}{k_1 k_2} = \frac{r}{k_1 k_2} \leq \frac{rc_s}{n_1 n_2}.$$

A similar argument yields $\|\mathbf{A}_{(k,l)} \mathbf{E}_R^*\|_F^2 \leq \frac{c_s r}{n_1 n_2}$. Combining $\sigma_{\min}(\mathbf{E}_L^* \mathbf{E}_L) \geq \frac{1}{\mu_1}$ and $\sigma_{\min}(\mathbf{E}_R \mathbf{E}_R^*) \geq \frac{1}{\mu_1}$, (33) follows by plugging these facts into the above equations.

To show (34), since $|\langle \mathbf{A}_b, \mathcal{P}_T \mathbf{A}_a \rangle| = |\langle \mathcal{P}_T \mathbf{A}_b, \mathbf{A}_a \rangle|$, we only need to examine the situation where $\omega_b < \omega_a$. Observe that

$$|\langle \mathbf{A}_b, \mathcal{P}_T \mathbf{A}_a \rangle| \leq |\langle \mathbf{A}_b, \mathbf{U} \mathbf{U}^* \mathbf{A}_a \rangle| + |\langle \mathbf{A}_b, \mathbf{A}_a \mathbf{V} \mathbf{V}^* \rangle| + |\langle \mathbf{A}_b, \mathbf{U} \mathbf{U}^* \mathbf{A}_a \mathbf{V} \mathbf{V}^* \rangle|.$$

Owing to the multi-fold Hankel structure of \mathbf{A}_a , the matrix $\mathbf{U} \mathbf{U}^* \sqrt{\omega_a} \mathbf{A}_a$ consists of ω_a columns of $\mathbf{U} \mathbf{U}^*$. Since there are only ω_b nonzero entries in \mathbf{A}_b each of magnitude $\frac{1}{\sqrt{\omega_b}}$, we can derive

$$\begin{aligned} |\langle \mathbf{A}_b, \mathbf{U} \mathbf{U}^* \mathbf{A}_a \rangle| &\leq \|\mathbf{A}_b\|_1 \|\mathbf{U} \mathbf{U}^* \mathbf{A}_a\|_\infty = \omega_b \cdot \frac{1}{\sqrt{\omega_b}} \cdot \max_{\alpha, \beta} |(\mathbf{U} \mathbf{U}^* \mathbf{A}_a)_{\alpha, \beta}| \\ &\leq \sqrt{\frac{\omega_b}{\omega_a}} \max_{\alpha, \beta} |(\mathbf{U} \mathbf{U}^*)_{\alpha, \beta}|. \end{aligned}$$

Each entry of $\mathbf{U} \mathbf{U}^*$ is bounded in magnitude by

$$\begin{aligned} |(\mathbf{U} \mathbf{U}^*)_{k,l}| &= |e_k^\top \mathbf{E}_L (\mathbf{E}_L^* \mathbf{E}_L)^{-1} \mathbf{E}_L^* e_l| \\ &\leq \|e_k^\top \mathbf{E}_L\|_F \left\| (\mathbf{E}_L^* \mathbf{E}_L)^{-1} \right\| \|\mathbf{E}_L^* e_l\|_F \\ &\leq \frac{r}{k_1 k_2} \frac{1}{\sigma_{\min}(\mathbf{E}_L^* \mathbf{E}_L)} \leq \frac{\mu_1 c_s r}{n_1 n_2}, \end{aligned} \tag{79}$$

which immediately implies that

$$|\langle \mathbf{A}_b, \mathbf{U} \mathbf{U}^* \mathbf{A}_a \rangle| \leq \sqrt{\frac{\omega_b}{\omega_a}} \frac{\mu_1 c_s r}{n_1 n_2}. \tag{80}$$

Similarly, one can derive

$$|\langle \mathbf{A}_b, \mathbf{A}_a \mathbf{V} \mathbf{V}^* \rangle| \leq \sqrt{\frac{\omega_b}{\omega_a}} \frac{\mu_1 c_s r}{n_1 n_2}. \tag{81}$$

We still need to bound the magnitude of $\langle \mathbf{U} \mathbf{U}^* \mathbf{A}_a \mathbf{V} \mathbf{V}^*, \mathbf{A}_b \rangle$. One can observe that for the k th row of $\mathbf{U} \mathbf{U}^*$:

$$\begin{aligned} \|e_k^\top \mathbf{U} \mathbf{U}^*\|_F &\leq \|e_k^\top \mathbf{E}_L (\mathbf{E}_L^* \mathbf{E}_L)^{-1} \mathbf{E}_L^*\|_F \\ &\leq \|e_k^\top \mathbf{E}_L\|_F \left\| (\mathbf{E}_L^* \mathbf{E}_L)^{-1} \mathbf{E}_L^* \right\| \\ &\leq \sqrt{\frac{\mu_1 c_s r}{n_1 n_2}}. \end{aligned}$$

Similarly, for the l th column of $\mathbf{V} \mathbf{V}^*$, one has $\|\mathbf{V} \mathbf{V}^* e_l\|_F \leq \sqrt{\frac{\mu_1 c_s r}{n_1 n_2}}$. The magnitude of the entries of $\mathbf{U} \mathbf{U}^* \mathbf{A}_a \mathbf{V} \mathbf{V}^*$ can now be bounded by

$$\begin{aligned} |(\mathbf{U} \mathbf{U}^* \mathbf{A}_a \mathbf{V} \mathbf{V}^*)_{k,l}| &\leq \|\mathbf{A}_a\| \|e_k^\top \mathbf{U} \mathbf{U}^*\|_F \|\mathbf{V} \mathbf{V}^* e_l\|_F \\ &\leq \frac{1}{\sqrt{\omega_a}} \frac{\mu_1 c_s r}{n_1 n_2}, \end{aligned}$$

where we used $\|\mathbf{A}_a\| = 1/\sqrt{\omega_a}$. Since \mathbf{A}_b has only ω_b nonzero entries each has magnitude $\frac{1}{\sqrt{\omega_b}}$, one can verify that

$$|\langle \mathbf{U} \mathbf{U}^* \mathbf{A}_a \mathbf{V} \mathbf{V}^*, \mathbf{A}_b \rangle| \leq \left(\max_{k,l} |(\mathbf{U} \mathbf{U}^* \mathbf{A}_a \mathbf{V} \mathbf{V}^*)_{k,l}| \right) \cdot \frac{1}{\sqrt{\omega_b}} \omega_b = \sqrt{\frac{\omega_b}{\omega_a}} \frac{\mu_1 c_s r}{n_1 n_2}. \tag{82}$$

The above bounds (80), (81) and (82) taken together lead to (34).

D Proof of Lemma 3

Define a family of operators

$$\mathcal{Z}_{(k,l)} := \frac{n_1 n_2}{m} \mathcal{P}_T \mathcal{A}_{(k,l)} \mathcal{P}_T - \frac{1}{m} \mathcal{P}_T \mathcal{A} \mathcal{P}_T.$$

for any $(k, l) \in [n_1] \times [n_2]$. For any matrix \mathbf{M} , we can compute

$$\begin{aligned} \mathcal{P}_T \mathcal{A}_{(k,l)} \mathcal{P}_T (\mathbf{M}) &= \mathcal{P}_T (\langle \mathbf{A}_{(k,l)}, \mathcal{P}_T \mathbf{M} \rangle \mathbf{A}_{(k,l)}) \\ &= \mathcal{P}_T (\mathbf{A}_{(k,l)}) \langle \mathcal{P}_T (\mathbf{A}_{(k,l)}), \mathbf{M} \rangle, \end{aligned} \quad (83)$$

and hence

$$\begin{aligned} (\mathcal{P}_T \mathcal{A}_{(k,l)} \mathcal{P}_T)^2 (\mathbf{M}) &= [\mathcal{P}_T \mathcal{A}_{(k,l)} \mathcal{P}_T (\mathbf{A}_{(k,l)})] \langle \mathcal{P}_T (\mathbf{A}_{(k,l)}), \mathbf{M} \rangle \\ &= \langle \mathbf{A}_{(k,l)}, \mathcal{P}_T (\mathbf{A}_{(k,l)}) \rangle \mathcal{P}_T (\mathbf{A}_{(k,l)}) \langle \mathcal{P}_T (\mathbf{A}_{(k,l)}), \mathbf{M} \rangle \\ &= \|\mathcal{P}_T (\mathbf{A}_{(k,l)})\|_{\text{F}}^2 \mathcal{P}_T \mathcal{A}_{(k,l)} \mathcal{P}_T (\mathbf{M}) \\ &\leq \frac{2\mu_1 c_s r}{n_1 n_2} \mathcal{P}_T \mathcal{A}_{(k,l)} \mathcal{P}_T (\mathbf{M}), \end{aligned} \quad (84)$$

where the last inequality follows from (35). This further gives

$$\|\mathcal{P}_T \mathcal{A}_{(k,l)} \mathcal{P}_T\| \leq \frac{2\mu_1 c_s r}{n_1 n_2}. \quad (85)$$

Let \mathbf{a}_i ($1 \leq i \leq m$) be m independent indices uniformly drawn from $[n_1] \times [n_2]$, then we have $\mathbb{E}(\mathcal{Z}_{\mathbf{a}_i}) = 0$ and

$$\|\mathcal{Z}_{\mathbf{a}_i}\| \leq 2 \max_{(k,l) \in [n_1] \times [n_2]} \frac{n_1 n_2}{m} \|\mathcal{P}_T \mathbf{A}_{(k,l)} \mathcal{P}_T\| \leq \frac{4\mu_1 c_s r}{m}.$$

following from (85). Further,

$$\begin{aligned} \mathbb{E} \mathcal{Z}_{\mathbf{a}_i}^2 &= \mathbb{E} \left(\frac{n_1 n_2}{m} \mathcal{P}_T \mathcal{A}_{\mathbf{a}_i} \mathcal{P}_T \right)^2 - \left(\mathbb{E} \left(\frac{n_1 n_2}{m} \mathcal{P}_T \mathcal{A}_{\mathbf{a}_i} \mathcal{P}_T \right) \right)^2 \\ &= \frac{n_1^2 n_2^2}{m^2} \mathbb{E} (\mathcal{P}_T \mathcal{A}_{\mathbf{a}_i} \mathcal{P}_T)^2 - \frac{1}{m^2} (\mathcal{P}_T \mathcal{A} \mathcal{P}_T)^2, \end{aligned}$$

We can then bound the operator norm as

$$\begin{aligned} \sum_{i=1}^m \|\mathbb{E}(\mathcal{Z}_{\mathbf{a}_i}^2)\| &\leq \sum_{i=1}^m \frac{n_1^2 n_2^2}{m^2} \|\mathbb{E}(\mathcal{P}_T \mathcal{A}_{\mathbf{a}_i} \mathcal{P}_T)^2\| + \frac{1}{m} \|(\mathcal{P}_T \mathcal{A} \mathcal{P}_T)^2\| \\ &\leq \frac{n_1^2 n_2^2}{m} \frac{2\mu_1 c_s r}{n_1 n_2} \|\mathbb{E}(\mathcal{P}_T \mathcal{A}_{\mathbf{a}_i} \mathcal{P}_T)\| + \frac{1}{m} \end{aligned} \quad (86)$$

$$\begin{aligned} &= \frac{2\mu_1 c_s r n_1 n_2}{m} \frac{1}{n_1 n_2} \|\mathcal{P}_T \mathcal{A} \mathcal{P}_T\| + \frac{1}{m^2} \\ &\leq \frac{4\mu_1 c_s r}{m}, \end{aligned} \quad (87)$$

where (86) uses (85). Applying Lemma 11 yields that there exists some constant $0 < \epsilon \leq \frac{1}{2}$ such that

$$\left\| \sum_{i=1}^m \mathcal{Z}_{\mathbf{a}_i} \right\| \leq \epsilon$$

with probability exceeding $1 - (n_1 n_2)^{-4}$, provided that $m > c_1 \mu_1 c_s r \log(n_1 n_2)$ for some universal constant $c_1 > 0$.

E Proof of Lemma 4

Suppose that $\mathcal{A}_\Omega = \sum_{i=1}^m \mathcal{A}_{\mathbf{a}_i}$, where \mathbf{a}_i , $1 \leq i \leq m$, are m independent indices drawn uniformly at random from $[n_1] \times [n_2]$. Define

$$\mathbf{S}_{(k,l)} := \frac{n_1 n_2}{m} \mathcal{A}_{(k,l)}(\mathbf{M}) - \frac{1}{m} \mathcal{A}(\mathbf{M}), \quad (k,l) \in [n_1] \times [n_2],$$

which obeys $\mathbb{E}[\mathbf{S}_{\mathbf{a}_i}] = \mathbf{0}$ and

$$\left(\frac{n_1 n_2}{m} \mathcal{A}_\Omega - \mathcal{A} \right)(\mathbf{M}) := \sum_{i=1}^m \mathbf{S}_{\mathbf{a}_i}.$$

In order to apply Lemma 11, one needs to bound $\|\mathbb{E}[\sum_{i=1}^m \mathbf{S}_{\mathbf{a}_i} \mathbf{S}_{\mathbf{a}_i}^*]\|$ and $\|\mathbf{S}_{\mathbf{a}_i}\|$, which we tackle separately in the sequel. Observe that

$$\begin{aligned} \mathbf{0} \preceq \mathbf{S}_{(k,l)} \mathbf{S}_{(k,l)}^* &= \left(\frac{n_1 n_2}{m} \mathcal{A}_{(k,l)}(\mathbf{M}) - \frac{1}{m} \mathcal{A}(\mathbf{M}) \right) \left(\frac{n_1 n_2}{m} \mathcal{A}_{(k,l)}(\mathbf{M}) - \frac{1}{m} \mathcal{A}(\mathbf{M}) \right)^* \\ &\preceq \left(\frac{n_1 n_2}{m} \right)^2 \mathcal{A}_{(k,l)}(\mathbf{M}) (\mathcal{A}_{(k,l)}(\mathbf{M}))^* \\ &= \left(\frac{n_1 n_2}{m} \right)^2 |\langle \mathbf{A}_{(k,l)}, \mathbf{M} \rangle|^2 \mathbf{A}_{(k,l)} \cdot \mathbf{A}_{(k,l)}^\top \\ &\preceq \left(\frac{n_1 n_2}{m} \right)^2 \frac{|\langle \mathbf{A}_{(k,l)}, \mathbf{M} \rangle|^2}{\omega_{k,l}} \mathbf{I}, \end{aligned}$$

where the first inequality follows since $\mathbb{E}[\frac{n_1 n_2}{m} \mathcal{A}_{(k,l)}(\mathbf{M})] = \frac{1}{m} \mathcal{A}(\mathbf{M})$, and the last inequality arises from the fact that all non-zero entries of $\mathbf{A}_{(k,l)} \cdot \mathbf{A}_{(k,l)}^\top$ lie on its diagonal and are bounded in magnitude by $\frac{1}{\omega_{k,l}}$. This immediately suggests

$$\begin{aligned} \left\| \mathbb{E} \left[\sum_{i=1}^m \mathbf{S}_{\mathbf{a}_i} \mathbf{S}_{\mathbf{a}_i}^* \right] \right\| &= \frac{m}{n_1 n_2} \left\| \sum_{(k,l) \in [n_1] \times [n_2]} \mathbf{S}_{(k,l)} \mathbf{S}_{(k,l)}^* \right\| \\ &\leq \frac{m}{n_1 n_2} \left\| \left(\frac{n_1 n_2}{m} \right)^2 \left(\sum_{(k,l) \in [n_1] \times [n_2]} \frac{|\langle \mathbf{A}_{(k,l)}, \mathbf{M} \rangle|^2}{\omega_{k,l}} \right) \mathbf{I} \right\| \\ &= \frac{n_1 n_2}{m} \|\mathbf{M}\|_{\mathcal{A},2}^2, \end{aligned} \tag{88}$$

where the last equality follows from the definition of $\|\mathbf{M}\|_{\mathcal{A},2}$. Following the same argument, one can derive the same bound for $\|\mathbb{E}[\sum_{i=1}^m \mathbf{S}_{\mathbf{a}_i}^* \mathbf{S}_{\mathbf{a}_i}]\|$ as well.

On the other hand, the operator norm of each $\mathbf{S}_{(k,l)}$ can be bounded as follows

$$\begin{aligned} \|\mathbf{S}_{(k,l)}\| &\leq \left\| \frac{n_1 n_2}{m} \mathcal{A}_{(k,l)}(\mathbf{M}) \right\| + \left\| \frac{1}{m} \mathcal{A}(\mathbf{M}) \right\| \\ &\leq 2 \max_{(k,l) \in [n_1] \times [n_2]} \left\| \frac{n_1 n_2}{m} \mathcal{A}_{(k,l)}(\mathbf{M}) \right\| \\ &= \frac{2n_1 n_2}{m} \max_{(k,l) \in [n_1] \times [n_2]} \|\langle \mathbf{A}_{(k,l)}, \mathbf{M} \rangle \mathbf{A}_{(k,l)}\| \\ &= \frac{2n_1 n_2}{m} \max_{(k,l) \in [n_1] \times [n_2]} \left| \frac{\langle \mathbf{A}_{(k,l)}, \mathbf{M} \rangle}{\sqrt{\omega_{k,l}}} \right| = \frac{2n_1 n_2}{m} \|\mathbf{M}\|_{\mathcal{A},\infty}, \end{aligned} \tag{89}$$

where (89) holds since $\|\mathbf{A}_{(k,l)}\| = \frac{1}{\sqrt{\omega_{k,l}}}$ and the last equality follows by applying the definition of $\|\cdot\|_{\mathcal{A},\infty}$.

Finally, we combine the above two bounds together with Bernstein inequality (Lemma 11) to obtain

$$\left\| \left(\frac{n_1 n_2}{m} \mathcal{A}_\Omega - \mathcal{A} \right)(\mathbf{M}) \right\| \leq c_2 \left(\sqrt{\frac{n_1 n_2 \log(n_1 n_2)}{m}} \|\mathbf{M}\|_{\mathcal{A},2} + \frac{2n_1 n_2 \log(n_1 n_2)}{m} \|\mathbf{M}\|_{\mathcal{A},\infty} \right)$$

with high probability, where $c_2 > 0$ is some absolute constant.

F Proof of Lemma 5

Write $\mathcal{A}_\Omega = \sum_{i=1}^m \mathcal{A}_{\mathbf{a}_i}$, where \mathbf{a}_i ($1 \leq i \leq m$) are m independent indices uniformly drawn from $[n_1] \times [n_2]$. By the definition of $\|\mathbf{M}\|_{\mathcal{A},2}$, we need to examine the components

$$\frac{1}{\sqrt{\omega_{k,l}}} \left\langle \mathbf{A}_{(k,l)}, \left(\frac{n_1 n_2}{m} \mathcal{P}_T \mathcal{A}_\Omega - \mathcal{P}_T \mathcal{A} \right) (\mathbf{M}) \right\rangle$$

for all $(k,l) \in [n_1] \times [n_2]$.

Define a set of variables $z_{(\alpha,\beta)}$'s to be

$$z_{(\alpha,\beta)}^{(k,l)} := \frac{1}{\sqrt{\omega_{k,l}}} \left\langle \mathbf{A}_{(k,l)}, \frac{n_1 n_2}{m} \mathcal{P}_T \mathcal{A}_{(\alpha,\beta)} (\mathbf{M}) - \frac{1}{m} \mathcal{P}_T \mathcal{A} (\mathbf{M}) \right\rangle, \quad (90)$$

thus resulting in

$$\frac{1}{\sqrt{\omega_{k,l}}} \left\langle \mathbf{A}_{(k,l)}, \left(\frac{n_1 n_2}{m} \mathcal{P}_T \mathcal{A}_\Omega - \mathcal{P}_T \mathcal{A} \right) (\mathbf{M}) \right\rangle := \sum_{i=1}^m z_{\mathbf{a}_i}^{(k,l)}.$$

The definition of $\|\mathbf{M}\|_{\mathcal{A},2}$ allows us to express

$$\left\| \left(\frac{n_1 n_2}{m} \mathcal{P}_T \mathcal{A}_\Omega - \mathcal{P}_T \mathcal{A} \right) (\mathbf{M}) \right\|_{\mathcal{A},2} = \left\| \sum_{i=1}^m z_{\mathbf{a}_i} \right\|_2, \quad (91)$$

where $z_{(\alpha,\beta)}$'s are defined to be $n_1 n_2$ -dimensional vector

$$\mathbf{z}_{(\alpha,\beta)} := \left[z_{(\alpha,\beta)}^{(k,l)} \right]_{(k,l) \in [n_1] \times [n_2]}, \quad (\alpha, \beta) \in [n_1] \times [n_2].$$

For any random vector $\mathbf{v} \in \mathcal{V}$, one can easily bound $\|\mathbf{v} - \mathbb{E}\mathbf{v}\|_2 \leq 2 \sup_{\tilde{\mathbf{v}} \in \mathcal{V}} \|\tilde{\mathbf{v}}\|_2$. Observing that $\mathbb{E}[\mathbf{z}_{(\alpha,\beta)}] = \mathbf{0}$, we can bound

$$\begin{aligned} \|\mathbf{z}_{(\alpha,\beta)}\|_2 &\leq 2 \sqrt{\sum_{k,l} \frac{1}{\omega_{k,l}} \left| \left\langle \mathbf{A}_{(k,l)}, \frac{2n_1 n_2}{m} \mathcal{P}_T \mathcal{A}_{(\alpha,\beta)} (\mathbf{M}) \right\rangle \right|^2} \\ &= \frac{2n_1 n_2}{m} \sqrt{\sum_{k,l} \frac{1}{\omega_{k,l}} \left| \left\langle \mathbf{A}_{(k,l)}, \mathcal{P}_T (\mathbf{A}_{(\alpha,\beta)}) \right\rangle \left\langle \mathbf{A}_{(\alpha,\beta)}, \mathbf{M} \right\rangle \right|^2} \\ &= \frac{2n_1 n_2}{m} \frac{|\langle \mathbf{A}_{(\alpha,\beta)}, \mathbf{M} \rangle|}{\sqrt{\omega_{\alpha,\beta}}} \sqrt{\sum_{k,l} \frac{\omega_{\alpha,\beta} |\langle \mathbf{A}_{(k,l)}, \mathcal{P}_T (\mathbf{A}_{(\alpha,\beta)}) \rangle|^2}{\omega_{k,l}}} \\ &\leq \frac{2n_1 n_2}{m} \frac{|\langle \mathbf{A}_{(\alpha,\beta)}, \mathbf{M} \rangle|}{\sqrt{\omega_{\alpha,\beta}}} \sqrt{\frac{\mu_5 r}{n_1 n_2}} = 2 \sqrt{\frac{n_1 n_2}{m}} \cdot \frac{\mu_5 r}{m} \frac{|\langle \mathbf{A}_{(\alpha,\beta)}, \mathbf{M} \rangle|}{\sqrt{\omega_{\alpha,\beta}}}, \end{aligned} \quad (92)$$

where (92) follows from the definition of μ_5 in (43). Now it follows that

$$\begin{aligned} \|\mathbf{z}_{\mathbf{a}_i}\|_2 &\leq \max_{\alpha,\beta} \|\mathbf{z}_{(\alpha,\beta)}\|_2 \\ &\leq \max_{\alpha,\beta} 2 \sqrt{\frac{n_1 n_2}{m}} \cdot \frac{\mu_5 r}{m} \frac{|\langle \mathbf{A}_{(\alpha,\beta)}, \mathbf{M} \rangle|}{\sqrt{\omega_{\alpha,\beta}}} \\ &\leq 2 \sqrt{\frac{n_1 n_2}{m}} \cdot \frac{\mu_5 r}{m} \|\mathbf{M}\|_{\mathcal{A},\infty}, \end{aligned} \quad (93)$$

where (93) follows from (40). On the other hand,

$$\begin{aligned}
\left| \mathbb{E} \left[\sum_{i=1}^m \mathbf{z}_{\mathbf{a}_i}^* \mathbf{z}_{\mathbf{a}_i} \right] \right| &= \frac{m}{n_1 n_2} \sum_{\alpha, \beta} \|\mathbf{z}_{(\alpha, \beta)}\|_2^2 \\
&\leq \frac{m}{n_1 n_2} \sum_{\alpha, \beta} 4 \frac{n_1 n_2}{m} \cdot \frac{\mu_5 r}{m} \frac{|\langle \mathbf{A}_{(\alpha, \beta)}, \mathbf{M} \rangle|^2}{\omega_{\alpha, \beta}} \\
&= \frac{4\mu_5 r}{m} \|\mathbf{M}\|_{\mathcal{A}, 2}^2.
\end{aligned}$$

which again follows from (41). Since $\mathbf{z}_{\mathbf{a}_i}$'s are vectors, we immediately obtain $\|\mathbb{E} [\sum_{i=1}^m \mathbf{z}_{\mathbf{a}_i} \mathbf{z}_{\mathbf{a}_i}^*]\| = \|\mathbb{E} [\sum_{i=1}^m \mathbf{z}_{\mathbf{a}_i}^* \mathbf{z}_{\mathbf{a}_i}]\|$. Applying Lemma 11 then suggests that

$$\left\| \left(\frac{n_1 n_2}{m} \mathcal{P}_T \mathcal{A}_\Omega - \mathcal{P}_T \mathcal{A} \right) (\mathbf{M}) \right\|_{\mathcal{A}, 2} \leq c_3 \left(\sqrt{\frac{\mu_5 r \log(n_1 n_2)}{m}} \|\mathbf{M}\|_{\mathcal{A}, 2} + \sqrt{\frac{n_1 n_2}{m} \cdot \frac{\mu_5 r}{m} \log(n_1 n_2)} \|\mathbf{M}\|_{\mathcal{A}, \infty} \right)$$

with high probability for some numerical constant $c_3 > 0$, which completes the proof.

G Proof of Lemma 6

From Appendix F, it is straightforward that

$$\left\| \left(\frac{n_1 n_2}{m} \mathcal{P}_T \mathcal{A}_\Omega - \mathcal{P}_T \mathcal{A} \right) (\mathbf{M}) \right\|_{\mathcal{A}, \infty} = \max_{k, l} \left| \sum_{i=1}^m z_{\mathbf{a}_i}^{(k, l)} \right|, \quad (94)$$

where $z_{\mathbf{a}_i}^{(k, l)}$'s are defined as (90). Using similar techniques as (92), we can obtain

$$\begin{aligned}
\left| z_{(\alpha, \beta)}^{(k, l)} \right| &\leq 2 \max_{k, l} \frac{1}{\sqrt{\omega_{k, l}}} \left| \left\langle \mathbf{A}_{(k, l)}, \frac{n_1 n_2}{m} \mathcal{P}_T (\mathbf{A}_{(\alpha, \beta)}) \langle \mathbf{A}_{(\alpha, \beta)}, \mathbf{M} \rangle \right\rangle \right| \\
&\leq 2 \max_{k, l} \frac{1}{\sqrt{\omega_{k, l}}} \sqrt{\frac{\omega_{k, l}}{\omega_{\alpha, \beta}}} \frac{3\mu_1 c_s r}{n_1 n_2} \frac{n_1 n_2}{m} |\langle \mathbf{A}_{(\alpha, \beta)}, \mathbf{M} \rangle| \\
&= \frac{6\mu_1 c_s r}{m} \frac{1}{\sqrt{\omega_{\alpha, \beta}}} |\langle \mathbf{A}_{(\alpha, \beta)}, \mathbf{M} \rangle|.
\end{aligned}$$

which follows from (34). Therefore $\left| z_{(\alpha, \beta)}^{(k, l)} \right| \leq \frac{6\mu_1 c_s r}{m} \|\mathbf{M}\|_{\mathcal{A}, \infty}$ and

$$\begin{aligned}
\mathbb{E} \left[\sum_{i=1}^m |z_{\mathbf{a}_i}^{(k, l)}|^2 \right] &= \frac{m}{n_1 n_2} \sum_{\alpha, \beta} \left| z_{(\alpha, \beta)}^{(k, l)} \right|^2 \\
&\leq \frac{m}{n_1 n_2} \left(\frac{6\mu_1 c_s r}{m} \right)^2 \sum_{\alpha, \beta} \frac{1}{\omega_{\alpha, \beta}} |\langle \mathbf{A}_{(\alpha, \beta)}, \mathbf{M} \rangle|^2 \\
&= \frac{36\mu_1^2 c_s^2 r^2}{m n_1 n_2} \|\mathbf{M}\|_{\mathcal{A}, 2}^2.
\end{aligned}$$

The Bernstein inequality in Lemma 11 taken collectively with the union bound yields that

$$\begin{aligned}
&\left\| \left(\frac{n_1 n_2}{m} \mathcal{P}_T \mathcal{A}_\Omega - \mathcal{P}_T \mathcal{A} \right) (\mathbf{M}) \right\|_{\mathcal{A}, \infty} \\
&\leq c_4 \left(\sqrt{\frac{\mu_1 c_s r \log(n_1 n_2)}{m}} \cdot \sqrt{\frac{\mu_1 c_s r}{n_1 n_2}} \|\mathbf{M}\|_{\mathcal{A}, 2} + \frac{\mu_1 c_s r \log(n_1 n_2)}{m} \|\mathbf{M}\|_{\mathcal{A}, \infty} \right)
\end{aligned}$$

with high probability for some constant $c_4 > 0$, completing the proof.

H Proof of Lemma 7

To bound $\|UV^*\|_{\mathcal{A},\infty}$, observe that there exists a unitary matrix B such that

$$UV^* = E_L (E_L^* E_L)^{-\frac{1}{2}} B (E_R E_R^*)^{-\frac{1}{2}} E_R.$$

For any $(k, l) \in [n_1] \times [n_2]$, we can then bound

$$\begin{aligned} |(UV^*)_{k,l}| &= |e_k^\top E_L (E_L^* E_L)^{-\frac{1}{2}} B (E_R E_R^*)^{-\frac{1}{2}} E_R e_l| \\ &\leq \|e_k^\top E_L\|_F \left\| (E_L^* E_L)^{-\frac{1}{2}} \right\| \|B\| \left\| (E_R^* E_R)^{-\frac{1}{2}} \right\| \|E_R e_l\|_F \\ &\leq \sqrt{\frac{r}{k_1 k_2}} \mu_1 \sqrt{\frac{r}{(n_1 - k_1 + 1)(n_2 - k_2 + 1)}} \\ &\leq \frac{\mu_1 c_s r}{n_1 n_2}. \end{aligned}$$

Since $A_{(k,l)}$ has only $\omega_{k,l}$ nonzero entries each of magnitude $\frac{1}{\sqrt{\omega_{k,l}}}$, this leads to

$$\begin{aligned} \|UV^*\|_{\mathcal{A},\infty} &= \frac{1}{\omega_{k,l}} \left| \sum_{(\alpha,\beta) \in \Omega_e(k,l)} (UV^*)_{\alpha,\beta} \right| \\ &\leq \max_{k,l} |(UV^*)_{k,l}| \leq \frac{\mu_1 c_s r}{n_1 n_2}. \end{aligned}$$

The rest is to bound $\|UV^*\|_{\mathcal{A},2}$ and $\|\mathcal{P}_T(\sqrt{\omega_{k,l}} A_{(k,l)})\|_{\mathcal{A},2}$. Observe that the i th row of UV^* obeys

$$\begin{aligned} \|e_i^\top UV^*\|_F^2 &= \|e_i^\top U\|_F^2 = \|e_i^\top E_L (E_L^* E_L)^{-\frac{1}{2}}\|_F^2 \leq \|e_i^\top E_L\|_F^2 \|(E_L^* E_L)^{-1}\|_F \\ &\leq \mu_1 \|e_i^\top E_L\|_F^2 \leq \frac{\mu_1 c_s r}{n_1 n_2}. \end{aligned} \tag{95}$$

That said, the total energy allocated to any row of UV^* cannot exceed $\frac{\mu_1 c_s r}{n_1 n_2}$.

Moreover, the matrix $\mathcal{P}_T(\sqrt{\omega_{\alpha,\beta}} A_{(\alpha,\beta)})$ exhibits the above property as well, which we briefly reason as follows. First, the matrix $UU^*(\sqrt{\omega_{\alpha,\beta}} A_{(\alpha,\beta)})$ obeys

$$\|e_i^\top UU^*(\sqrt{\omega_{\alpha,\beta}} A_{(\alpha,\beta)})\|_F^2 \leq \|e_i^\top U\|_F^2 \|U^*\|^2 \|\sqrt{\omega_{\alpha,\beta}} A_{(\alpha,\beta)}\|^2 \leq \frac{\mu_1 c_s r}{n_1 n_2},$$

since the operator norm of U and $\sqrt{\omega_{\alpha,\beta}} A_{(\alpha,\beta)}$ are both bounded by 1. The same bound for $\sqrt{\omega_{\alpha,\beta}} A_{(\alpha,\beta)} VV^*$ can be demonstrated via the same argument as for $UU^*(\sqrt{\omega_{\alpha,\beta}} A_{(\alpha,\beta)})$. Additionally, for $UU^*(\sqrt{\omega_{\alpha,\beta}} A_{(\alpha,\beta)}) VV^*$ one has

$$\begin{aligned} \|e_i^\top UU^*(\sqrt{\omega_{\alpha,\beta}} A_{(\alpha,\beta)}) VV^*\|_F^2 &\leq \|e_i^\top U\|_F^2 \|U^*\|^2 \|VV^*\|^2 \|\sqrt{\omega_{\alpha,\beta}} A_{(\alpha,\beta)}\|^2 \\ &\leq \frac{\mu_1 c_s r}{n_1 n_2}. \end{aligned}$$

By definition of \mathcal{P}_T ,

$$\begin{aligned} \|e_i^\top \mathcal{P}_T(\sqrt{\omega_{\alpha,\beta}} A_{(\alpha,\beta)})\|_F^2 &\leq 3 \|e_i^\top UU^*(\sqrt{\omega_{\alpha,\beta}} A_{(\alpha,\beta)})\|_F^2 + 3 \|e_i^\top (\sqrt{\omega_{\alpha,\beta}} A_{(\alpha,\beta)}) VV^*\|_F^2 \\ &\quad + 3 \|e_i^\top UU^*(\sqrt{\omega_{\alpha,\beta}} A_{(\alpha,\beta)}) VV^*\|_F^2 \\ &\leq \frac{9\mu_1 c_s r}{n_1 n_2}. \end{aligned}$$

Now our task boils down to bounding $\|M\|_{\mathcal{A},2}$ for some matrix M satisfying some energy constraints per row, which subsumes $\|UV^*\|_{\mathcal{A},2}$ and $\|\mathcal{P}_T(\sqrt{\omega_{k,l}} A_{(k,l)})\|_{\mathcal{A},2}$ as special cases. We can then conclude the proof by applying the following lemma.

Lemma 12. Denote by the set \mathcal{M} of feasible matrices satisfying

$$\max_i \|\mathbf{e}_i^\top \mathbf{M}\|_F^2 \leq \frac{3\mu_1 c_s r}{n_1 n_2}. \quad (96)$$

Then there exists some universal constant $c_3 > 0$ such that

$$\max_{\mathbf{M} \in \mathcal{M}} \|\mathbf{M}\|_{\mathcal{A},2}^2 \leq c_3 \frac{\mu_1 c_s r}{n_1 n_2} \log(n_1 n_2). \quad (97)$$

Proof. For ease of presentation, we split any matrix \mathbf{M} into 4 parts, which are defined as follows

- $\mathbf{M}^{(1)}$: the matrix containing all upper triangular components of all upper triangular blocks of \mathbf{M} ;
- $\mathbf{M}^{(2)}$: the matrix containing all lower triangular components of all upper triangular blocks of \mathbf{M} ;
- $\mathbf{M}^{(3)}$: the matrix containing all upper triangular components of all lower triangular blocks of \mathbf{M} ;
- $\mathbf{M}^{(4)}$: the matrix containing all lower triangular components of all lower triangular blocks of \mathbf{M} .

Here, we use the term “upper triangular” and “lower triangular” in short for “left upper triangular” and “right lower triangular”, which are more natural for Hankel matrices. Instead of maximizing $\|\mathbf{M}\|_{\mathcal{A},2}$ directly, we will handle $\max_{\mathbf{M} \in \mathcal{M}} \|\mathbf{M}^{(l)}\|_{\mathcal{A},2}^2$ for each $1 \leq l \leq 4$ separately, owing to the fact that

$$\max_{\mathbf{M} \in \mathcal{M}} \|\mathbf{M}\|_{\mathcal{A},2}^2 \leq \sum_{l=1}^4 \max_{\mathbf{M}: \mathbf{M}^{(l)} \in \mathcal{M}} \|\mathbf{M}^{(l)}\|_{\mathcal{A},2}^2. \quad (98)$$

In the sequel, we only demonstrate how to control $\|\mathbf{M}^{(1)}\|_{\mathcal{A},2}$. Similar bounds can be derived for $\|\mathbf{M}^{(l)}\|_{\mathcal{A},2}$ ($2 \leq l \leq 4$) via the same argument.

To facilitate analysis, we divide the entire index set into several subsets $\mathcal{W}_{i,j}$ such that for all $1 \leq i \leq \lceil \log(n_1) \rceil$ and $1 \leq j \leq \lceil \log(n_2) \rceil$,

$$\mathcal{W}_{i,j} := \bigcup \{ \Omega_e(k,l) \mid (k,l) \in [2^{i-1}, 2^i] \times [2^{j-1}, 2^j] \}. \quad (99)$$

Consequently, for each $\Omega_e(k,l) \subseteq \mathcal{W}_{i,j}$, one has

$$2^{i-1} \cdot 2^{j-1} \leq \omega_{k,l} \leq 2^{i+j}.$$

This allows us to derive for each $\mathcal{W}_{i,j}$ that

$$\sum_{(k,l) \in \mathcal{W}_{i,j}} \frac{1}{\omega_{k,l}^2} \left| \sum_{(\alpha,\beta) \in \Omega_e(k,l)} \mathbf{M}_{\alpha,\beta}^{(1)} \right|^2 \leq \sum_{(k,l) \in \mathcal{W}_{i,j}} \frac{1}{\omega_{k,l}} \sum_{(\alpha,\beta) \in \Omega_e(k,l)} \left| \mathbf{M}_{\alpha,\beta}^{(1)} \right|^2 \quad (100)$$

$$\leq \frac{1}{2^{i+j-2}} \sum_{(k,l) \in \mathcal{W}_{i,j}} \sum_{(\alpha,\beta) \in \Omega_e(k,l)} \left| \mathbf{M}_{\alpha,\beta}^{(1)} \right|^2, \quad (101)$$

where (100) follows from the RMS-AM (root-mean square v.s. arithmetic mean) inequality.

Observe that the indices contained in $\mathcal{W}_{i,j}$ reside within no more than $2^i \cdot 2^j$ rows. By assumption (96), the total energy allocated to $\mathcal{W}_{i,j}$ must be bounded above by

$$\sum_{(k,l) \in \mathcal{W}_{i,j}} \sum_{(\alpha,\beta) \in \Omega_e(k,l)} \left| \mathbf{M}_{\alpha,\beta}^{(1)} \right|^2 \leq 2^i \cdot 2^j \max_i \|\mathbf{e}_i^\top \mathbf{M}\|_F^2 \leq 2^{i+j} \cdot \frac{3\mu_1 c_s r}{n_1 n_2}.$$

Substituting it into (101) immediately leads to

$$\sum_{(k,l) \in \mathcal{W}_{i,j}} \frac{1}{\omega_{k,l}^2} \left| \sum_{(\alpha,\beta) \in \Omega_e(k,l)} \mathbf{M}_{\alpha,\beta}^{(1)} \right|^2 \leq \frac{12\mu_1 c_s r}{n_1 n_2}. \quad (102)$$

By definition,

$$\|\mathbf{M}\|_{\mathcal{A},2}^2 = \sum_{1 \leq i \leq \lceil \log n_1 \rceil, 1 \leq j \leq \lceil \log n_2 \rceil} \sum_{(k,l) \in \mathcal{W}_{i,j}} \frac{\left| \sum_{(\alpha,\beta) \in \Omega_e(k,l)} \mathbf{M}_{\alpha,\beta} \right|^2}{\omega_{k,l}^2}.$$

Combining the above bounds over all $\mathcal{W}_{i,j}$ then gives

$$\left\| \mathbf{M}^{(1)} \right\|_{\mathcal{A},2}^2 \leq \frac{12\mu_1 c_s r \lceil \log(n_1) \rceil \cdot \lceil \log(n_2) \rceil}{n_1 n_2}$$

as claimed. \square

I Proof of Lemma 8

Suppose there is a non-zero perturbation (\mathbf{H}, \mathbf{T}) such that $(\mathbf{X} + \mathbf{H}, \mathbf{S} + \mathbf{T})$ is the optimizer of Robust-EMaC. One can easily verify that $\mathcal{P}_{\Omega^\perp}(\mathbf{S} + \mathbf{T}) = 0$, otherwise we can always set $\mathbf{S} + \mathbf{T}$ as $\mathcal{P}_{\Omega}(\mathbf{S} + \mathbf{T})$ to yield a better estimate. This together with the fact that $\mathcal{P}_{\Omega^\perp}(\mathbf{S}) = 0$ implies that $\mathcal{P}_{\Omega}(\mathbf{T}) = \mathbf{T}$. Observe that the constraints of Robust-EMaC indicate

$$\mathcal{P}_{\Omega}(\mathbf{X} + \mathbf{S}) = \mathcal{P}_{\Omega}(\mathbf{X} + \mathbf{H} + \mathbf{S} + \mathbf{T}) \Rightarrow \mathcal{P}_{\Omega}(\mathbf{H} + \mathbf{T}) = 0,$$

which is equivalent to requiring $\mathcal{A}'_{\Omega}(\mathbf{H}_e) = -\mathcal{A}'_{\Omega}(\mathbf{T}_e) = -\mathbf{T}_e$ and $\mathcal{A}^{\perp}(\mathbf{H}_e) = 0$.

Recall that \mathbf{H}_e and \mathbf{S}_e are the enhanced forms of \mathbf{H} and \mathbf{S} , respectively. Set $\mathbf{W}_0 \in T^{\perp}$ to be a matrix satisfying $\langle \mathbf{W}_0, \mathcal{P}_{T^{\perp}}(\mathbf{H}_e) \rangle = \|\mathcal{P}_{T^{\perp}}(\mathbf{H}_e)\|_*$ and $\|\mathbf{W}_0\| \leq 1$, then $UV^* + \mathbf{W}_0$ is a sub-gradient of the nuclear norm at \mathbf{X}_e . This gives

$$\begin{aligned} \|\mathbf{X}_e + \mathbf{H}_e\|_* &\geq \|\mathbf{X}_e\|_* + \langle UV^* + \mathbf{W}_0, \mathbf{H}_e \rangle \\ &= \|\mathbf{X}_e\|_* + \langle UV^*, \mathbf{H}_e \rangle + \|\mathcal{P}_{T^{\perp}}(\mathbf{H}_e)\|_*. \end{aligned} \quad (103)$$

Owing to the fact that $\text{support}(\mathbf{S}) \subseteq \Omega^{\text{dirty}}$, one has $\mathbf{S}_e = \mathcal{A}'_{\Omega^{\text{dirty}}}(\mathbf{S}_e)$. Combining this and the fact that $\text{support}(\mathbf{S}_e + \mathbf{T}_e) \subseteq \Omega$ yields

$$\|\mathbf{S}_e + \mathbf{T}_e\|_1 = \|\mathcal{A}'_{\Omega^{\text{clean}}}(\mathbf{T}_e)\|_1 + \|\mathbf{S}_e + \mathcal{A}'_{\Omega^{\text{dirty}}}(\mathbf{T}_e)\|_1,$$

which further gives

$$\begin{aligned} \|\mathbf{S}_e + \mathbf{T}_e\|_1 - \|\mathbf{S}_e\|_1 &= \|\mathcal{A}'_{\Omega^{\text{clean}}}(\mathbf{T}_e)\|_1 + \|\mathbf{S}_e + \mathcal{A}'_{\Omega^{\text{dirty}}}(\mathbf{T}_e)\|_1 - \|\mathbf{S}_e\|_1 \\ &\geq \|\mathcal{A}'_{\Omega^{\text{clean}}}(\mathbf{T}_e)\|_1 + \langle \text{sgn}(\mathbf{S}_e), \mathcal{A}'_{\Omega^{\text{dirty}}}(\mathbf{T}_e) \rangle \end{aligned} \quad (104)$$

$$= \|\mathcal{A}'_{\Omega^{\text{clean}}}(\mathbf{T}_e)\|_1 - \langle \text{sgn}(\mathbf{S}_e), \mathcal{A}'_{\Omega^{\text{dirty}}}(\mathbf{H}_e) \rangle \quad (105)$$

$$\begin{aligned} &= \|\mathcal{A}'_{\Omega^{\text{clean}}}(\mathbf{T}_e)\|_1 - \langle \mathcal{A}'_{\Omega^{\text{dirty}}}(\text{sgn}(\mathbf{S}_e)), \mathbf{H}_e \rangle \\ &= \|\mathcal{A}'_{\Omega^{\text{clean}}}(\mathbf{H}_e)\|_1 - \langle \text{sgn}(\mathbf{S}_e), \mathbf{H}_e \rangle. \end{aligned} \quad (106)$$

Here, (104) follows from the fact that $\text{sgn}(\mathbf{S}_e)$ is the sub-gradient of $\|\cdot\|_1$ at \mathbf{S}_e , and (105) arises from the identity $\mathcal{P}_{\Omega^{\text{dirty}}}(\mathbf{H} + \mathbf{T}) = 0$ and hence $\mathcal{A}'_{\Omega^{\text{dirty}}}(\mathbf{H}_e) = -\mathcal{A}'_{\Omega^{\text{dirty}}}(\mathbf{T}_e)$. The inequalities (103) and (106) taken collectively lead to

$$\begin{aligned} &\|\mathbf{X}_e + \mathbf{H}_e\|_* + \lambda \|\mathbf{S}_e + \mathbf{T}_e\|_1 - (\|\mathbf{X}_e\|_* + \lambda \|\mathbf{S}_e\|_1) \\ &\geq \langle UV^*, \mathbf{H}_e \rangle + \|\mathcal{P}_{T^{\perp}}(\mathbf{H}_e)\|_* + \lambda \|\mathcal{A}'_{\Omega^{\text{clean}}}(\mathbf{H}_e)\|_1 - \lambda \langle \text{sgn}(\mathbf{S}_e), \mathbf{H}_e \rangle \\ &\geq -\langle \lambda \text{sgn}(\mathbf{S}_e) - UV^*, \mathbf{H}_e \rangle + \|\mathcal{P}_{T^{\perp}}(\mathbf{H}_e)\|_* + \lambda \|\mathcal{A}'_{\Omega^{\text{clean}}}(\mathbf{H}_e)\|_1. \end{aligned} \quad (107)$$

It remains to show that the right-hand side of (107) cannot be negative. For a dual matrix \mathbf{W} satisfying

Conditions (56), one can derive

$$\begin{aligned}
& \langle \lambda \text{sgn}(\mathbf{S}_e) - \mathbf{UV}^*, \mathbf{H}_e \rangle \\
&= \langle \mathbf{W} + \lambda \text{sgn}(\mathbf{S}_e) - \mathbf{UV}^*, \mathbf{H}_e \rangle - \langle \mathbf{W}, \mathbf{H}_e \rangle \\
&= \langle \mathcal{P}_T(\mathbf{W} + \lambda \text{sgn}(\mathbf{S}_e) - \mathbf{UV}^*), \mathcal{P}_T(\mathbf{H}_e) \rangle + \langle \mathcal{P}_{T^\perp}(\mathbf{W} + \lambda \text{sgn}(\mathbf{S}_e) - \mathbf{UV}^*), \mathcal{P}_{T^\perp}(\mathbf{H}_e) \rangle \\
&\quad - \langle \mathcal{A}'_{\Omega^{\text{clean}}}(\mathbf{W}), \mathcal{A}'_{\Omega^{\text{clean}}}(\mathbf{H}_e) \rangle - \langle \mathcal{A}'_{(\Omega^{\text{clean}})^\perp}(\mathbf{W}), \mathcal{A}'_{(\Omega^{\text{clean}})^\perp}(\mathbf{H}_e) \rangle. \\
&\leq \frac{\lambda}{n_1^2 n_2^2} \|\mathcal{P}_T(\mathbf{H}_e)\|_F + \frac{1}{4} \|\mathcal{P}_{T^\perp}(\mathbf{H}_e)\|_* + \frac{\lambda}{4} \|\mathcal{A}'_{\Omega^{\text{clean}}}(\mathbf{H}_e)\|_1,
\end{aligned} \tag{108}$$

where the last inequality follows from the four properties of \mathbf{W} in (56). Since $(\mathbf{X} + \mathbf{H}, \mathbf{S} + \mathbf{T})$ is assumed to be the optimizer, substituting (108) into (107) then yields

$$0 \geq \|\mathbf{X}_e + \mathbf{H}_e\|_* + \lambda \|\mathbf{S}_e + \mathbf{T}_e\|_1 - (\|\mathbf{X}_e\|_* + \lambda \|\mathbf{S}_e\|_1) \tag{109}$$

$$\begin{aligned}
&\geq \frac{3}{4} \|\mathcal{P}_{T^\perp}(\mathbf{H}_e)\|_* + \frac{3}{4} \lambda \|\mathcal{A}'_{\Omega^{\text{clean}}}(\mathbf{H}_e)\|_1 - \frac{\lambda}{n_1^2 n_2^2} \|\mathcal{P}_T(\mathbf{H}_e)\|_F \\
&\geq \frac{3}{4} \|\mathcal{P}_{T^\perp}(\mathbf{H}_e)\|_* + \frac{3}{4} \lambda \|\mathcal{A}'_{\Omega^{\text{clean}}}(\mathbf{H}_e)\|_F - \frac{\lambda}{n_1^2 n_2^2} \|\mathcal{P}_T(\mathbf{H}_e)\|_F,
\end{aligned} \tag{110}$$

where (110) arises due to the inequality $\|\mathbf{M}\|_F \leq \|\mathbf{M}\|_1$.

The invertibility condition (54) on $\mathcal{P}_T \mathcal{A}_{\Omega^{\text{clean}}} \mathcal{P}_T$ is equivalent to

$$\left\| \mathcal{P}_T - \mathcal{P}_T \left(\frac{1}{\rho(1-s)} \mathcal{A}_{\Omega^{\text{clean}}} + \mathcal{A}^\perp \right) \mathcal{P}_T \right\| \leq \frac{1}{2},$$

indicating that

$$\frac{1}{2} \|\mathcal{P}_T(\mathbf{H}_e)\|_F \leq \left\| \mathcal{P}_T \left(\frac{1}{\rho(1-s)} \mathcal{A}_{\Omega^{\text{clean}}} + \mathcal{A}^\perp \right) \mathcal{P}_T(\mathbf{H}_e) \right\|_F \leq \frac{3}{2} \|\mathcal{P}_T(\mathbf{H}_e)\|_F.$$

One can, therefore, bound $\|\mathcal{P}_T(\mathbf{H}_e)\|_F$ as follows

$$\begin{aligned}
\|\mathcal{P}_T(\mathbf{H}_e)\|_F &\leq 2 \left\| \mathcal{P}_T \left(\frac{1}{\rho(1-s)} \mathcal{A}_{\Omega^{\text{clean}}} + \mathcal{A}^\perp \right) \mathcal{P}_T(\mathbf{H}_e) \right\|_F \\
&\leq \frac{2}{\rho(1-s)} \|\mathcal{P}_T \mathcal{A}_{\Omega^{\text{clean}}} \mathcal{P}_T(\mathbf{H}_e)\|_F + 2 \|\mathcal{P}_T \mathcal{A}^\perp \mathcal{P}_T(\mathbf{H}_e)\|_F \\
&\leq \frac{2}{\rho(1-s)} (\|\mathcal{P}_T \mathcal{A}_{\Omega^{\text{clean}}}(\mathbf{H}_e)\|_F + \|\mathcal{P}_T \mathcal{A}_{\Omega^{\text{clean}}} \mathcal{P}_{T^\perp}(\mathbf{H}_e)\|_F) \\
&\quad + 2 \|\mathcal{P}_T \mathcal{A}^\perp(\mathbf{H}_e)\|_F + 2 \|\mathcal{P}_T \mathcal{A}^\perp \mathcal{P}_{T^\perp}(\mathbf{H}_e)\|_F \\
&\leq \frac{2}{\rho(1-s)} (\|\mathcal{A}_{\Omega^{\text{clean}}}(\mathbf{H}_e)\|_F + \|\mathcal{A}_{\Omega^{\text{clean}}} \mathcal{P}_{T^\perp}(\mathbf{H}_e)\|_F) + 2 \|\mathcal{P}_{T^\perp}(\mathbf{H}_e)\|_F,
\end{aligned} \tag{111}$$

where the last inequality exploit the facts that $\mathcal{A}^\perp(\mathbf{H}_e) = 0$ and $\|\mathcal{P}_T(\mathbf{M})\|_F \leq \|\mathbf{M}\|_F$.

Recall that $\mathcal{A}_{\Omega^{\text{clean}}}$ corresponds to sampling with replacement. Condition (55) together with (111) leads to

$$\begin{aligned}
\|\mathcal{P}_T(\mathbf{H}_e)\|_F &\leq \frac{20 \log(n_1 n_2)}{\rho(1-s)} (\|\mathcal{A}'_{\Omega^{\text{clean}}}(\mathbf{H}_e)\|_F + \|\mathcal{A}'_{\Omega^{\text{clean}}} \mathcal{P}_{T^\perp}(\mathbf{H}_e)\|_F) + 2 \|\mathcal{P}_{T^\perp}(\mathbf{H}_e)\|_F \\
&\leq \frac{20 \log(n_1 n_2)}{\rho(1-s)} \|\mathcal{A}'_{\Omega^{\text{clean}}}(\mathbf{H}_e)\|_F + \left(\frac{20 \log(n_1 n_2)}{\rho(1-s)} + 2 \right) \|\mathcal{P}_{T^\perp}(\mathbf{H}_e)\|_F \\
&\leq \frac{20 \log(n_1 n_2)}{\rho(1-s)} \|\mathcal{A}'_{\Omega^{\text{clean}}}(\mathbf{H}_e)\|_F + \left(\frac{20 \log(n_1 n_2)}{\rho(1-s)} + 2 \right) \|\mathcal{P}_{T^\perp}(\mathbf{H}_e)\|_*,
\end{aligned} \tag{112}$$

where the last inequality follows from the fact that $\|\mathbf{M}\|_F \leq \|\mathbf{M}\|_*$. Substituting (112) into (110) yields

$$\left(\frac{3}{4} - \frac{\lambda}{n_1^2 n_2^2} \left(\frac{20 \log(n_1 n_2)}{\rho(1-s)} + 2\right)\right) \|\mathcal{P}_{T^\perp}(\mathbf{H}_e)\|_* + \lambda \left(\frac{3}{4} - \frac{20 \log(n_1 n_2)}{\rho(1-s) n_1^2 n_2^2}\right) \|\mathcal{A}'_{\Omega^{\text{clean}}}(\mathbf{H}_e)\|_F \leq 0. \quad (113)$$

Since $\lambda < 1$ and $\rho n_1^2 n_2^2 \gg \log(n_1 n_2)$, both terms on the left-hand side of (113) are positive. This can only occur when

$$\mathcal{P}_{T^\perp}(\mathbf{H}_e) = 0 \quad \text{and} \quad \mathcal{A}'_{\Omega^{\text{clean}}}(\mathbf{H}_e) = 0. \quad (114)$$

(1) Consider first the situation where

$$\|\mathcal{P}_T(\mathbf{H}_e)\|_F \leq \frac{n_1^2 n_2^2}{2} \|\mathcal{P}_{T^\perp}(\mathbf{H}_e)\|_F. \quad (115)$$

One can immediately see that

$$\|\mathcal{P}_T(\mathbf{H}_e)\|_F \leq \frac{n_1^2 n_2^2}{2} \|\mathcal{P}_{T^\perp}(\mathbf{H}_e)\|_F = 0$$

which implies $\mathcal{P}_T(\mathbf{H}_e) = \mathcal{P}_{T^\perp}(\mathbf{H}_e) = 0$, and therefore $\mathbf{H}_e = 0$. That said, Robust-EMaC succeeds in finding \mathbf{X}_e under Condition (115).

(2) Consider instead the complement situation where

$$\|\mathcal{P}_T(\mathbf{H}_e)\|_F > \frac{n_1^2 n_2^2}{2} \|\mathcal{P}_{T^\perp}(\mathbf{H}_e)\|_F.$$

Note that $\mathcal{A}'_{\Omega^{\text{clean}}}(\mathbf{H}_e) = \mathcal{A}^\perp(\mathbf{H}_e) = 0$ and $\left\| \mathcal{P}_T \mathcal{A} \mathcal{P}_T - \frac{1}{\rho(1-s)} \mathcal{P}_T \mathcal{A}_{\Omega^{\text{clean}}} \mathcal{P}_T \right\| \leq \frac{1}{2}$. Using the same argument as in the proof of Lemma 1 (see the second part of Appendix B) with Ω replaced by Ω^{clean} , we can conclude $\mathbf{H}_e = 0$.

J Proof of Lemma 9

We first state the following useful inequality in the proof. For any $\mathbf{b} \in [n_1] \times [n_2]$, one has

$$\sum_{\mathbf{a} \in [n_1] \times [n_2]} |\langle \mathcal{P}_T \mathbf{A}_b, \mathbf{A}_a \rangle|^2 \omega_a \leq \sum_{\mathbf{a} \in [n_1] \times [n_2]} \left(\sqrt{\frac{\omega_b}{\omega_a}} \frac{3\mu_1 c_s r}{n_1 n_2} \right)^2 \omega_a \quad (116)$$

$$= \omega_b \sum_{\mathbf{a} \in [n_1] \times [n_2]} \left(\frac{3\mu_1 c_s r}{n_1 n_2} \right)^2 = \omega_b \frac{9\mu_1^2 c_s^2 r^2}{n_1 n_2}, \quad (117)$$

where (116) follows from (34).

By definition, Ω^{dirty} is the set of *distinct* locations that appear in Ω but not in Ω^{clean} . To simplify the analysis, we introduce an auxiliary multi-set $\tilde{\Omega}^{\text{dirty}}$ that contains $\rho s n_1 n_2$ i.i.d. entries. Specifically, suppose that $\Omega = \{\mathbf{a}_i \mid 1 \leq i \leq \rho n_1 n_2\}$, $\Omega^{\text{clean}} = \{\mathbf{a}_i \mid 1 \leq i \leq \rho(1-s)n_1 n_2\}$ and $\tilde{\Omega}^{\text{dirty}} = \{\mathbf{a}_i \mid \rho(1-s)n_1 n_2 < i \leq \rho n_1 n_2\}$, where \mathbf{a}_i 's are independently and uniformly selected from $[n_1] \times [n_2]$.

In addition, we consider an equivalent model for $\text{sgn}(\mathbf{S})$ as follows

- Define $\mathbf{K} = (K_{\alpha, \beta})_{1 \leq \alpha \leq n_1, 1 \leq \beta \leq n_2}$ to be a random $n_1 \times n_2$ matrix such that all of its entries are independent and have amplitude 1 (i.e. in the real case, all entries are either 1 or -1 , and in the complex case, all entries have amplitude 1 and arbitrary phase on the unit circle). We assume that $\mathbb{E}\mathbf{K} = \mathbf{0}$.
- Set $\text{sgn}(\mathbf{S})$ such that $\text{sgn}(\mathbf{S}_{\alpha, \beta}) = K_{\alpha, \beta} \mathbf{1}_{\{(\alpha, \beta) \in \Omega^{\text{dirty}}\}}$, and hence

$$\text{sgn}(\mathbf{S}_e) = \sum_{(\alpha, \beta) \in \Omega^{\text{dirty}}} K_{\alpha, \beta} \sqrt{\omega_{\alpha, \beta}} \mathbf{A}_{\alpha, \beta}.$$

Recall that $\text{support}(\mathbf{S}) \subseteq \Omega^{\text{dirty}}$. Rather than directly studying $\text{sgn}(\mathbf{S}_e)$, we will first examine an auxiliary matrix

$$\tilde{\mathbf{S}}_e := \sum_{i=\rho(1-s)n_1n_2+1}^{\rho n_1 n_2} K_{\mathbf{a}_i} \sqrt{\omega_{\mathbf{a}_i}} \mathbf{A}_{\mathbf{a}_i},$$

and then bound the difference between $\tilde{\mathbf{S}}_e$ and $\text{sgn}(\mathbf{S}_e)$.

For any given pair $(k, l) \in [n_1] \times [n_2]$, define a random variable

$$\mathcal{Z}_{\alpha, \beta} := \sqrt{\frac{\omega_{\alpha, \beta}}{\omega_{k, l}}} \langle \mathcal{P}_T \mathbf{A}_{(k, l)}, K_{\alpha, \beta} \mathbf{A}_{\alpha, \beta} \rangle.$$

Thus, conditioned on \mathbf{K} , $\mathcal{Z}_{\mathbf{a}_i}$'s are conditionally independent and $\frac{1}{\sqrt{\omega_{k, l}}} \langle \mathbf{A}_{(k, l)}, \mathcal{P}_T(\tilde{\mathbf{S}}_e) \rangle$ is equivalent to $\sum_{i=\rho(1-s)n_1n_2+1}^{\rho n_1 n_2} \mathcal{Z}_{\mathbf{a}_i}$ in distribution. The conditional mean and variance of $\mathcal{Z}_{\mathbf{a}_i}$ are given as

$$\mathbb{E}(\mathcal{Z}_{\mathbf{a}_i} | \mathbf{K}) = \frac{1}{n_1 n_2} \frac{1}{\sqrt{\omega_{k, l}}} \langle \mathcal{P}_T \mathbf{A}_{(k, l)}, \mathbf{K}_e \rangle,$$

where \mathbf{K}_e is the enhanced matrix of \mathbf{K} , and

$$\begin{aligned} \text{Var}(\mathcal{Z}_{\mathbf{a}_i} | \mathbf{K}) &\leq \mathbb{E}(\mathcal{Z}_{\mathbf{a}_i} \mathcal{Z}_{\mathbf{a}_i}^* | \mathbf{K}) = \frac{1}{n_1 n_2} \frac{1}{\omega_{k, l}} \sum_{\mathbf{b} \in [n_1] \times [n_2]} \omega_{\mathbf{b}} |\langle \mathcal{P}_T \mathbf{A}_{(k, l)}, \mathbf{A}_{\mathbf{b}} \rangle|^2 \\ &\leq \frac{9\mu_1^2 c_s^2 r^2}{n_1^2 n_2^2}, \end{aligned}$$

where the last inequality follows from (117). Besides, from (34), the magnitude of $\mathcal{Z}_{\alpha, \beta}$ can be bounded as follows

$$|\mathcal{Z}_{\alpha, \beta}| \leq \frac{3\mu_1 c_s r}{n_1 n_2}. \quad (118)$$

Applying Lemma 11 then yields that with probability exceeding $1 - (n_1 n_2)^{-4}$,

$$\begin{aligned} \frac{1}{\sqrt{\omega_{k, l}}} \left| \langle \mathbf{A}_{(k, l)}, \mathcal{P}_T(\tilde{\mathbf{S}}_e) \rangle - \rho s \langle \mathcal{P}_T \mathbf{A}_{(k, l)}, \mathbf{K}_e \rangle \right| &\leq c_{13} \mu_1 c_s r \left(\sqrt{\frac{\rho s \log(n_1 n_2)}{n_1 n_2}} + \frac{\log(n_1 n_2)}{n_1 n_2} \right) \\ &\leq 2c_{13} \mu_1 c_s r \sqrt{\frac{\rho s \log(n_1 n_2)}{n_1 n_2}} \end{aligned} \quad (119)$$

for some constant $c_{13} > 0$ provided $\rho s n_1 n_2 \gg \log(n_1 n_2)$.

The next step is to bound $\frac{\rho s}{\sqrt{\omega_{k, l}}} \langle \mathcal{P}_T \mathbf{A}_{(k, l)}, \mathbf{K}_e \rangle$. For convenience of analysis, we represent \mathbf{K}_e as

$$\mathbf{K}_e = \sum_{\mathbf{a} \in [n_1] \times [n_2]} z_{\mathbf{a}} \sqrt{\omega_{\mathbf{a}}} \mathbf{A}_{\mathbf{a}}, \quad (120)$$

where $z_{\mathbf{a}}$'s are independent (not necessarily i.i.d.) zero-mean random variables satisfying $|z_{\mathbf{a}}| = 1$. Let

$$\mathcal{Y}_{\mathbf{a}} := \frac{1}{\sqrt{\omega_{k, l}}} \langle \mathcal{P}_T \mathbf{A}_{(k, l)}, z_{\mathbf{a}} \sqrt{\omega_{\mathbf{a}}} \mathbf{A}_{\mathbf{a}} \rangle,$$

then $\mathbb{E} \mathcal{Y}_{\mathbf{a}} = 0$, (34) and (117) allow us to bound

$$|\mathcal{Y}_{\mathbf{a}}| = \frac{1}{\sqrt{\omega_{k, l}}} |\langle \mathcal{P}_T \mathbf{A}_{(k, l)}, \sqrt{\omega_{\mathbf{a}}} \mathbf{A}_{\mathbf{a}} \rangle| \leq \frac{3\mu_1 c_s r}{n_1 n_2},$$

and

$$\sum_{\mathbf{a} \in [n_1] \times [n_2]} \mathbb{E} \mathcal{Y}_{\mathbf{a}} \mathcal{Y}_{\mathbf{a}}^* = \frac{1}{\omega_{k, l}} \sum_{\mathbf{a} \in [n_1] \times [n_2]} |\langle \mathcal{P}_T \mathbf{A}_{(k, l)}, \sqrt{\omega_{\mathbf{a}}} \mathbf{A}_{\mathbf{a}} \rangle|^2 \leq \frac{9\mu_1^2 c_s^2 r^2}{n_1 n_2}.$$

Applying Lemma 11 suggests that there exists a constant $c_{14} > 0$ such that

$$\frac{1}{\sqrt{\omega_{k,l}}} |\langle \mathcal{P}_T \mathbf{A}_{(k,l)}, \mathbf{K}_e \rangle| = \left| \sum_{\mathbf{a} \in [n_1] \times [n_2]} \mathcal{Y}_{\mathbf{a}} \right| \leq c_{14} \mu_1 c_s r \sqrt{\frac{\log(n_1 n_2)}{n_1 n_2}}$$

with high probability provided $n_1 n_2 \gg \log(n_1 n_2)$. This together with (119) suggests that

$$\begin{aligned} \frac{1}{\sqrt{\omega_{k,l}}} \left| \langle \mathbf{A}_{(k,l)}, \mathcal{P}_T(\tilde{\mathbf{S}}_e) \rangle \right| &\leq \frac{1}{\sqrt{\omega_{k,l}}} \left| \langle \mathbf{A}_{(k,l)}, \mathcal{P}_T(\tilde{\mathbf{S}}_e) \rangle - \rho s \langle \mathcal{P}_T \mathbf{A}_{(k,l)}, \mathbf{K}_e \rangle \right| + \frac{\rho s}{\sqrt{\omega_{k,l}}} |\langle \mathcal{P}_T \mathbf{A}_{(k,l)}, \mathbf{K}_e \rangle| \\ &\leq c_{15} \mu_1 c_s r \sqrt{\frac{\rho s \log(n_1 n_2)}{n_1 n_2}} \end{aligned} \quad (121)$$

for some constant $c_{15} > 0$ with high probability.

We still need to bound the deviation of $\tilde{\mathbf{S}}_e$ from $\text{sgn}(\mathbf{S}_e)$. Observe that the difference between them arise from sampling with replacement, i.e. there are a few entries in $\{\mathbf{a}_i \mid \rho(1-s)n_1 n_2 < i \leq \rho n_1 n_2\}$ that either fall within Ω^{clean} or have appeared more than once. A simple Chernoff bound argument (e.g. [53]) indicates the number of aforementioned conflicts is upper bounded by $10 \log(n_1 n_2)$ with high probability. That said, one can find a collection of entry locations $\{\mathbf{b}_1, \dots, \mathbf{b}_N\}$ such that

$$\tilde{\mathbf{S}}_e - \text{sgn}(\mathbf{S}_e) = \sum_{i=1}^N K_{\mathbf{b}_i} \sqrt{\omega_{\mathbf{b}_i}} \mathbf{A}_{\mathbf{b}_i}, \quad (122)$$

where $N \leq 10 \log(n_1 n_2)$ with high probability. Therefore, we can bound

$$\begin{aligned} \frac{1}{\sqrt{\omega_{k,l}}} \left| \langle \mathbf{A}_{(k,l)}, \mathcal{P}_T(\tilde{\mathbf{S}}_e - \text{sgn}(\mathbf{S}_e)) \rangle \right| &\leq \sum_{i=1}^N \frac{1}{\sqrt{\omega_{k,l}}} |\langle \mathbf{A}_{(k,l)}, \mathcal{P}_T(\sqrt{\omega_{\mathbf{b}_i}} \mathbf{A}_{\mathbf{b}_i}) \rangle| \\ &\leq N \frac{3\mu_1 c_s r}{n_1 n_2} \leq \frac{30\mu_1 c_s r \log(n_1 n_2)}{n_1 n_2}. \end{aligned}$$

following (34). Putting the above inequality and (121) together yields that for every $(k, l) \in [n_1] \times [n_2]$,

$$\begin{aligned} \frac{1}{\sqrt{\omega_{k,l}}} |\langle \mathbf{A}_{(k,l)}, \mathcal{P}_T(\text{sgn}(\mathbf{S}_e)) \rangle| &\leq \frac{1}{\sqrt{\omega_{k,l}}} \left| \langle \mathbf{A}_{(k,l)}, \mathcal{P}_T(\tilde{\mathbf{S}}_e - \text{sgn}(\mathbf{S}_e)) \rangle \right| + \frac{1}{\sqrt{\omega_{k,l}}} \left| \langle \mathbf{A}_{(k,l)}, \mathcal{P}_T(\tilde{\mathbf{S}}_e) \rangle \right| \\ &\leq c_{15} \mu_1 c_s r \sqrt{\frac{\rho s \log(n_1 n_2)}{n_1 n_2}} + \frac{30\mu_1 c_s r \log(n_1 n_2)}{n_1 n_2} \\ &\leq c_9 \mu_1 c_s r \sqrt{\frac{\rho s \log(n_1 n_2)}{n_1 n_2}} \end{aligned}$$

for some constant $c_9 > 0$ provided $\rho s n_1 n_2 > \log(n_1 n_2)$. This completes the proof.

K Proof of Lemma 10

Consider the model of $\text{sgn}(\mathbf{S})$, \mathbf{K} and $\tilde{\mathbf{S}}_e$ as introduced in the proof of Lemma 9 in Appendix J. For any $(\alpha, \beta) \in [n_1] \times [n_2]$, define

$$\tilde{\mathcal{Z}}_{\alpha, \beta} := \mathcal{A}_{\alpha, \beta}(\mathbf{K}_e) = \sqrt{\omega_{\alpha, \beta}} K_{\alpha, \beta} \mathbf{A}_{\alpha, \beta}.$$

With this notation, we can see that $\tilde{\mathcal{Z}}_{\mathbf{a}_i}$'s are conditionally independent given \mathbf{K} , and satisfy

$$\mathbb{E}(\tilde{\mathcal{Z}}_{\mathbf{a}_i} | \mathbf{K}) = \frac{1}{n_1 n_2} \sum_{(\alpha, \beta) \in [n_1] \times [n_2]} \sqrt{\omega_{\alpha, \beta}} \mathbf{A}_{\alpha, \beta} K_{\alpha, \beta} = \frac{1}{n_1 n_2} \mathbf{K}_e,$$

$$\|\tilde{\mathcal{Z}}_{\alpha, \beta}\| = \|\sqrt{\omega_{\alpha, \beta}} \mathbf{A}_{\alpha, \beta}\| = 1,$$

and

$$\left\| \mathbb{E} \left(\tilde{\mathbf{Z}}_{\mathbf{a}_i} \tilde{\mathbf{Z}}_{\mathbf{a}_i}^* | \mathbf{K} \right) \right\| \leq \frac{1}{n_1 n_2} \sum_{(\alpha, \beta) \in [n_1] \times [n_2]} \left\| \omega_{\alpha, \beta} \mathbf{A}_{\alpha, \beta} \mathbf{A}_{\alpha, \beta}^* \right\| = 1.$$

Since $\tilde{\mathbf{S}}_e = \sum_{i=(1-s)\rho n_1 n_2 + 1}^{\rho n_1 n_2} \tilde{\mathbf{Z}}_{\mathbf{a}_i}$, applying Lemma 11 implies that conditioned on \mathbf{K} , there exists a constant $c_{16} > 0$ such that

$$\left\| \tilde{\mathbf{S}}_e - \rho s \mathbf{K}_e \right\| < \sqrt{c_{16} \rho s n_1 n_2 \log(n_1 n_2)} \quad (123)$$

with probability at least $1 - n_1^{-5} n_2^{-5}$.

The next step is to bound the operator norm of $\rho s \mathbf{K}_e$. Recall the decomposition form of \mathbf{K}_e in (120). Let $\mathcal{Y}_{\mathbf{a}} := z_{\mathbf{a}} \sqrt{\omega_{\mathbf{a}}} \mathbf{A}_{\mathbf{a}}$, then we have $\mathbb{E} \mathcal{Y}_{\mathbf{a}} = 0$, $\|\mathcal{Y}_{\mathbf{a}}\| = 1$, and

$$\left\| \sum_{\mathbf{a} \in [n_1] \times [n_2]} \mathbb{E} \mathcal{Y}_{\mathbf{a}} \mathcal{Y}_{\mathbf{a}}^* \right\| = \left\| \sum_{\mathbf{a} \in [n_1] \times [n_2]} \omega_{\mathbf{a}} \mathbf{A}_{\mathbf{a}} \mathbf{A}_{\mathbf{a}}^* \right\| \leq n_1 n_2$$

Therefore, applying Lemma 11 yields that there exists a constant $c_{17} > 0$ such that

$$\|\mathbf{K}_e\| \leq \sqrt{c_{17} n_1 n_2 \log(n_1 n_2)}$$

with high probability. This and (123), taken collectively, yield

$$\left\| \tilde{\mathbf{S}}_e \right\| \leq \left\| \tilde{\mathbf{S}}_e - \rho s \mathbf{K}_e \right\| + \rho s \|\mathbf{K}_e\| < 2\sqrt{c_{18} \rho s n_1 n_2 \log(n_1 n_2)}$$

with high probability, where $c_{18} = \max\{c_{16}, c_{17}\}$. On the other hand, (122) implies that,

$$\left\| \tilde{\mathbf{S}}_e - \text{sgn}(\mathbf{S}_e) \right\| \leq \sum_{i=1}^N \left\| \sqrt{\omega_{\mathbf{b}_i}} \mathbf{A}_{\mathbf{b}_i} \right\| = N \leq 10 \log(n_1 n_2) \leq \sqrt{c_{18} \rho s n_1 n_2 \log(n_1 n_2)}$$

with high probability, provided $\rho s n_1 n_2 > 100 \log(n_1 n_2) / c_{18}$. Consequently, for a sufficiently small constant s ,

$$\begin{aligned} \|\mathcal{P}_{T^\perp}(\lambda \text{sgn}(\mathbf{S}_e))\| &\leq \lambda \|\text{sgn}(\mathbf{S}_e)\| \leq \lambda \left\| \tilde{\mathbf{S}}_e - \text{sgn}(\mathbf{S}_e) \right\| + \lambda \left\| \tilde{\mathbf{S}}_e \right\| \\ &\leq 3\lambda \sqrt{c_{18} \rho s n_1 n_2 \log(n_1 n_2)} \\ &= 3\sqrt{c_{18} s} \leq \frac{1}{8} \end{aligned}$$

with probability exceeding $1 - n_1^{-5} n_2^{-5}$.

L Proof of Theorem 2

We prove this theorem under the conditions of Lemma 1, i.e. (29)–(32). Note that these conditions are satisfied with high probability, as we have shown in the proof of Theorem 1.

Denote the solution of Noisy-EMaC as $\hat{\mathbf{X}}_e = \mathbf{X}_e + \mathbf{H}_e$. Since \mathbf{H}_e is a two-fold Hankel matrix, i.e. $\mathbf{H}_e = \mathcal{A}_\Omega(\mathbf{H}_e) + \mathcal{A}_{\Omega^\perp}(\mathbf{H}_e)$, we can obtain

$$\begin{aligned} \|\mathbf{X}_e\|_* &\geq \|\hat{\mathbf{X}}_e\|_* = \|\mathbf{X}_e + \mathbf{H}_e\|_* \\ &\geq \|\mathbf{X}_e + \mathcal{A}_{\Omega^\perp}(\mathbf{H}_e)\|_* - \|\mathcal{A}_\Omega(\mathbf{H}_e)\|_*. \end{aligned} \quad (124)$$

The second term can be bounded using the triangle inequality as

$$\|\mathcal{A}_\Omega(\mathbf{H}_e)\|_F \leq \left\| \mathcal{A}_\Omega(\hat{\mathbf{X}}_e - \mathbf{X}_e^\circ) \right\|_F + \|\mathcal{A}_\Omega(\mathbf{X}_e - \mathbf{X}_e^\circ)\|_F. \quad (125)$$

Since the constraint of Noisy-EMaC requires $\|\mathcal{P}_\Omega(\hat{\mathbf{X}} - \mathbf{X}^\circ)\|_F \leq \delta$ and $\|\mathcal{P}_\Omega(\mathbf{X} - \mathbf{X}^\circ)\|_F \leq \delta$, the Hankel structure of the enhanced form allows us to bound $\|\mathcal{A}_\Omega(\hat{\mathbf{X}}_e - \mathbf{X}_e^\circ)\|_F \leq \sqrt{n_1 n_2} \delta$ and $\|\mathcal{A}_\Omega(\mathbf{X}_e - \mathbf{X}_e^\circ)\|_F \leq \sqrt{n_1 n_2} \delta$, which immediately leads to

$$\|\mathcal{A}_\Omega(\mathbf{H}_e)\|_F \leq 2\sqrt{n_1 n_2} \delta.$$

Using the same analysis as for (73) allows us to bound the perturbation $\mathcal{A}_{\Omega^\perp}(\mathbf{H}_e)$ as follows

$$\|\mathbf{X}_e + \mathcal{A}_{\Omega^\perp}(\mathbf{H}_e)\|_* \geq \|\mathbf{X}_e\|_* + \frac{1}{4} \|\mathcal{P}_{T^\perp} \mathcal{A}_{\Omega^\perp}(\mathbf{H}_e)\|_F.$$

Combining this with (124), we have

$$\begin{aligned} \|\mathcal{P}_{T^\perp} \mathcal{A}_{\Omega^\perp}(\mathbf{H}_e)\|_F &\leq 4\|\mathcal{A}_\Omega(\mathbf{H}_e)\|_* \\ &\leq 4\sqrt{n_1 n_2} \|\mathcal{A}_\Omega(\mathbf{H}_e)\|_F \leq 8n_1 n_2 \delta. \end{aligned}$$

Further from Lemma 1, we know that

$$\|\mathcal{P}_T \mathcal{A}_{\Omega^\perp}(\mathbf{H}_e)\|_F \leq \frac{n_1 n_2}{m} \sqrt{2} \|\mathcal{P}_{T^\perp} \mathcal{A}_{\Omega^\perp}(\mathbf{H}_e)\|_F. \quad (126)$$

Therefore, combining all the above results give

$$\begin{aligned} \|\mathbf{H}_e\|_F &\leq \|\mathcal{A}_\Omega(\mathbf{H}_e)\|_F + \|\mathcal{P}_T \mathcal{A}_{\Omega^\perp}(\mathbf{H}_e)\|_F + \|\mathcal{P}_{T^\perp} \mathcal{A}_{\Omega^\perp}(\mathbf{H}_e)\|_F \\ &\leq \left\{ 2\sqrt{n_1 n_2} + 8n_1 n_2 + \frac{8\sqrt{2}n_1^2 n_2^2}{m} \right\} \delta. \end{aligned}$$

References

- [1] M. Lustig, D. Donoho, and J. M. Pauly, "Sparse MRI: The application of compressed sensing for rapid MR imaging," *Magnetic Resonance in Medicine*, vol. 58, no. 6, pp. 1182–1195, 2007.
- [2] L. Potter, E. Ertin, J. Parker, and M. Cetin, "Sparsity and compressed sensing in radar imaging," *Proceedings of the IEEE*, vol. 98, no. 6, pp. 1006–1020, 2010.
- [3] L. Borcea, G. Papanicolaou, C. Tsogka, and J. Berryman, "Imaging and time reversal in random media," *Inverse Problems*, vol. 18, no. 5, p. 1247, 2002.
- [4] L. Schermelleh, R. Heintzmann, and H. Leonhardt, "A guide to super-resolution fluorescence microscopy," *The Journal of cell biology*, vol. 190, no. 2, pp. 165–175, 2010.
- [5] Y. Chi, Y. Xie, and R. Calderbank, "Compressive demodulation of mutually interfering signals," *submitted to IEEE Transactions on Information Theory*, 2013. [Online]. Available: <http://arxiv.org/abs/1303.3904>
- [6] J. A. Tropp, J. N. Laska, M. F. Duarte, J. K. Romberg, and R. G. Baraniuk, "Beyond nyquist: Efficient sampling of sparse bandlimited signals," *Information Theory, IEEE Transactions on*, vol. 56, no. 1, pp. 520–544, 2010.
- [7] R. Prony, "Essai experimental et analytique," *J. de l'Ecole Polytechnique (Paris)*, vol. 1, no. 2, pp. 24–76, 1795.
- [8] R. Roy and T. Kailath, "ESPRIT-estimation of signal parameters via rotational invariance techniques," *IEEE Transactions on Acoustics, Speech and Signal Processing*, vol. 37, no. 7, pp. 984–995, Jul 1989.
- [9] Y. Hua and T. K. Sarkar, "Matrix pencil method for estimating parameters of exponentially damped/undamped sinusoids in noise," *IEEE Transactions on Acoustics, Speech and Signal Processing*, vol. 38, no. 5, pp. 814–824, may 1990.

- [10] D. Tufts and R. Kumaresan, "Estimation of frequencies of multiple sinusoids: Making linear prediction perform like maximum likelihood," *Proceedings of the IEEE*, vol. 70, no. 9, pp. 975 – 989, sept. 1982.
- [11] M. Vetterli, P. Marziliano, and T. Blu, "Sampling signals with finite rate of innovation," *IEEE Transactions on Signal Processing*, vol. 50, no. 6, pp. 1417–1428, 2002.
- [12] K. Gedalyahu, R. Tur, and Y. C. Eldar, "Multichannel sampling of pulse streams at the rate of innovation," *IEEE Transactions on Signal Processing*, vol. 59, no. 4, pp. 1491–1504, 2011.
- [13] P. L. Dragotti, M. Vetterli, and T. Blu, "Sampling moments and reconstructing signals of finite rate of innovation: Shannon meets strang-fix," *IEEE Transactions on Signal Processing*, vol. 55, no. 5, pp. 1741 –1757, May 2007.
- [14] E. J. Candes, J. Romberg, and T. Tao, "Robust uncertainty principles: exact signal reconstruction from highly incomplete frequency information," *IEEE Transactions on Information Theory*, vol. 52, no. 2, pp. 489–509, Feb. 2006.
- [15] D. Donoho, "Compressed sensing," *IEEE Transactions on Information Theory*, vol. 52, no. 4, pp. 1289 –1306, April 2006.
- [16] E. J. Candes, J. K. Romberg, and T. Tao, "Stable signal recovery from incomplete and inaccurate measurements," *Communications on Pure and Applied Mathematics*, vol. 59, no. 8, pp. 1207–1223, 2006.
- [17] X. Li, "Compressed sensing and matrix completion with constant proportion of corruptions," *Constructive Approximation*, vol. 37, pp. 73–99, 2013.
- [18] Y. Chi, L. Scharf, A. Pezeshki, and A. Calderbank, "Sensitivity to basis mismatch in compressed sensing," *IEEE Transactions on Signal Processing*, vol. 59, no. 5, pp. 2182–2195, May 2011.
- [19] Y. Hua, "Estimating two-dimensional frequencies by matrix enhancement and matrix pencil," *IEEE Transactions on Signal Processing*, vol. 40, no. 9, pp. 2267 –2280, Sep 1992.
- [20] J. A. Cadzow, "Spectral estimation: An overdetermined rational model equation approach," *Proceedings of the IEEE*, vol. 70, no. 9, pp. 907–939, 1982.
- [21] E. Candes and Y. Plan, "A probabilistic and RIPless theory of compressed sensing," *IEEE Transactions on Information Theory*, vol. 57, no. 11, pp. 7235–7254, 2011.
- [22] M. Duarte and R. Baraniuk, "Spectral compressive sensing," *Applied and Computational Harmonic Analysis*, 2012.
- [23] A. C. Fannjiang, T. Strohmer, and P. Yan, "Compressed remote sensing of sparse objects," *SIAM Journal on Imaging Sciences*, vol. 3, no. 3, pp. 595–618, 2010.
- [24] E. J. Candes and C. Fernandez-Granda, "Towards a mathematical theory of super-resolution," *to appear in Communications on Pure and Applied Mathematics*, 2013.
- [25] —, "Super-resolution from noisy data," November 2012. [Online]. Available: <http://arxiv.org/abs/1211.0290>
- [26] G. Tang, B. N. Bhaskar, P. Shah, and B. Recht, "Compressed sensing off the grid," July 2012. [Online]. Available: <http://arxiv.org/abs/1207.6053>
- [27] E. J. Candes and B. Recht, "Exact matrix completion via convex optimization," *Foundations of Computational Mathematics*, vol. 9, no. 6, pp. 717–772, April 2009.
- [28] R. H. Keshavan, A. Montanari, and S. Oh, "Matrix completion from a few entries," *IEEE Transactions on Information Theory*, vol. 56, no. 6, pp. 2980–2998, 2010.

- [29] E. Candes and T. Tao, “The power of convex relaxation: Near-optimal matrix completion,” *IEEE Transactions on Information Theory*, vol. 56, no. 5, pp. 2053–2080, May 2010.
- [30] D. Gross, “Recovering low-rank matrices from few coefficients in any basis,” *IEEE Transactions on Information Theory*, vol. 57, no. 3, pp. 1548–1566, March 2011.
- [31] Y. Chen, “Incoherence-optimal matrix completion,” *arXiv preprint arXiv:1310.0154*, 2014.
- [32] E. J. Candès, X. Li, Y. Ma, and J. Wright, “Robust principal component analysis?” *Journal of ACM*, vol. 58, no. 3, pp. 11:1–11:37, Jun 2011.
- [33] S. Negahban and M. Wainwright, “Restricted strong convexity and weighted matrix completion: Optimal bounds with noise,” *The Journal of Machine Learning Research*, vol. 98888, pp. 1665–1697, May 2012.
- [34] V. Chandrasekaran, S. Sanghavi, P. A. Parrilo, and A. S. Willsky, “Rank-sparsity incoherence for matrix decomposition,” *SIAM Journal on Optimization*, vol. 21, no. 2, pp. 572–596, 2011.
- [35] Y. Chen, H. Xu, C. Caramanis, and S. Sanghavi, “Robust matrix completion with corrupted columns,” *International Conference on Machine Learning (ICML)*, June 2011.
- [36] Y. Chen, A. Jalali, S. Sanghavi, and C. Caramanis, “Low-rank matrix recovery from errors and erasures,” *IEEE Transactions on Information Theory*, vol. 59, no. 7, pp. 4324–4337, 2013.
- [37] M. Wu, “Collaborative filtering via ensembles of matrix factorizations,” vol. 2007, 2007.
- [38] T. Zhang, J. M. Pauly, and I. R. Levesque, “Accelerating parameter mapping with a locally low rank constraint,” *Magnetic Resonance in Medicine*, DOI: 10.1002/mrm.25161, 2014.
- [39] B. Recht, M. Fazel, and P. A. Parrilo, “Guaranteed minimum-rank solutions of linear matrix equations via nuclear norm minimization,” *SIAM Review*, vol. 52, no. 3, pp. 471–501, 2010.
- [40] Y. Chen and Y. Chi, “Spectral compressed sensing via structured matrix completion,” *International Conference on Machine Learning (ICML)*, June 2013.
- [41] E. J. Candes and Y. Plan, “Matrix completion with noise,” *Proceedings of the IEEE*, vol. 98, no. 6, pp. 925–936, June 2010.
- [42] G. Tang, B. Bhaskar, and B. Recht, “Near minimax line spectral estimation,” 2013. [Online]. Available: <http://arxiv.org/abs/1303.4348>
- [43] M. Fazel, T. K. Pong, D. Sun, and P. Tseng, “Hankel matrix rank minimization with applications in system identification and realization,” 2011.
- [44] I. Markovsky, “Structured low-rank approximation and its applications,” *Automatica*, vol. 44, no. 4, pp. 891–909, 2008.
- [45] B. Balle and M. Mohri, “Spectral learning of general weighted automata via constrained matrix completion,” *Advances in Neural Information Processing Systems (NIPS)*, pp. 2168–2176, 2012.
- [46] A. Sankaranarayanan, P. Turaga, R. Baraniuk, and R. Chellappa, “Compressive acquisition of dynamic scenes,” *Computer Vision–ECCV 2010*, pp. 129–142, 2010.
- [47] P. J. Shin, P. E. Larson, M. A. Ohliger, M. Elad, J. M. Pauly, D. B. Vigneron, and M. Lustig, “Calibrationless parallel imaging reconstruction based on structured low-rank matrix completion,” *submitted to Magnetic Resonance in Medicine*, 2012.
- [48] M. Fazel, H. Hindi, and S. P. Boyd, “Log-det heuristic for matrix rank minimization with applications to Hankel and Euclidean distance matrices,” *American Control Conference*, vol. 3, pp. 2156–2162 vol.3, June 2003.
- [49] J. F. Cai, E. J. Candes, and Z. Shen, “A singular value thresholding algorithm for matrix completion,” *SIAM Journal on Optimization*, vol. 20, no. 4, pp. 1956–1982, 2010.

- [50] M. Grant, S. Boyd, and Y. Ye, “CVX: Matlab software for disciplined convex programming,” *Online accessible: <http://stanford.edu/~boyd/cvx>*, 2008.
- [51] S. Chen, D. L. Donoho, and M. A. Saunders, “Atomic decomposition by basis pursuit,” *SIAM Review*, vol. 43, no. 1, pp. 129–159, 2001.
- [52] L. L. Scharf, *Statistical signal processing*. Addison-Wesley Reading, MA, 1991, vol. 98.
- [53] N. Alon and J. H. Spencer, *The Probabilistic Method (3rd Edition)*. Wiley, 2008.
- [54] J. A. Tropp, “User-friendly tail bounds for sums of random matrices,” *Foundations of Computational Mathematics*, vol. 12, no. 4, pp. 389–434, 2012.